UNIVERSIDADE FEDERAL DE SÃO CARLOS
CENTRO DE CIÊNCIAS BIOLÓGICAS E DA SAÚDE
PROGRAMA DE PÓS-GRADUAÇÃO EM GENÉTICA E EVOLUÇÃO

ESTUDO *IN VITRO* DE CITO E FOTOTOXICIDADE DAS DROGAS NITROHETEROCÍCLICAS NITRACRINA E QUINIFURYL.

Marcelo Muniz Rossa

São Carlos – SP
2005

CENTRO DE CIÊNCIAS BIOLÓGICAS E DA SAÚDE
PROGRAMA DE PÓS-GRADUAÇÃO EM GENÉTICA E EVOLUÇÃO

TESE DE DOUTORADO

ESTUDO *IN VITRO* DE CITO E FOTOTOXICIDADE DAS DROGAS NITROHETEROCÍCLICAS NITRACRINA E QUINIFURYL.

Marcelo Muniz Rossa

Orientadora:
Dra. Heloísa S. Selistre de Araújo

Co-orientador:
Dr. Igor Anatolievich Degterev

Tese de doutorado apresentada ao Programa de Pós-Graduação em Genética e Evolução do Centro de Ciências Biológicas e da Saúde da Universidade Federal de São Carlos (UFSCar), como parte dos requisitos para a obtenção do Título de Doutor em Ciências Biológicas, na área de concentração: Genética e Evolução.

São Carlos – SP
2005

Ficha catalográfica elaborada pelo DePT da Biblioteca Comunitária/UFSCar

R823ev

Rossa, Marcelo Muniz.
Estudo *in vitro* de cito e fototoxicidade das drogas nitroheterocíclicas Nitracrina e Quinifuryl / Marcelo Muniz Rossa. -- São Carlos : UFSCar, 2005.
120 p.

Tese (Doutorado) -- Universidade Federal de São Carlos, 2005.

1. Bioquímica. 2. Drogas nitroheterocíclicas. 3. Terapia fotoquímica. 4. Carregadores de drogas. I. Título.

CDD: 574.192 (20ª)

Orientadora:

Profa. Dra. Heloísa Sobreiro Selistre de Araújo

à Renata Fogaça

Agradecimentos:

Antes de tudo, devo agradecer a Dra. Heloisa Sobreiro Selistre de Araújo pela imprescindível presença em todo o desenvolvimento desse trabalho. Sem a sua disponibilização de toda a parte logística, este projeto não teria sido realizado. Dra Heloisa, sinceramente, muito obrigado pelas excelentes condições de trabalho.

Devo agradecer também ao Dr. Igor A. Degterev pela condução intelectual do projeto, pelo afinco e dedicação que sempre demonstrou no ambiente de trabalho.

Gostaria também de mencionar todo o pessoal do Departamento de Fisiologia, em especial aos meus companheiros de laboratório Renner e Oscar, pela disposição em colaborar na realização prática e teórica dos diversos experimentos realizados.

Agradeço ao pessoal da secretaria de pós-graduação pela realização da parte burocrática.

À todo o pessoal do Instituto de Química da UFSCar, em especial ao Prof. Alzir do laboratório de Química inorgânica.

Ao grupo da USP de Ribeirão Preto, agradeço a todos em nome do Prof. Iouri Borissevich.

Ao Prof. Dr. Antonio Cláudio Tedesco do Depto de Química/FFCLRP/USP .

À CAPES pelo suporte financeiro.

Sumário

Lista de Figuras

Lista de Tabelas

Abreviaturas

ATCC - American Type Culture Collection

DMSO - Dimetilsulfóxido

DMEM - Dubelcco´s Modified Eagle´s Medium

DNHC - drogas nitroheterocíclicas

DSPC - distearoilfosfatidilcolina

EDTA - ácido etilenodiamina tetraacético

ERO´s - espécies reativas do oxigênio

ERN´s - espécies reativas do nitrogênio

ET - efeito tóxico

FBS - soro fetal bovino (fetal bovine serum)

FT - fototerapia

K562 - células de eritroleucemia humana

LC_{50} - concentração letal 50%

MTT - sal tetrazolium

NIH3T3 - fibroblastos embrionários de camundongos

$O^{\bullet}$ - oxigênio singlete

O_2 - oxigênio molecular

O_2^- - ânion superóxido

$^{\bullet}OH$ - radical hidroxila

P388 - células de linfoleucemia de camundongos

PBS - Tampão Fosfato em solução fisiológica salina

PEG - Polietilenoglicol

ROL - região de ondas longas

RPM - rotações por minuto

TFQ - terapia fotoquímica

v/v - volume por volume

w/v - peso por volume

τ^{50} - tempo requerido para matar 50% das células

Resumo

A Nitracrina, um agente antitumoral polonês, e o Quinifuryl, um anti-séptico russo, são compostos nitroheterocíclicos. A citotoxicidade dessas drogas foi investigada sobre três linhagens de células em condições de normoxia. Foi dada ênfase na comparação dos efeitos das drogas em tecidos tumorogênicos (células leucêmicas P388 e K562), e não tumorogênicos (células fibroblásticas NIH3T3). Ambas as drogas mostraram significativa citotoxicidade para todas as linhagens de células. A toxicidade sobre as células leucêmicas P388 de camundongos foi significativamente maior comparada com as células fibroblásticas NIH3T3 de camundongos. Adicionalmente, a taxa de morte celular foi 2 - 3 vezes maior no caso das células P388 versus NIH3T3. As células K562 de eritroleucemia humana demonstraram incorporação das drogas 10 minutos após sua adição, enquanto que os valores de LC_{50} foram atingidos após um atraso de 3 horas devido às transformações intracelulares requeridas para matar as células.

Também foi investigada a fotocitotoxicidade de ambas as drogas contra células tumorais e não transformadas de camundongos e de células de eritroleucemia humana. A citotoxicidade dessas drogas foi medida no escuro e no claro, sob iluminação com luz visível. Ambas as drogas mostraram elevada citotoxicidade quando iluminadas com valores de LC_{50} 7 - 35 vezes menores, após 1 hora de iluminação, comparado à incubação por 1 hora no escuro. A citotoxicidade da Nitracrina contra todas as células estudadas excede às do Quinifuryl, tanto no escuro como sob iluminação. O efeito tóxico geral foi calculado pela morte celular direta e pela contenção da proliferação celular.

As micelas (PEG-2000-estearato) e os lipossomos unilamelares (DSPC) foram escolhidos como veículos de transporte. A citotoxicidade das drogas livres e imobilizadas também foi estudada. Nossos resultados mostraram que o Quinifuryl e a Nitracrina podem ser efetivamente imobilizadas por micelas e lipossomos unilamelares. Ambas as drogas continuaram altamente tóxicas contra as linhagens de células quando imobilizadas em lipossomos DSPC. Um efeito protetor das micelas contra a toxicidade da Nitracrina sobre células P388 foi observado em baixa concentração da droga (0,2 nmol/ml), mas não em concentração mais alta (2 nmol/ml). As micelas também protegeram as células P388 contra a toxicidade do Quinifuryl.

Abstract

The cytotoxicity of two nitroheterocyclic compounds, Polish antitumor agent, Nitracrine and Russian antiseptic, Quinifuryl, towards three lines of cells were determined under normoxia conditions. Special emphasis has been placed on the comparisons of the drugs effects in highly tumorogenic, leukaemic P388 and K562 and non-tumorogenic, fibroblast cells NIH3T3. Both drugs showed significant cytotoxicity to all cell lines. Toxicity of both drugs toward murine leukaemia was substantially higher, compared to non-transformed murine fibroblasts. At the drug concentrations of 2 nmol/ml, it took 2-3 times less time to reach the LC_{50} with P388 compared to NIH3T3. Uptake of drugs by human erythroleukaemia cells was observed starting 10 min from the addition of the drug, while the LC_{50} values were achieved after 3 hr of incubation. This delay in cell killing may be due to the intracellular transformation of drugs required for cell killing.

It was also investigated the cellular phototoxicity of both drugs towards murine leukaemia, fibroblast and human erythroleukaemia cells. The cytotoxicity of these drugs towards two lines of leukaemic cells and a line of non-transformed cells, was measured in comparison, on the dark and under illumination. Both drugs showed highly elevated cytotoxicity when illuminated with LC_{50} values 7-35 times lower after 1 h illumination compared to 1 h incubation of cells incubation with drug on the dark. Cytotoxicity of Nitracrine toward all cell lines studied exceeded that of Quinifuryl, both on the dark and under illumination, so that 10 times lower concentration of former drug was needed to reach the same toxicity as the latter. General toxic effect was calculated as a direct cell kill and a cell proliferation arrest.

Micelles (PEG-2000-stearate) and small unilamellar liposomes (DSPC) were chosen as vehicles and cytotoxicity of free and immobilized drugs was studied. We show that both drugs are effectively immobilized and strongly retained by both micelles and unilamellar liposomes. Both drugs are highly toxic against all line cells, when is immobilized in liposomes DSPC. A protective effect of micelles against Nitracrine toxicity toward P388 cells was observed at low drug concentration (0.2 nmol/ml), but not at higher concentration (2 nmol/ml). Micelles also protected P388 cells against cytotoxicity of Quinifuryl.

INTRODUÇÃO

Os avanços na área médica tiveram um grande impacto na perspectiva e na qualidade de vida de pessoas com câncer. Essa evolução tem ocorrido como um resultado do diagnóstico precoce e desenvolvimento de abordagens terapêuticas cada vez mais efetivas.

Quase todos os tipos de câncer começam como resultado da anormalidade de uma única célula (Adams & Stratford, 1994). Existe uma grande variação no tempo em que um tumor leva para dobrar de tamanho; esse "tempo de duplicação" pode variar de alguns dias a muitos anos. O desenvolvimento do câncer envolve o acúmulo de sucessivas anormalidades genéticas ao longo dos anos. As células contêm genes supressores de tumor, cuja função normal é frear a divisão. Muitos tipos de câncer são causados por danos que reduzem a atividade do gene supressor de tumor (Wood et al., 1996). Alguns genes podem levar a célula a eliminar drogas anticancerígenas; outros genes são responsáveis pela fabricação de proteínas importantes que habilitam o câncer a invadir tecidos adjacentes e se espalhar para diferentes partes do corpo. Em alguns casos, estas células podem invadir tecidos linfáticos e sanguíneos, causando o desenvolvimento de crescimentos secundários conhecidos como metástase.

A morte celular apoptótica serve para causar o suicídio de células tumorais e está sob controle genético. Porém, um dano genético pode resultar em células que não morrem, o que pode ser um fator importante tanto para o desenvolvimento do câncer quanto sua resistência ao tratamento com drogas.

TRATAMENTOS ANTICANCERÍGENOS

O câncer pode ser tratado com cirurgia, radioterapia (tratamento com irradiação de alta energia) ou quimioterapia (tratamento com drogas). Em geral, a cirurgia é o tratamento mais efetivo, porém, diferentes tipos de câncer são tratados de maneiras muito diversas. A radioterapia e a quimioterapia são capazes de destruir os cânceres**.** Para muitos pacientes, a melhor possibilidade de cura é obtida com a combinação de tratamentos (Gareth, 2001). A quimioterapia e a radioterapia têm sido freqüentemente utilizadas aliadas à cirurgia, com o objetivo de erradicar quaisquer traços microscópicos de câncer não retirados. A cirurgia pode falhar na remoção completa do câncer porque pode haver células cancerosas que foram deixadas no local da operação, ou por causa de metástase. Se a quantidade de câncer residual for de proporções microscópicas, ainda existe a possibilidade de que o câncer seja completamente erradicado por um tratamento adicional com drogas, que têm o potencial de agir em todo o corpo. Alguns pacientes com câncer, cujo principal tratamento é a radioterapia, também se beneficiarão de tratamento adicional com drogas (Adams & Stratford, 1994).

Nosso trabalho procurou aprofundar metodologias usadas na quimioterapia, introduzindo as novas drogas potenciais acoplado com abordagens de fototerapia e entrega dirigida das drogas para os alvos cancerígenos (Daghastanli et al., 2004).

QUIMIOTERAPIA

As drogas anti-cancerígenas são transportadas pela circulação para quase todas as partes do corpo. Podem matar células cancerosas onde quer que estejam, sendo úteis no tratamento de cânceres que se espalharam do seu tumor original (metástase). Utiliza-se drogas no combate ao câncer para tentar destruí-lo completamente, erradicando qualquer vestígio residual deixado após cirurgia ou radioterapia, ou ainda, diminuindo o tumor para facilitar esses tratamentos.

Existem duas categorias principais de drogas usadas para tratar o câncer: quimioterápicas (citotóxicas) e hormonais (endócrinas). Freqüentemente, a quimioterapia tem um efeito significativo em células normais, bem como, em células cancerosas, resultando em diversos efeitos colaterais. Os tratamentos hormonais são bem mais suaves, porém, a sua aplicação é limitada a cânceres de mama e próstata. Entretanto, a quimioterapia é ativa contra uma variedade mais ampla de cânceres e também tende a agir mais rápido. O tratamento com quimioterapia visa matar células cancerosas e evitar efeitos colaterais intoleráveis.

A maioria das quimioterapias envolve a combinação de drogas para reduzir a possibilidade de fracasso devido à resistência do tumor. Podem ser utilizadas drogas que interferem em diferentes estágios da mitose. Uma vez bem sucedido o tratamento para inibir a divisão celular, o tumor não crescerá, e as suas células morrerão por envelhecimento, sem serem repostas. Para minimizar os efeitos colaterais do tratamento quimioterápico, pode ser administrada doses mais baixas (Wood et al., 1996).

DROGAS NITROHETEROCÍCLICAS (DNHC)

Um grande número de compostos heterocíclicos vêm sendo empregado para fins medicinais, como antibióticos, agentes antifúngicos e antiparasitários. Os mais utilizados são os derivados de 5-nitroimidazol, 5-nitrofurano e 1-nitroacridina. Essas drogas possuem alta atividade citostática e radiosensibilizante sobre as células cancerígenas *in vitro* (Franko, 1986). *DNHC* fluorescentes podem também servir como marcadores moleculares potenciais permitindo a seleção de células tumorais em frações derivadas de regiões aeróbicas e anaeróbicas (Hay et al., 1995). Alguns problemas limitam a aplicação de DNHC no tratamento do câncer, incluindo: 1) não satisfatória atividade terapêutica *in vivo* e alta citotoxicidade *in vitro*; 2) efeitos colaterais; 3) baixa solubilidade em soluções aquosas. Embora a aplicação de *DNHC* no tratamento do câncer no momento seja limitada, estas drogas continuam a despertar um grande interesse de pesquisadores que, recentemente, descreveram a síntese de novas DNHC (Wood et al., 1996; Rauth et al., 1998; Viode et al., 1999)

A família dos derivados do 5-nitrofuran-ethenyl-quinolina, que inclui o Quinifuryl, foi sintetizada no início dos anos 70 pelo Dr. N. M. Sukhova no Instituto de Síntese Orgânica da Academia de Ciências da Letônia, com o intuito de ser utilizado como agente anti-tumoral. O Quinifuryl foi escolhido para a realização deste estudo pelas seguintes razões:

a) é altamente tóxico para diversas linhagens de células tumorais (Degterev, 1991; Buzukov & Degterev, 1995), inclusive sobre as linhagens que dificilmente são tratadas com quimioterapia, como melanoma B16 e eritroleucemia

humana K562 (Verovskiy et al., 1990; Degterev et al., 1991; Rossa et al., 2003; Daghastanli et al., 2004);

b) é fotolábil e produz intermediários reativos do oxigênio e nitrogênio durante a fotodecomposição (Smirnov et al., 1989 e 1989a; Tatarskaya et al., 1989; Borisevich & Degterev, 1992; Borisevich et al., 2003), o que leva a célula cancerígena atacada a um estresse oxidativo, causado pela alta citotoxicidade na luz, que é maior que a citotoxicidade da droga no escuro (Daghastanli et al., 2004 e 2004a).

c) o monitoramento da decomposição metabólica e fotolítica da droga foi desenvolvido em trabalhos anteriores (Degterev et al., 1999; Borissevich et al., 2003), facilitando os estudos de cinética do decaimento fotolítico e a formação de produtos e de intermediários reativos, possibilitando o estudo dos mecanismos da toxicidade.

d) a atividade do Quinifuryl ainda não foi completamente caracterizada, em contraste com a Nitracrina, que é um candidato à agente anticancerígeno ainda sem aplicação prática (Gniazdowski et al., 1995; Wilson et al., 1986; Gorleuska et al., 2001).

A Nitracrina, pertencente ao grupo dos derivados de 1-nitro-9-aminoacridina, foi sintetizada por um grupo de químicos Poloneses liderados pelo Dr. Andjei Ledokhowsky no início dos anos 60, sendo um composto que apresenta satisfatória atividade citotóxica e propriedades antitumorais (Degterev et al., 1986; Wilson et al., 1986). A Nitracrina foi escolhida para a realização deste estudo para, sendo uma droga promissora para uso clínico, servir de referência para compararmos com os dados obtidos com o Quinifuryl.

Desenvolvendo a idéia de uso prático das DNHC na terapia dos cânceres e de algumas outras doenças graves, iniciamos estudos pioneiros de fototoxicidade destas drogas contra os alvos cancerígenos. Visando o uso prático das DNHC na terapia no escuro e na fototerapia, começamos os estudos de aplicação tópica e/ou de entrega dirigida das mesmas.

FOTOTERAPIA

A fototerapia baseia-se na introdução de um agente fotossensível (geralmente um corante) para os tecidos patogênicos (Foot, 1990) e, consequentemente, a exposição de tais tecidos à luz senssibilizante. O mecanismo de ação terapêutico consiste na excitação do corante por meio da irradiação de luz (Handerson & Douguerty, 1992), com isso, o corante transfere a energia de excitação para a molécula de oxigênio, gerando oxigênio singlet ($^1O_2$) e outros radicais livres, acarretando em danos irreparáveis no tecido-alvo (Sobolev et al., 2000).

A maioria dos agentes fotosensibilizantes são distribuídos e acumulam-se em tecidos normais e neoplásicos (Chan et al, 1998). No entanto, a distribuição da droga em tecidos tumorais ainda não foi bem definida, sendo este um dos aspectos não esclarecidos da terapia fotodinâmica. Sabe-se que a absorção da luz pelo agente fotosensibilizante pode limitar a sua penetração no tecido, este fenômeno é chamado de “self-shielding” (Foot, 1990). Muitos sensibilizantes são propensos à auto-destruição durante a exposição à luz, um processo chamado “photo-bleaching” (Handerson & Douguerty, 1992). A luz visível com comprimento de onda maior que 600 nm é preferível na fototerapia devido a sua penetração ser mais profunda nos tecidos.

Gradualmente, os métodos de tratamento vêm diversificando-se, e sendo aplicados no tratamento de doenças auto-imunes (Moan et al., 1992; Kick et al., 1996; Bethea et al., 1998), e em outras causadas por agentes microbianos (Dall'Amico et al., 1996). Experiências sucessivas foram realizadas com diferentes drogas, incluindo as nitroheterocíclicas (Adams & Stratford, 1994; Bremner et al.,

1994), o que aumentou o arsenal terapêutico de substâncias usadas em fototerapia. Vários experimentos foram realizados usando luz com $\lambda \geq 400$ nm (Yoshimura et al., 1996; van Iperena et al., 1997; Wainwright et al., 1999). Existem evidências de que o oxigênio singlete, junto ao ânion superóxido (O_2^-), são as espécies mais danosas em fototerapia, sugerindo que os efeitos da fototerapia são oxigênio-dependentes (Foot, 1990; Handerson & Douguerty, 1992). Em normoxia, os danos celulares mediados pelo O_2 ocorrerão próximos ou não aos sítios de geração, e podem afetar virtualmente todos os componentes celulares (Sobolev et al; 2000). Os efeitos da fototerapia nas células envolvem foto-oxidação de membranas, alterando a permeabilidade celular, perda de fluido e inativação de sistemas de transporte enzimáticos e de receptores, inibição de enzimas reparadoras de DNA, inativação de enzimas mitocondriais (o que é considerado um evento-chave na letalidade celular pela fototerapia), destruição de lisossomos, severos danos ao DNA e a membrana nuclear, perda da integridade celular e finalmente, a liberação de fatores de necrose de tumor e danos vasculares (Handerson & Douguerty, 1992; Jori, 1996).

O primeiro passo para se tratar um tumor pela fototerapia consiste em introduzir a droga no organismo por meio de um sistema de entrega dirigida do agente fotossensibilizante ao tecido alvo; ou seja, a administração da droga e a sua distribuição pelas células e tecidos. No segundo passo, o agente fotossensibilizante acumulado no tecido alvo é exposto à irradiação de luz com comprimento de onda apropriado para penetrar até o tecido e ser absorvido pela droga. A fluência da luz pelos tecidos decresce exponencialmente com a distância,

a profundidade de penetração efetiva varia de tecido para tecido (Sobolev et al; 2000).

TRANSPORTE DIRIGIDO

Os obstáculos que limitam a aplicação de drogas DNHC podem ser superados usando-se veículos de transporte dirigido. Embora essa abordagem apresente um grande desenvolvimento durante a última década (Kwona & Okanob, 1996; Kwona, 1998), até o momento não foi utilizada para DNHC. Estes carregadores de drogas visam reduzir a toxicidade causada pela droga livre, preservando as células sadias, uma vez que seus componentes são atóxicos e biodegradáveis. Entre os carregadores, encontram-se micelas que podem ser usadas para transporte de drogas hidrofóbicas em altas concentrações (Yua et al., 1998; Kidchob et al., 1998). Uma vantagem das partículas micelares é a tendência de acumularem-se espontaneamente em tumores sólidos (Chelvi et al., 1995). Outra vantagem é o seu fácil preparo em larga escala e a reprodutibilidade do ensaio. Além disso, a sua peculiaridade estrutural permite que as micelas permaneçam no sangue (ou tecidos) por um longo período de tempo, sem ser reconhecido por imunoglobulinas e /ou células fagocitárias (Sobolev et al; 2000).

Os lipossomos (lipoproteínas artificiais), conhecidos como partículas LDE (*Low Density Emulsion)*, são veículos que podem funcionar para o transporte dirigido de DNHC. Os lipossomos vêm sendo desenvolvidos desde os anos 70, e a sua utilização inclui o uso como carregador de drogas sintéticas para o tratamento de combate ao câncer e vacinas lipossomais para uso clínico em humanos (Gregoreadis, 1995).

Sabe-se que as células tumorais têm até 100 vezes mais receptores de LDL que as células normais, assim, os lipossomos tendem concentrar-se em células

mais vascularizadas, típicas dos tumores, como carcinoma e melanoma de camundongos e leucemia humana (Sobolev et al., 2000). O uso de lipossomos ligados com os anticorpos monoclonais aumenta a possibilidade de sucesso do transporte dirigido para os alvos cancerígenos (Park et al., 1997). Até o momento esta abordagem não foi utilizada para DNHC. A utilização de veículos de transporte permite a administração de doses até dez vezes superior a dose máxima normalmente usada, com toxicidade mínima, o que é particularmente interessante na terapia com DNHC.

OBJETIVOS

Visando aumentar o uso clínico de compostos nitroheterocíclicos e ampliar o arsenal terapêutico para o tratamento do câncer, o presente trabalho tem como objetivos:

1) Estudar os mecanismos de citotoxicidade de DNHC sobre células cancerígenas.

2) Desenvolver uma abordagem da Terapia Fotoquímica para DNHC.

3) Imobilizar as DNHC em lipossomos e micelas.

MATERIAIS E MÉTODOS

Drogas.

O Quinifuryl (M-106), 2-(5'-nitro-2'-furanyl)ethenyl-4-{N-[4'-(N,N-diethylamino)-1'-methylbutyl] carbamoyl} quinoline, é um derivado do 5-nitrofuril-etenil-quinolina. Foi sintetizado pelo Dr. N. M. Sukhova (Instituto de Síntese Orgânica da Academia de Ciências de Riga, República da Lituânia). A Nitracrina (Ledakrina, C-283), 1-nitro-9'(3'3'-dimethylaminopropylamino) acridina adquirida de Polfa (Polônia), foi sintetizada por um grupo de químicos Poloneses liderados pelo Dr. Andjei Ledokhowsky. Ambas as drogas foram cedidas pelo Prof. Dr. Igor A. Degterev (Depto. de Fisiologia/CCBS/UFSCar).

As soluções de estoque 40 mM e 20 mM para o Quinifuryl e para a Nitracrina, respectivamente, cujos tampões foram preparadas em água Milli-Q (Millipore), pH 7,0. A autenticidade estrutural de ambas as drogas foi verificada por análises de ressonância magnética nuclear (RMN). A fórmula estrutural de ambas as drogas são mostradas nos esquemas 1A e 1B.

Tecidos biológicos.

As células de fibroblastos embrionários de camundongo NIH3T3, as células de eritroleucemia humana K562 e as células de linfoleucemia de camundongos P388 foram usados, para avaliar citotoxicidade de drogas livres e encapsuladas. As células P388 foram cultivadas em meio Fisher suplementado com 10% de soro fetal bovino (FBS) em frascos de 175 cm^2 a 37ºC com 5% de CO_2. As células

NIH3T3 e K562 foram cultivadas em Dulbecco's Modified Eagle's Medium (DMEM) suplementado com 10% de soro fetal bovino (FBS), 1% L-glutamina, 50 unid/ml penicilina, 50 mg/ml streptomicina e 250 mg/ml anfotericina-B em frascos de 175 cm^2 em um incubador (CellStar, USA) a 37ºC com 5% de CO_2. As células P388 foram obtidas do American Type Culture Collection (ATCC Nº CCL46) e cedidas pelo Departamento de Química/FFCLRP/USP (Prof. Dr. Antonio C. Tedesco).

O número de células em suspensão foi calculado utilizando-se uma câmara de Neubauer (0,0025mm^2). As densidades semeadas variaram de 2×10^4 a 6×10^4 células/ml. A viabilidade foi avaliada pelo método de contagem com *Trypan Blue* que é o método de exclusão do corante. O método recebe este nome porque este corante não passa pela membrana das células vivas, ligando-se apenas aos fragmentos de células mortas (Freshney, 1994). Estas medidas foram feitas no início de cada experimento, sendo a exclusão sempre superior a 96%.

Testes de citotoxicidade

Os testes de citotoxicidade das drogas foram feitos baseados na metodologia (Freshney, 1994) adaptada para nossos fins. Os testes foram baseados no ensaio com MTT e realizados de dois modos: medindo-se tanto o efeito letal direto da droga (Teste 1) ou o efeito tóxico geral que inclui a contenção da proliferação celular (Teste 2) (Rossa et al., 2003). O sal tetrazolium 3-(4,5-dimethylthiazol-2-yl)-2-5 diphenyl tetrazolium bromide (MTT) é reduzido nas células viáveis para produzir um produto colorido que pode ser interpretado como uma medida de viabilidade (Mosmann, 1983).

Para os ensaios com MTT, as células foram semeadas em meio DMEM contendo 5% de FBS em placas tipo ELISA com 96 poços. As placas foram semeadas com aproximadamente 10^4 células por poço em colunas de seis poços cada e expostas a uma gama de diferentes concentrações de droga de 0,02 a 2 nmol/ml (para Nitracrina) ou 0,2 a 20 nmol/ml (para Quinifuryl), por intervalos de tempo que variaram de zero a 24 horas (nos experimentos no escuro) ou de 10 a 90 minutos (nos experimento sob iluminação).

As colunas foram divididas em grupos controle e experimento. Os grupos de experimento foram divididos em conjuntos de seis poços cada, de acordo com o tempo de incubação, que geralmente variaram de zero a noventa minutos de incubação nos experimentos sob iluminação ou de zero a 24 horas em experimentos no escuro. Em experimentos feitos no escuro, os grupos de controle continham células sem droga (geralmente duas colunas de seis poços, ver figura pág. 25). Em experimentos feitos sob irradiação, os grupos de controle continham células com droga não irradiadas e células sem drogas irradiadas, pelo mesmo período de tempo.

As placas foram centrifugadas logo após a incubação a 3700 rpm (centrífuga Eppendorf 5804 R com rotor de placas A-2-DWP) e o sobrenadante foi vertido. Nos poços foi adicionado corante tetrazolium amarelo (MTT), que é reduzido a um produto (cristais de formazan) de cor púrpura somente pelas células vivas (que é um indicativo da integridade mitocondrial e, portanto, da integridade celular) e incubado durante 3 horas no escuro. Após este período, as placas foram novamente centrifugadas e o sobrenadante foi novamente descartado. O corante precipitado foi diluído em dimetilsulfóxido (DMSO) e a

leitura de absorbância foi feita em Leitor de Placas Dynex MRX (Dynex Technologies Inc.) a 570 nm.

No final do período de exposição às drogas, as placas foram centrifugadas a um preciptado de células e o sobrenadante contendo a droga foi descartado e substituído tanto por MTT dissolvido em DMSO (Teste 1) ou por meio de cultura fresco (Teste 2). Neste segundo caso, as células foram incubadas por um período adicional (2-3 vezes o tempo de duplicação da população) que variou de 36 a 72 horas, dependendo da linhagem celular trabalhada, com o meio trocado diariamente, seguido de ensaio com MTT. Em ambos os testes, as placas com MTT foram incubadas no escuro por 4 horas. Em seguida, os cristais de MTT-formazan insolúveis em água foram dissolvidos em DMSO, e a absorbância foi lida a 570 nm em um leitor de placas ELISA Dynex MRX (Dynex Technologies Inc.).

A visualização deste experimento está na figura abaixo, que mostra uma placa de ELISA no fim do experimento.

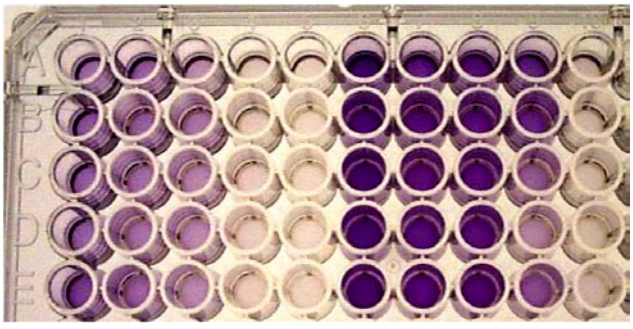

Figura 1: Placa de ELISA corada no experimento de toxicidade durante 24 horas. A distribuição das colunas feita conforme descrito anteriormente.

Irradiação/Fotólise.

A irradiação das placas-teste (contendo células e incubadas com as drogas) foi feita com lâmpada de tungstênio (150 W) e filtro de vidro (5-57 KOPP color glass filter) onde o intervalo de espectro da irradiação ficou entre 360 e 440 nm. A intensidade da radiação foi de 22 mW/cm^2 (medida no Spectra-Physics 407A Radiometer) e o tempo de exposição à luz variou de 0 a 90 minutos. Os experimentos foram realizados a temperatura de 24ºC.

Estudo da incorporação de DNHC em células K562 e metabolismo intracelular destas drogas.

A incorporação das drogas em células K562 foi medida utilizando-se do seguinte procedimento: cada droga foi adicionada à 1ml de suspensão celular ($1x10^6$ céls/ml) em 20mM de tampão Hepes até uma concentração final de 2nmol/ml. As misturas foram incubadas à 37ºC por intervalos de tempo variando entre 0 a 3 horas em contínua agitação em um agitador orbital (Forma Scientific, USA). Após incubação, as células foram centrifugadas a 3700 rpm (centrífuga eppendorff, 5804 R) e repetidamente lavadas até que nenhum espectro da droga pudesse ser detectado no sobrenadante. As células do pellet foram lisadas com solução Triton X-100 (0,5%) em água Milli-Q. O espectro de absorção do lisado preparado das células incubadas com droga foi medido contra o controle de células não-tratadas (que não receberam a droga), mas incubadas sobre idênticas condições, e comparados com os espectros das drogas intactas medidas contra os lisados preparados das células controle.

Carregadores de drogas.

A encapsulação das DNHC foi feita em micelas (estearato de PEG-2000) e lipossomos (distearoilfosfatidilcolina - DSPC).

Micelizando as drogas, misturamos o estearato de PEG-2000 com solução da droga e submetemos à diálise até que a concentração externa à membrana de diálise se estabilizasse. A concentração da droga incorporada em micelas foi medida espectrofotometricamente (400 nm) usando em cubeta de referência uma suspensão de micelas sem droga.

Os lipossomos foram preparados pelo Prof. Dr. Antonio C. Tedesco (Depto. de Química/FFCLRP/USP). Para a preparação, o colesterol e os fosfolipídios (2:1) foram dissolvidos em uma mistura de isobutanol e clorofórmio (10:4) e o solvente orgânico foi removido sob pressão reduzida usando-se um evaporador rotatório (Speed Vac Plus SC210A, Thermo Savant). A fina camada de filme formada foi armazenada a vácuo durante a noite para remover qualquer traço de solvente orgânico e extrudado através de membranas de 0,2 μm usando um extruder “Lipex Biomembrane”. A concentração da droga imobilizada em lipossomos foi medida espectrofotometricamente (400 nm) após solubilização dos mesmos em DMSO, usando em cubeta de referência uma suspensão de lipossomos sem droga.

***Cálculos e Análise Estatística*.**

A dependência da concentração da droga e do tempo na morte celular foram calculados como: Efeito Tóxico (ET); sendo ET = [DC]/[Cel]^{controle}, onde [Cel]^{controle} é a concentração nas placas controle (células incubadas pelo mesmo período sem drogas) e [DC] é a concentração de células mortas. [DC] é calculado como [Cel]^{controle} – [Cel]^{final}, onde [Cel]^{final} é a concentração de células vivas nas placas expostas às drogas (Monks et al, 1991). A concentração de células foi medida usando-se uma curva de calibração feita para a linhagem P388 de células pelo método de coloração com MTT.

O efeito citotóxico (LC_{50}) dos compostos testados foi estimado como:
100 x (D^0 - D) / D^0 = 50; onde D^0 e D são as densidades ópticas das placas teste no tempo zero (quando os compostos foram adicionados) e após a exposição às drogas, respectivamente (Monks et al, 1991).

Os dados são apresentados como a média (±DP) de dois a cinco experimentos com seis séries de medições independentes em cada experimento. As análises estatísticas foram realizadas com o Student's *T-test*, utilizando o programa InStat Software Program for Windows (GraphPads software, San Diego, USA). Os gráficos foram elaborados com o programa Origin Microcal 6.1 (OriginLab software, USA).

ESQUEMA 1A. Estruturas do Quinifuryl e Nitracrina.

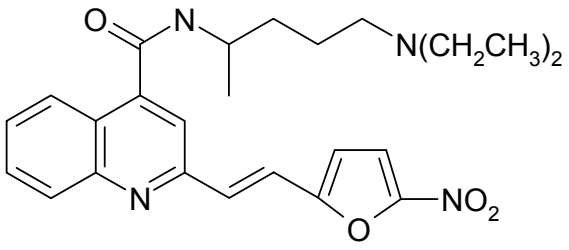

Quinifuryl:

2-(5'–nitro-2'–furanyl) ethenyl-4-{N-[4–(N,N-diethylamino)-1'–methylbutyl] carbamoyl}quinolina.

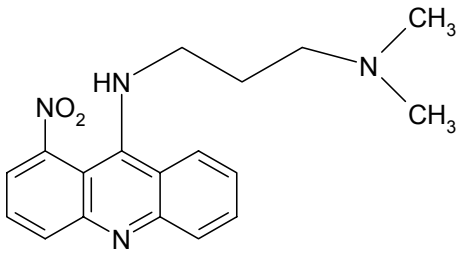

Nitracrina:

1-nitro-9(3'3'- dimethylaminopropylamino)acridina.

ESQUEMA 1B. Estruturas do Quinifuryl e Nitracrina.

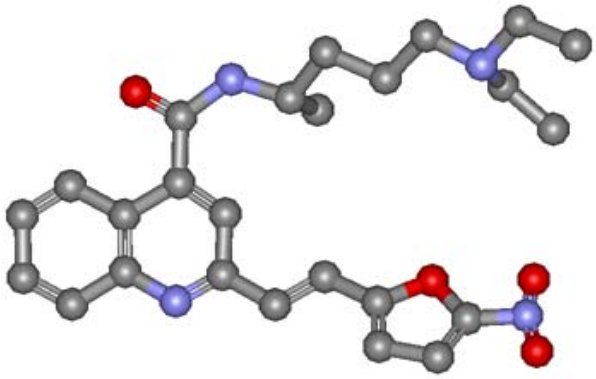

Quinifuryl:

2-(5'–nitro-2'–furanyl) ethenyl-4-{N-[4–(N,N-diethylamino)-1'–methylbutyl] carbamoyl}quinolina.

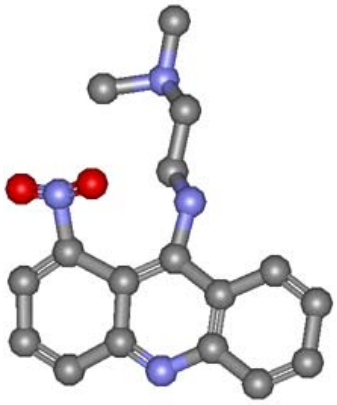

Nitracrina:

1-nitro-9(3'3'- dimethylaminopropylamino)acridina.

RESULTADOS

Citotoxicidade das DNHC no escuro sobre as células tumorais e não-transformadas.

Primeiro determinamos os efeitos tóxicos dose-dependentes de ambas as drogas. Os resultados mostram que a toxicidade da Nitracrina é maior que a do Quinifuryl em todas as concentrações usadas (figura 2). A Nitracrina atingiu o LC_{50} com 0,08 nmol/ml, enquanto o Quinifuryl precisou de 2 nmol/ml para atingir o mesmo valor de morte celular. Os valores dos efeitos tóxicos foram calculados como a proporção entre o número de células que morreram durante incubação com droga e a concentração inicial de células. Células incubadas sem droga serviram como controle em cada série de experimentos.

A tabela 1 mostra que a Nitracrina demonstra uma citotoxicidade significativamente maior que o Quinifuryl para todas as linhagens de células. Os valores de LC_{50} foram calculados baseando-se nos resultados de cinco séries independentes de experimentos com seis repetições das medidas em cada série.

A tabela 2 mostra que ambas as drogas são tóxicas para todas as linhagens de células ($LC_{50} \leq 2$ μM) e requerem menos de 24 horas para atingirem os valores de LC_{50}. Além do mais, a linhagem de células P388 de linfoleucemia de camundongos é mais sensível às duas drogas, quando comparadas à linhagem de células NIH3T3 não-transformadas de camundongos.

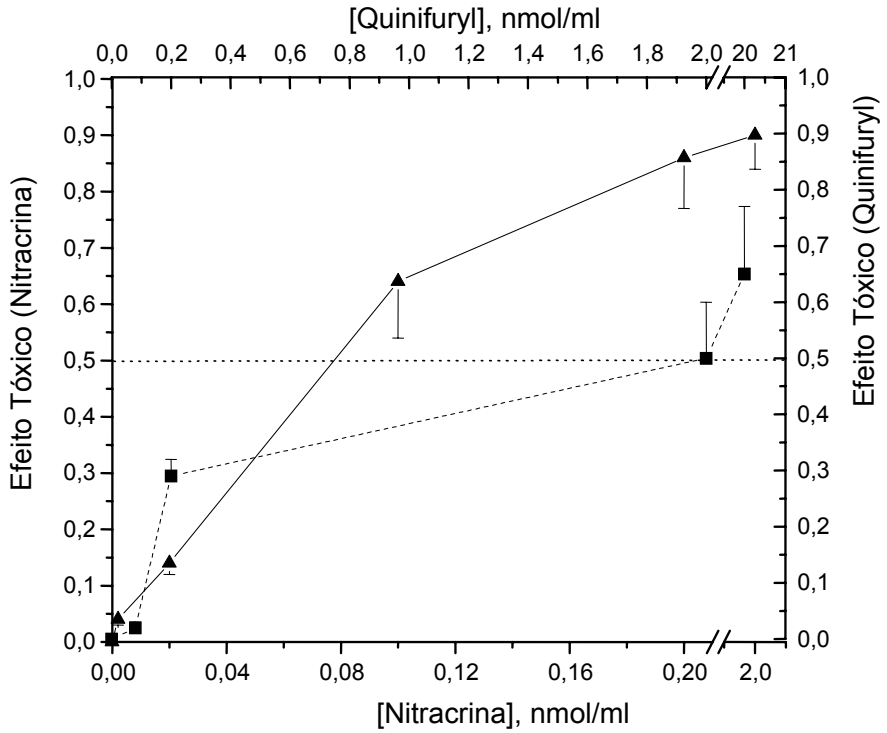

FIGURA 2. Dependência da morte celular de K562 na concentração de Nitracrina (▲) e Quinifuryl (■). Tempo de incubação das drogas nas células: 24 horas.

TABELA 1. Valores de LC_{50} para Quinifuryl e Nitracrina medidos em diferentes períodos de tempo. Cada valor de LC_{50} representa a média (± DP) de cinco séries independentes de experimentos com seis repetições.

Linhagem celular	Droga	Tempo, hs	LC_{50}, µM
K562 céls. leucêmicas	Quinifuryl	24	2 ±0,9
		12	12 ±2,2
	Nitracrina	24	0,12 ±0,07
		6	2,2 ±0,06
P388 céls. leucêmicas	Quinifuryl	24	1,1 ±0,2
	Nitracrina	24	0,16 ±0,06
		6	0,5 ±0,13
NIH3T3 céls. normais	Quinifuryl	24	1,2 ±0,17
		12	11 ±2,1
	Nitracrina	24	0,13 ±0,04
		12	1,4 ±0,2

TABELA 2. Período de tempo requerido para atingir o LC_{50} (τ^{50}) em diversas concentrações de ambas as drogas. Dados referentes às drogas livres representam às médias (± DP) de dois a cinco series independentes de experimentos com cinco ou seis repetições. * Diferenças significantes foram encontradas entre os valores de τ^{50} como se segue: $p < 0.01$ (b vs h, c vs i, e vs h, f vs i), $p < 0.05$ (a vs d, g vs j, b vs e). Nenhuma diferença significante foi observada entre c e f.

Linhagem de Células	Drogas	Concentração (μM)	τ^{50}, horas
K562	Quinifuryl	20	6,5 ±0,6[a]
		2	21 ±2,7[b]
	Nitracrina	2	8,4 ±0,6[c]
NIH3T3	Quinifuryl	20	3,7 ±0,2[d]
		2	16 ±0,2[e]
	Nitracrina	2	8,5 ±0,4[f]
		0,2	17 ±2[g]
P388	Quinifuryl	2	5,3 ±0,7[h]
	Nitracrina	2	3,5 ±0,1[i]
		0,2	12 ±2[j]

Os tempos de incubação requeridos para alcançar os valores de LC_{50} com concentração de 2 μM de ambas as drogas foram 2-3 vezes maiores tanto para NIH3T3 (16 hr e 8,5 hr para Quinifuryl e Nitracrina, respectivamente) como para K562 (21 hr e 8,4 hr para Quinifuryl e Nitracrina, respectivamente), oposto à P388 (5,3 hr e 3,5 hr para Quinifuryl e Nitracrina, respectivamente) como é mostrado na tabela 2. Além disso, os dados presentes na tabela 3 mostram que o efeito tóxico observado após 12 horas de incubação das drogas em células P388 foram significativamente maiores (0,79 e 0,64 para Quinifuryl e Nitracrina, respectivamente) que em células NIH3T3 (0,43 e 0,38 para Quinifuryl e Nitracrina, respectivamente).

Absorção das drogas pelas células tumorais e transformação metabólica intracelular.

Como o Quinifuryl, apesar de sua citotoxicidade *in vitro*, mostrou muito pouco efeito *in vivo* (Degterev et al.,1990), uma possível explicação é seu rápido metabolismo intracelular. Para testarmos esta possibilidade a incorporação de Quinifuryl e Nitracrina em células K562 foi medida. A incorporação intracelular das drogas pode ser visualmente detectada, uma vez que o pellet de células K562 torna-se amarelo brilhante após 10 minutos de incubação com Quinifuryl (a droga é amarelada), enquanto que o pellet das células controle permanece sem coloração. A incubação com Nitracrina resulta em uma mudança de cor do pellet de amarelo para marrom. Após incubação com drogas, o pellet contendo células foi lavado duas vezes e as células foram lisadas. Os diferentes espectros foram

TABELA 3. Efeito tóxico (TE) do Quinifuryl e da Nitracrina observado após 12 horas de incubação das drogas com células apropriadas. O TE foi medido imediatamente após a aplicação da droga (ET_{12}) e após três vezes o tempo requerido para o tempo de duplicação de linhagem celular ($ET_{36/72}$). Cada valor de representa a média (± DP) de uma série de experimentos com seis repetições. Os experimentos seguiram dois procedimentos (Teste 1 e 2) realizados em paralelo.

Droga	Linhagem Celular								
	K562			P388			NIH3T3		
	ET_{12}	ET_{72}	P	ET_{12}	ET_{36}	P	ET_{12}	ET_{72}	p
Quinifuryl, 2 μM	0,47 ± 0,08	0,58 ± 0,05	NS	0,79 ± 0,01	0,89 ± 0,04	< 0,05	0,43 ± 0,16	0,96 ± 0,01	< 0,05
Nitracrina, 0,2 μM	0,63 ± 0,09	0,81 ± 0,06	< 0,01	0,64 ± 0,11	0,88 ± 0,03	< 0,05	0,38 ± 0,1	0,94 ±0,005	< 0,05

lidos contra o conteúdo do meio intracelular das células controle que foram incubadas por 6 horas nas mesmas condições. Os espectros das drogas intactas também foram tirados contra o lisado de células controle para estimarmos o grau de biotransformação da droga.

Cinéticas das mudanças na concentração relativa de Quinifuryl no sobrenadante versus o pellet celular são mostradas na figura 3. O balanço foi calculado como soma da concentração de droga da mistura incubada e do lisado celular. Nossas tentativas de medir o balanço da Nitracrina falharam por causa do coeficiente de extinção muito baixo deste composto quando comparado ao do Quinifuryl (3,9 $mM^{-1}. cm^{-1}$ e 26,2 $mM^{-1}.cm^{-1}$, respectivamente).

A figura 4 mostra a dinâmica das mudanças do espectro no lisado de células K562 após a incubação com Quinifuryl (Painel A) ou Nitracrina (Painel B) em diferentes períodos de tempo. A absorção específica do Quinifuryl (396 nm) aumentou pelos 30 minutos iniciais após a adição da droga e depois começa a decrescer com o tempo. Esta perda de droga corresponde com o aparecimento de um mínimo próximo a 248 nm e de um pico a 276 nm, que corresponde à posição do mínimo no mesmo comprimento de onda observado no espectro da droga intacta.

Após os primeiros 10 minutos de incubação com Nitracrina, diferenças no espectro do conteúdo celular mostrou o aparecimento de um pico a 410 nm e um correspondente mínimo a 430 nm com valores flutuando entre $\Delta A^{409-430}$,que varia por 6 nm em comparação com a droga intacta. Após 1 hora de incubação, entretanto, dois novos picos aparecem no espectro a 573 nm e 627 nm com

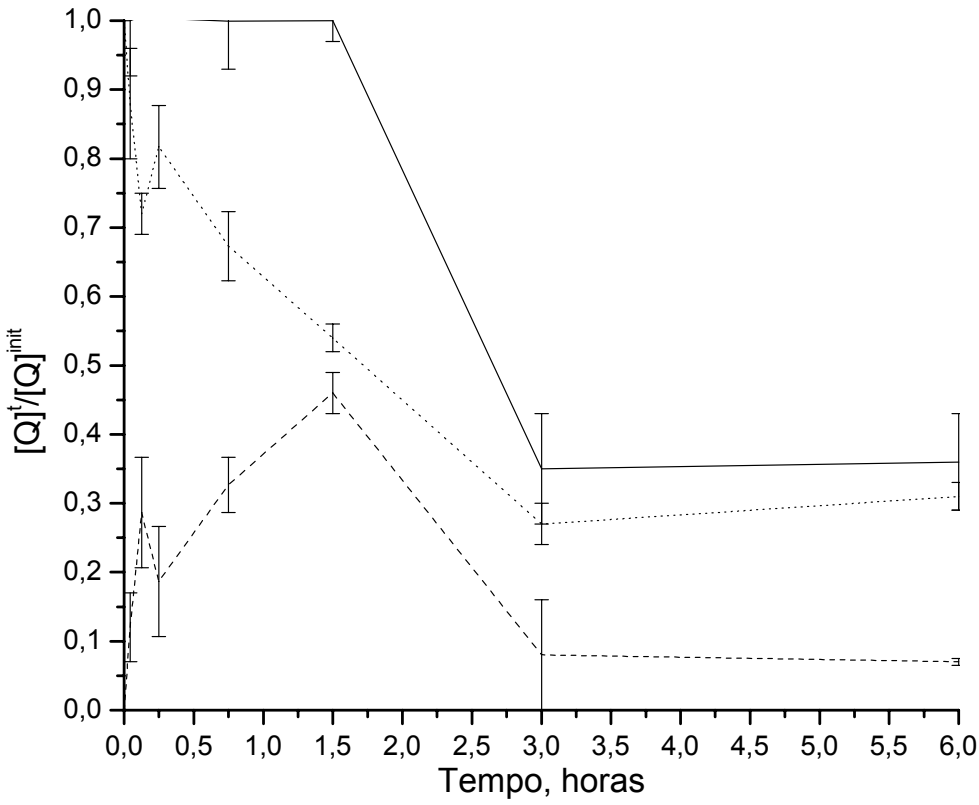

FIGURA 3. Cinética das mudanças da absorbância específica do Quinifuryl à 396 nm durante a incubação da droga com células K562 no sobrenadante (linha pontilhada), no conteúdo celular (linha tracejada), e balanço (linha sólida). $A_r = A^i/A^0$, onde A^0 e A^i – intensidades destes picos antes e durante a incubação da droga. Balanço - $A^i_s + A^i_c/A^0$, onde A^i_s e A^i_c são absorbâncias descobertas no sobrenadante e no conteúdo celular, respectivamente. Dados representam a média (± DP) de três medições.

absorção relativa e absoluta variáveis. Sobretudo, mudanças espectrais mostradas na figura 4 refletem uma substancial biotransformação de ambas as drogas no interior de células K562.

Fotocitotoxicidade das DNHC sobre as células tumorais e não-transformadas.

Um exemplo da citotoxicidade da droga medida é apresentado na figura 5 que mostra o desenvolvimento do efeito tóxico sobre células de eritroleucemia humana K562 como uma função do tempo de incubação celular com droga tanto sob iluminação com luz visível (Painel A) quanto no escuro (Painel B). Os valores do efeito tóxico foram calculados como descrito em *Materiais e Métodos*. Células incubadas sem droga serviram como controle em cada série de experimentos. Normalmente, nenhuma diferença significante nas taxas de células mortas foi observada nas placas controle até incubação de 24 horas no escuro e até 1,5 horas de iluminação.

Ambas as drogas foram muito mais citotóxicas sob iluminação que no escuro. A morte de 50% das células foi atingida sob iluminação em 45 minutos e 48 minutos para 2 nmol/ml de Quinifuryl e para 0,2 nmol/ml de Nitracrina, respectivamente (figura 5A), enquanto no escuro levou 8.4 horas para Nitracrina e 18,5 horas para o Quinifuryl (figura 5B). Nitracrina apresenta maior citotoxicidade que o Quinifuryl tanto no escuro quanto sob iluminação. Tanto que concentrações 10 vezes menor de Nitracrina produzem o mesmo efeito tóxico (sob iluminação, figura 5A) ou maior (no escuro, figura 5B) contra células K562 que o Quinifuryl.

A tabela 4 mostra que os valores de LC_{50} observados após 1 hora de iluminação foram mais baixos, comparados aos experimentos no escuro. Todas as linhagens de células mostraram-se mais sensíveis a Nitracrina, comparada ao Quinifuryl, tanto no escuro quanto sob iluminação.

Parte dos dados experimentais foram obtidos seguindo-se o Teste 1 e o método de coloração com MTT foi realizado imediatamente após o tratamento com droga. Esta abordagem limita os resultados observados apenas ao efeito de morte direta da droga. O efeito de morte direta (Teste 1) e o efeito tóxico geral (Teste 2) de ambas as drogas contra três linhagens de células medidos em paralelo estão presentes na tabela 5. Os experimentos de morte celular (Teste 1) e de toxicidade geral (Teste 2) foram realizados em paralelo, onde uma placa foi submetida à medição do efeito tóxico imediatamente após a adição da droga (Teste 1) e na segunda placa, as drogas foram substituías por meio de cultura completo e as células foram levadas para se proliferarem por 2-3 vezes o tempo de duplicação da população que foi de 72 horas (K562 e NIH3T3) ou 36 horas (P388). A tabela 5 confirma novamente que todas as células são mais sensíveis a Nitracrina, comparada com o Quinifuryl. Os valores de LC_{50} observados após uma hora de iluminação não foram significativos, comparados aos experimentos no escuro (teste 2).

Sendo aplicadas em mesma concentração, ambas as drogas matam células mais rapidamente quando iluminadas com luz visível. A tabela 6 mostra os tempos de incubação requeridos para se atingir a morte de 50% das células em diferentes concentrações tanto no escuro quanto sob iluminação com luz visível.

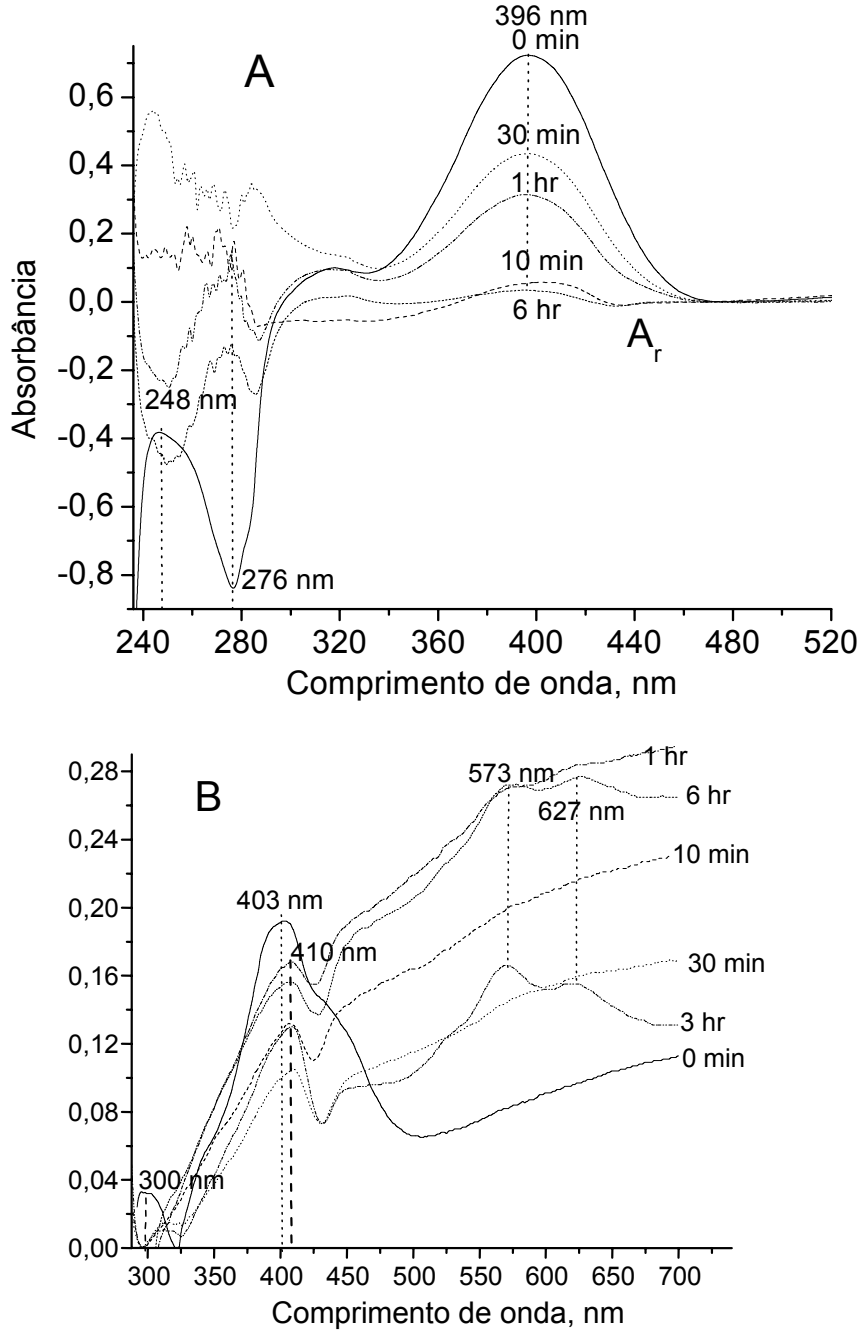

FIGURA 4. Espectro de absorção do conteúdo de células K562 após incubação com Quinifuryl (A) e Nitracrina (B). Diferenças no espectro de absorção do conteúdo de células K562 após incubação com Quinifuryl (A) e Nitracrina (B) para vários períodos, seguidos de lavagem e lise celular. Linhas sólidas representam o espectro das respectivas drogas antes da incubação com células. Todos os espectros foram lidas contra o conteúdo de células intactas que foram incubadas em paralelo sem nenhum aditivo. Cada medição representa a média (±DP) de três repetições das séries.

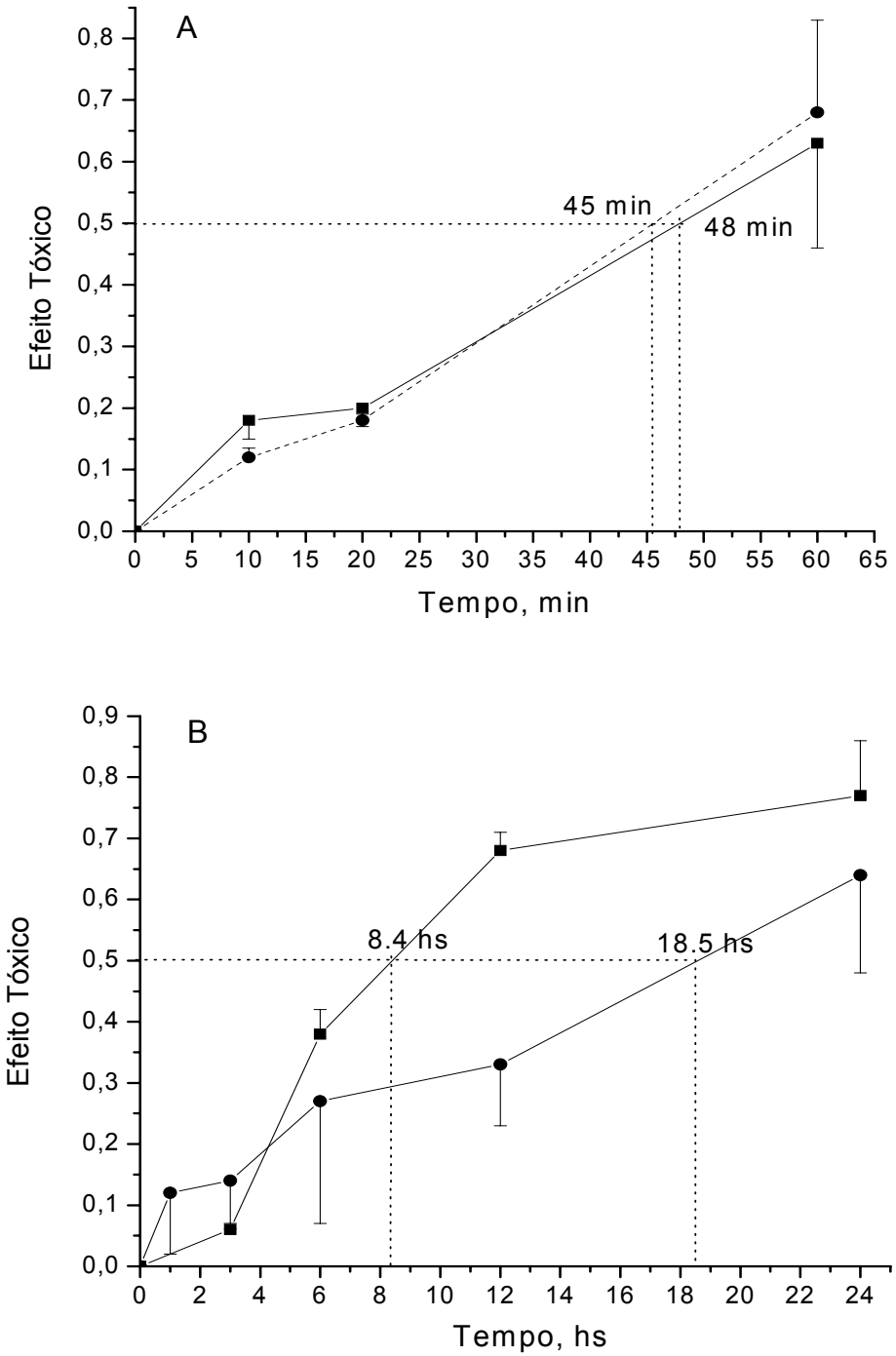

FIGURA 5. Fototoxicidade (A) e toxicidade no escuro (B) do Quinifuryl (●) e da Nitracrina (■) contra células de eritroleucemia humana K562 medidas pelo método de coloroção com MTT. Linhas pontilhadas verticais mostram o tempo requerido para alcançar a morte de 50% das células. As concentrações de droga foram como se segue: Quinifuryl – 2,0 μM; Nitracrina – 0,2 μM. O efeito tóxico foi medido como $[DC]/[Cel]^{controle}$, onde $[Cel]^{controle}$ é a concentração de células, nas placas controle (células incubadas pelo mesmo período de tempo sem drogas) e [DC] é a concentração de células mortas. Cada ponto representa a média (±DP) de seis experimentos.

TABELA 4. O LC_{50} para o Quinifuryl e para a Nitracrina foram medidos após 12 horas de incubação das células no escuro ou sob iluminação com luz visível por 1 hora. Cada valor de LC_{50} representa a média (± DP) de cinco séries independentes de experimentos com seis repetições.

Droga	**LC_{50}, µM**	
	Escuro	Iluminação
	Células P388	
Quinifuryl	79,7 ±18,1	11,8 ±3,8
Nitracrina	7,7 ±1,3	0,23 ±0,15
	Células NIH3T3	
Quinifuryl	18,6 ±6,0	1,6 ±0,7
Nitracrina	16,2 ±2,8	0,6 ±0,6
	Células K562	
Quinifuryl	*15,4 ±2,4	1,48 ±0,33
Nitracrina	*8,9 ±0,8	0,16 ±0,04

TABELA 5. Efeito da morte direta (Teste 1) e da toxicidade geral (Teste 2) do Quinifuryl e da Nitracrina contra células P388 tanto no escuro quanto sob iluminação com luz visível. Em cada coluna, o símbolo (*) marca a diferença estatisticamente significante ($p < 0,01$) entre os resultados do Teste 1. Nenhuma diferença significante foi observada entre o Teste 2 no escuro e sob iluminação em cada série de experimentos. Cada valor amostrado representa a média (± DP) de cinco séries independentes de experimentos com seis repetições.

Droga	[Droga], μM	**EFEITO TÓXICO**			
		Escuro, 12 h		Iluminação, 1h	
		Teste 1	Teste 2	Teste 1	Teste 2
		Células P388			
Quinifuryl	2,0	*0,48 ±0,1	0,97 ±0,16	*0,76 ±0,27	0,93 ±0,20
	0,2	*0,014±0,002	n. m.	*0,13 ±0,04	0,84 ±0,24
Nitracrina	0,2	0,59 ±0,2	0,97 ±0,15	*0,64 ±0,17	0,99 ±0,26
	0,02	*0,14 ±0,05	n. m.	*0,49 ±0,13	0,97 ±0,26
		Células NIH3T3			
Quinifuryl	2,0	*0,59 ±0,13	0,96 ±0,01	*0,43 ±0,16	0,93 ±0,04
	0,2	*0,0 ±0,06	0,0 ±0,12	*0,35 ±0,12	0,87 ±0,12
Nitracrina	2,0	0,56 ±0,1	0,96 ±0,15	n. m.	0,89 ±0,20
	0,2	*0,38 ±0,1	0,94 ±0,01	*0,65 ±0,14	0,89 ±0,12
	0,02	*0,25 ±0,03	0,89 ±0,2	*0,41 ±0,11	n. m.
		Células K562			
Quinifuryl	2,0	*0,33 ±0,1	n. m.	*0,68 ±0,15	n. m.
Nitracrina	0,2	0,63 ±0,03	n. m.	0,68 ±0,17	n. m.

TABELA 6. Tempo para atingir a morte de 50% das células (τ^{50}). Cada valor de representa a média (± DP) de cinco séries independentes de experimentos com cinco ou seis repetições.

Droga	[Droga], μM	**τ_{50}, min**	
		Escuro	Iluminação
Células P388			
Quinifuryl	20,0	231 ±51	25 ±7
	2,0	350 ±118	76 ±9
	0,2	1540 ±90	96 ±11
Nitracrina	0,2	390 ±179	76 ±9
	0,02	431 ±43	97 ±13
Células NIH3T3			
Quinifuryl	2,0	408 ±67	34 ±18
	0,2	> 500	56 ±17
Nitracrina	0,2	191 ±13	31 ±15
	0,02	622 ±115	58 ±28
Células K562			
Quinifuryl	2,0	n. m.	45 ±5
Nitracrina	0,2	n. m.	48 ±7

Entrega dirigida das DNHC.

Abordagens sobre a entrega dirigida das DNHC são extremamente úteis para uso clínico destas drogas no tratamento quimio-terapêutico do câncer, bem como na terapia fotoquímica do mesmo devido ao consumo intenso das mesmas em tecidos sadios e aos danos causados para o organismo-hospedeiro dos tumores.

Procuramos as condições propícias para entrega dirigida das DNHC aos alvos cancerígenos. Nesta etapa testamos micelas de PEG-2000-estearato e de lipossomos unilamelares distearoilfosfatidilcolina (DSPC) como os possíveis carregadores destas drogas.

Os resultados mostram que as drogas nitroheterocíclicas (Quinifuryl e Nitracrina) podem ser imobilizadas em micelas e lipossomos e entregues com sucesso às células cancerígenas causando a morte das mesmas. Os resultados são apresentados como a dependência de efeito tóxico no tempo de incubação das células com as drogas e estamos comparando os intervalos de *tempo necessário* para causar morte de 50% das células (τ^{50}).

Os resultados apresentados na figura 6 mostram que as micelas protegem as células de leucemia de camundongos (P388) contra a toxicidade do Quinifuryl em concentrações baixas. Ao contrário, a Nitracrina pura e imobilizada em micelas em concentração de 2 nmol/ml mostrou mesma toxicidade sob estas células, enquanto em baixa concentração (0,2 nmol/ml), droga imobilizada foi significativamente mais tóxica, tanto que foi preciso 5,6 horas para matar 50% das células contra 12,7 horas para a droga livre (figura 7).

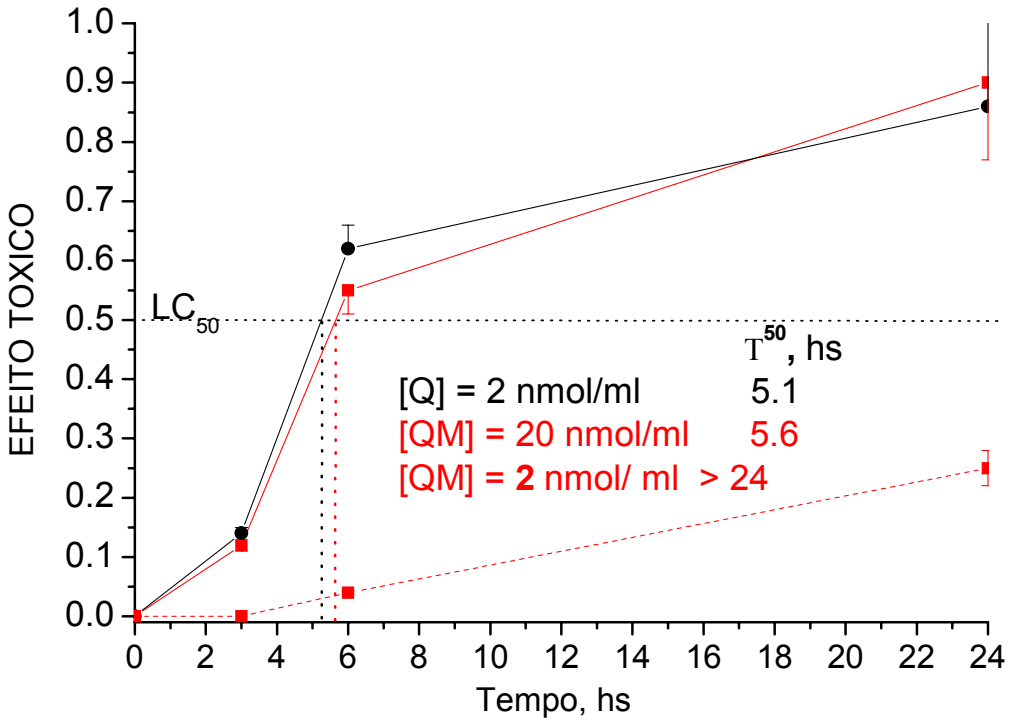

FIGURA 6. Citotoxicidade no escuro de Quinifuril puro (preto) e imobilizado em micelas de PEG-2000-estearato (vermelho) contra células P388. Cada ponto representa a média (± DP) de três experimentos.

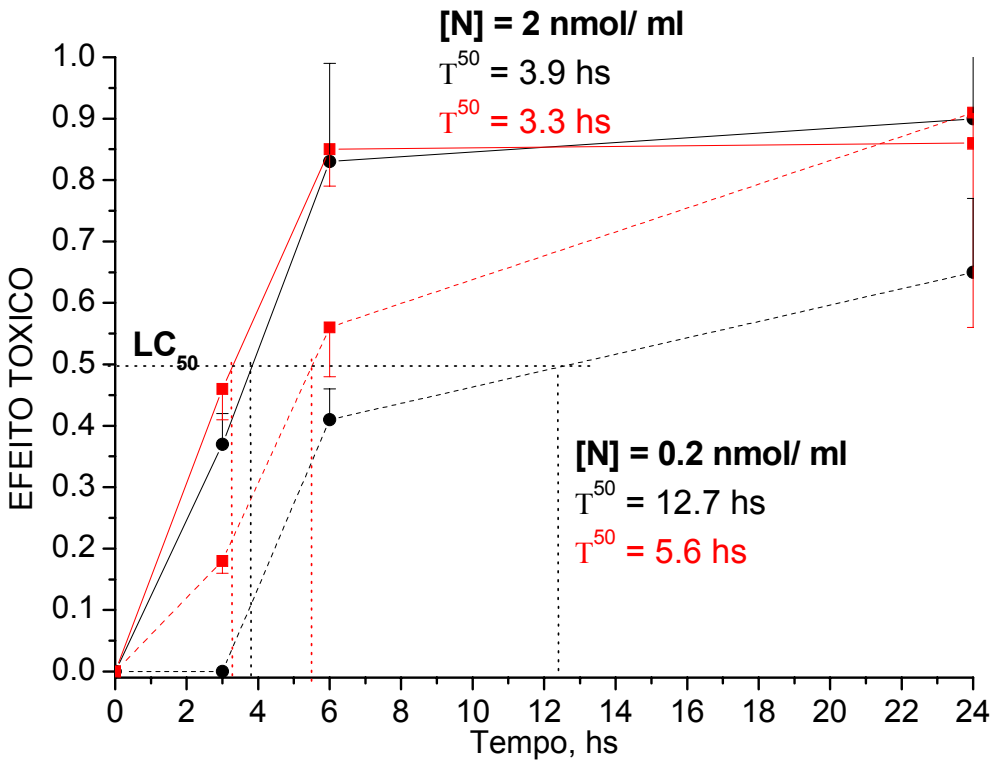

FIGURA 7. Citotoxicidade no escuro da Nitracrina pura (preto) e imobilizada em micelas em PEG-2000-estearato (vermelho) contra células P388. Cada ponto representa a média (± DP) de três experimentos.

Os experimentos feitos com Nitracrina imobilizada em micelas contra as células de eritroleucemia humana (K562) e fibroblastos não-transformadas de camundongo (NIH3T3) estão apresentados nas figuras 8 e 9, respectivamente. Parece que as micelas aumentam a toxicidade da Nitracrina contra as células K562, diminuído os valores de τ^{50} (figura 8), mas não alteram este parâmetro sobre os fibroblastos NIH3T3 (figura 9).

Os resultados dos primeiros experimentos com uso dos lipossomos DSPC estão apresentados nas figuras 10-12. Os resultados mostram que ambas drogas continuam a ser tóxicas quando imobilizadas em lipossomos contra todas as linhagens de células estudadas (figuras 10 e 11) e que o efeito tóxico depende de concentração da droga (figura 12). A figura 10 mostra que o tempo necessário para a Nitracrina lipossomizada atingir o LC_{50} de células K562 e NIH3T3 foi de 8,8 horas, enquanto que para células P388 foi de 7,9 horas. A figura 11 mostra que o Quinifuryl imobilizado em lipossomos continua a ser tóxico contra todas as linhagens de células estudadas, e o tempo necessário para atingir o LC_{50} foi de 21 horas para K562, 17 horas para NIH3T3 e 20 horas para P388. A figura 12 mostra a citotoxicidade da Nitracrina lipossomizada contra células P388 em concentrações que variaram de 1,6 nmol/ml a 0,02 nmol/ml.

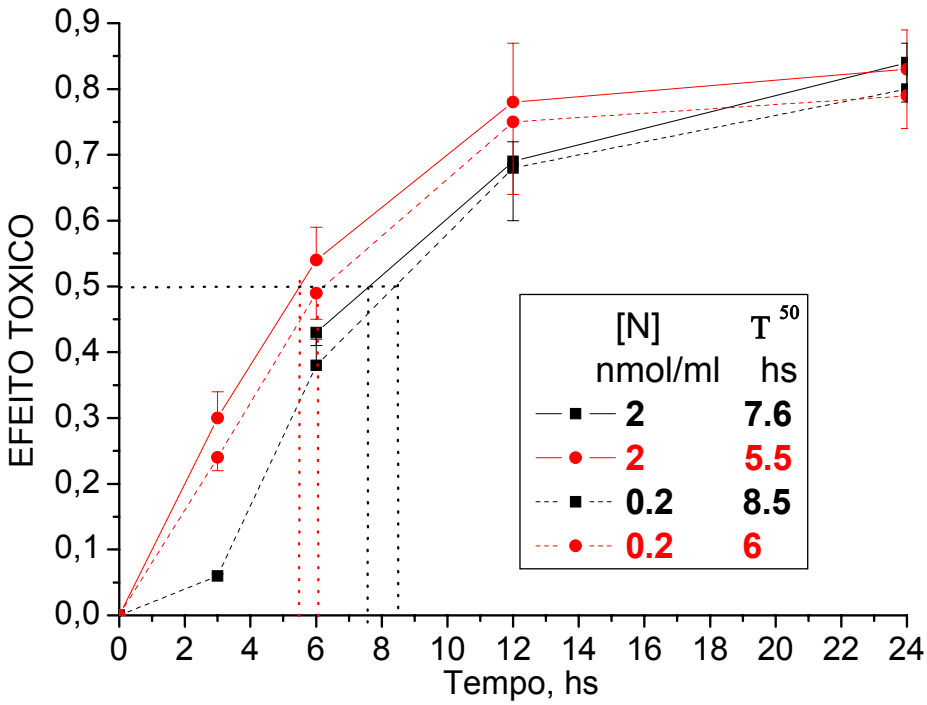

FIGURA 8. Citotoxicidade no escuro de Nitracrina pura (preto) e imobilizada em micelas em PEG-2000-estearato (vermelho) contra células K562. Cada ponto representa a média (± DP) de três experimentos.

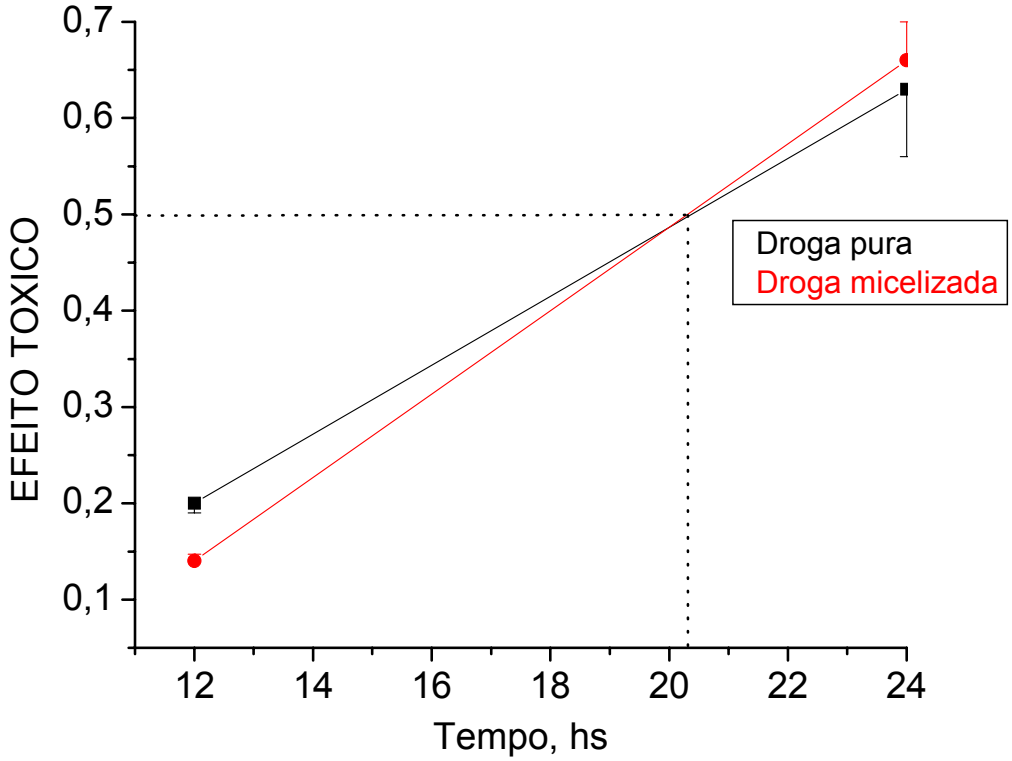

FIGURA 9. Citotoxicidade no escuro de Nitracrina pura (preto) e imobilizada em micelas em PEG-2000-estearato (vermelho) contra as células de fibroblasto (NIH3T3). Cada ponto representa a média (± DP) de três experimentos.

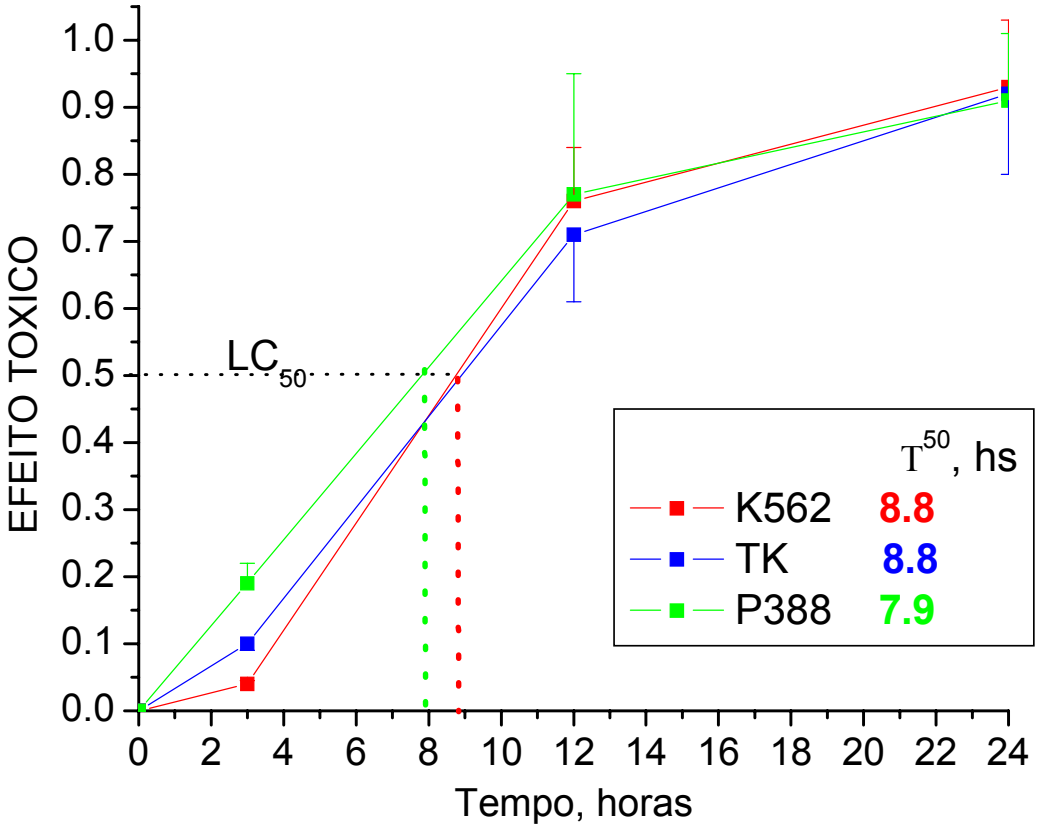

FIGURA 10. Toxicidade no escuro de Nitracrina imobilizada em lipossomos DSPC. [N] = 1,6 nmol/ml. Cada ponto representa a média (± DP) de três experimentos.

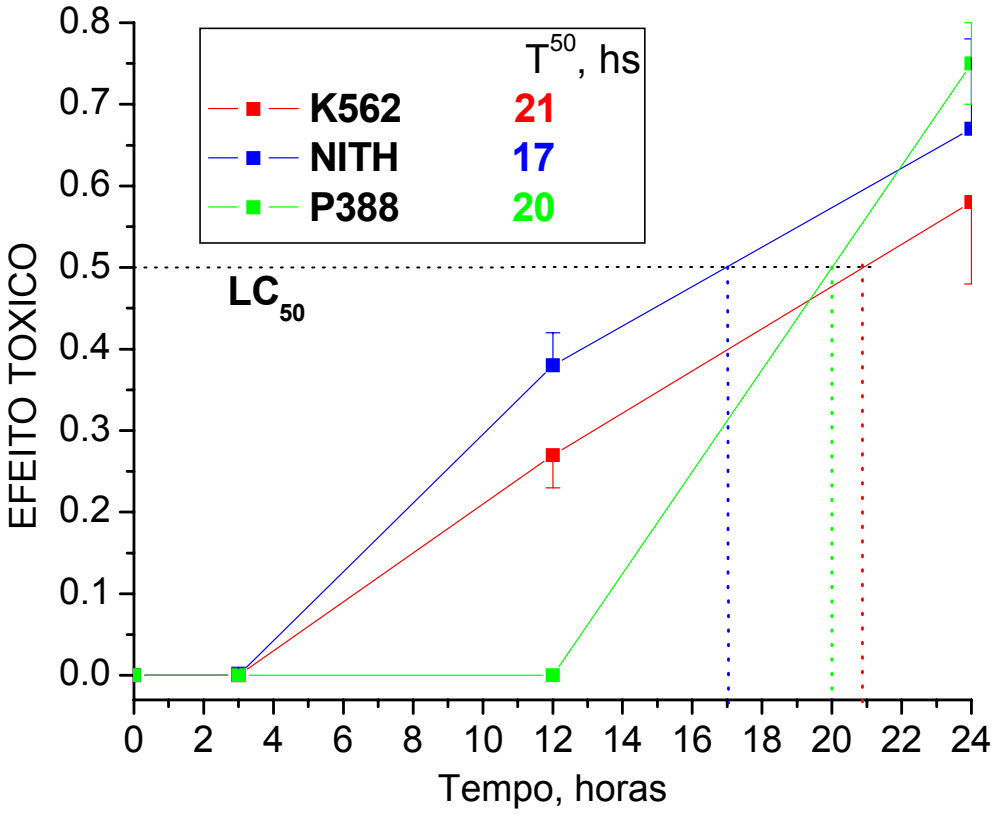

FIGURA 11. Toxicidade no escuro de Quinifuryl imobilizado em lipossomos DSPC. [Q] = 1,6 nmol/ml. Cada ponto representa a média (± DP) de três experimentos.

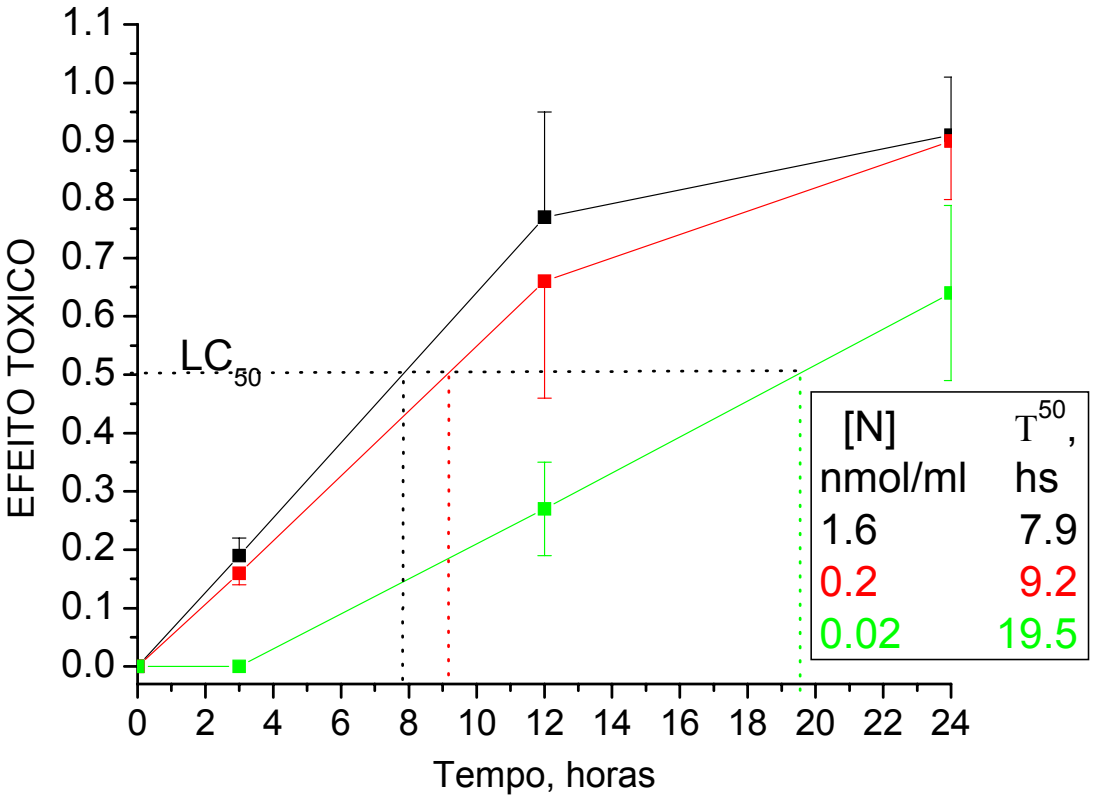

FIGURA 12. Toxicidade no escuro de Nitracrina imobilizada em lipossomos DSPC sobre as células P388. Dependência de concentração da droga. Cada ponto representa a média (± DP) de três experimentos.

DISCUSSÃO

Citotoxicidade das DNHC.

Os resultados do presente estudo demonstram que o Quinifuryl e a Nitracrina possuem alta citotoxicidade sobre células leucêmicas humanas (K562) e de camundongos (P388). Para todas as linhagens de células, a citotoxicidade da Nitracrina foi maior do que para o Quinifuryl. A Nitracrina é um reconhecido agente citotóxico seletivo para as células hipóxicas (Who, 1996) e um potente agente citotóxico hipoxia-seletivo *in vitro* (Gniazdowski et al., 1995; Gorlewska, et al., 2001). Sua toxicidade contra a linhagem de células de ovário de hamsters chineses (CHOW AA8) em condições de hipoxia foi demonstrada ser 10^5 vezes maior que o misonidazole (Degterev, et al., 1999). Os resultados do presente estudo demonstram que sob condições de normoxia, ambas as drogas são altamente tóxicas contra três linhagens de células, e os valores de LC_{50} obtidos após 24 horas de incubação foram ≤ 2 μM (tabela 1, figura 2).

Foi observado que ambas as drogas induziram rapidamente à morte celular, com o tempo de exposição requerido pelo Quinifuryl para alcançar o LC_{50} ficando entre 5 e 21 horas e para Nitracrina entre 3,5 e 8,5 horas (tabela 2). A Nitracrina é 10 vezes mais tóxica que o Quinifuryl para todas as linhagens de células. No entanto, o Quinifuryl mostrou citotoxicidade satisfatória (tabelas 1 e 2). Assim, esses resultados indicam que esse agente é um promissor candidato para o tratamento de tumores, pois seu efeito é 30 vezes menos danoso que o da

Nitracrina ao organismo-hospedeiro (Verovskiy et al., 1990). No entanto, essas observações *in vivo* deveriam ser melhor exploradas. O Quinifuryl e a Nitracrina aceleram muito a produção de ERO's em melanoma B16, em linfoleucemia P388 (Smirnov et al., 1989). Portanto, o estresse oxidativo possivelmente seja o mecanismo de toxicidade destas drogas contra células tumorais sob condições de normoxia.

No presente trabalho nós examinamos a citotoxicidade de duas drogas nitroheterocíclicas contra três linhagens de células (leucemia de camundongo P388, fibroblasto de camundongo NIH3T3 e eritroleucemia humana K562) a fim de iniciarmos um estudo do modo de ação destas drogas *in vivo*. Mesmo que ambas as drogas sejam de alguma forma tóxicas aos fibroblastos não tumorais de camundongo (NIH3T3), células de linfoleucemia de camundongo (P388) foram muito mais sensíveis a ambos os compostos. Um aspecto altamente desejável nas drogas anticancerígenas é que tenham elevada toxicidade contra células transformadas, mas baixa toxicidade às células não-transformadas. Além disso, a morte das células P388 causada por ambas as drogas, foi atingida 2,5 - 3 vezes mais rápida comparadas às células NIH3T3 (tabela 2).

Para avaliar os efeitos citotóxicos das drogas, experimentos paralelos, utilizando os Testes 1 e 2, foram comparados: no teste 1, o efeito tóxico foi medido imediatamente após o período de incubação; no teste 2, as drogas foram retiradas e meio de cultura DMEM foi adicionado para que as células proliferassem por um período adicional de 72 horas (K562 e NIH3T3) ou 36 horas (P388) (três vezes o "tempo de duplicação" para cada linhagem celular). Os resultados obtidos, usando-se este método (tabela 3), mostram que as drogas não

apenas causam morte celular, mas também atenuam a proliferação das células sobreviventes. Então, além do efeito citotóxico, ambas as drogas poderiam conter o crescimento do tumor.

Nossos resultados sugerem que o Quinifuryl, um anti-séptico usado em cirurgias para o tratamento de feridas e queimaduras, cuja atividade antitumoral ainda não foi bem estabelecida, merece atenção especial como um possível candidato para a terapia do câncer. Considerando sua alta citotoxicidade *in vitro* e relativamente baixa toxicidade aos hospedeiros, sugerimos que o Quinifuryl deva ser mais estudado a fim de ampliar o número das drogas em uso na medicina anticancerígena, em geral, e na terapia fotoquímica, em particular.

Absorção e metabolismo intracelular das DNHC.

Ambas as drogas foram incorporadas pelas células após 10 minutos de incubação (figura 4). Entretanto, os LC_{50} foram atingidos após 3 horas de incubação (tabela 2). Este atraso na indução da morte celular pode ser devido ao tempo requerido para a formação dos intermediários tóxicos resultantes do metabolismo intracelular (figura 3) ou para acumular uma concentração intracelular da droga capaz de exercer o efeito citotóxico. Considerando que os nossos resultados, apresentados na figura 4, sugerem que o metabolismo intracelular da droga é rápido, a primeira suposição parece mais correta.

Como mostrado na figura 3, o Quinifuryl presente no conteúdo intracelular aumentou pelos primeiros 90 minutos após a incubação da droga, refletindo a acumulação do composto que, posteriormente, começou a diminuir.

Concomitantemente com a perda da droga, um pico próximo a 280 nm apareceu no lugar de um mínimo no espectro do composto intacto (figura 4A). Estas mudanças no espectro são provavelmente referentes à transformação da droga no interior das células.

Em contraste com o Quinifuryl, a Nitracrina não perde a cor durante o metabolismo (Degterev et al., 1990). Entretanto, a Nitracrina mostrou deslocamento do seu espectro máximo para a região de ondas longas. De fato, a figura 4B mostra que o máximo do conteúdo intracelular das células K562 tratadas com Nitracrina tem deslocamento de 6 nm comparando com Nitracrina intacta. Este espectro também possui o mínimo perto de 420 nm e a relação A^{409}/A^{420} se muda com o tempo de incubação da droga. Dois novos picos adicionais também apareceram na região do vermelho após 1 hora de incubação da droga. Estas mudanças claramente indicam uma transformação intracelular da droga.

As análises do metabolismo intracelular destas drogas feitas para determinar sua susceptibilidade a biotransformação e para determinar o papel deste processo na toxicidade das DNHC, mostraram que a citotoxicidade dessas drogas deve-se ao metabolismo intracelular das mesmas.

Fototoxicidade de DNHC.

Os dados mostrados são os primeiros a indicar a possibilidade do uso de compostos nitroheterocíclicos como fotossensibilizantes para a terapia fotoquímica do câncer. Uma dramática aceleração na morte celular foi observada quando as linhagens de células foram expostas à iluminação com luz visível na presença das

drogas. Os resultados apresentados nas tabelas 4 e 6 mostram que a iluminação com luz visível diminui a concentração letal de ambos os agentes e diminui o tempo do efeito letal.

A tabela 5 mostra que os efeitos letais (Teste 1) de ambas as drogas, quando iluminadas com luz visível por 1 hora, foram similares aos observados após 12 horas de incubação com a droga no escuro para todas as linhagens de células. O efeito da Nitracrina foi maior, comparada ao Quinifuryl, tanto no escuro quanto sob iluminação. Uma significante toxicidade sobre as células P388 e NIH3T3 foi observada para baixas concentrações (0,2 nmol/ml) de Quinifuryl sob iluminação, enquanto que, baixa (P388) ou nenhuma (NIH3T3) toxicidade foi observada em 12 horas de incubação com droga no escuro nestas células. Estes resultados também mostram que as drogas não causam apenas a morte, mas também atenuam a proliferação das células que sobreviveram à ação da droga. Em contraste ao efeito letal direto, a toxicidade geral (Teste 2) de ambas as drogas sobre células P388 e NIH3T3 após 1 hora de iluminação e 12 horas de incubação no escuro foi similar.

Mecanismos da citotoxicidade no escuro do Quinifuryl e da Nitracrina são, provavelmente, devidos aos seus metabólitos. Ambas as drogas são metabolizadas em tecidos normais (Degterev et al., 1986; Degterev et al., 1990; Degterev et al., 1999) e em células cancerígenas (Veroviskiy et al., 1990; Degterev et al., 1986). Acredita-se que a Nitracrina produza intermediários reativos durante o metabolismo que causam modificações no DNA (Gorlewska et al., 2001). Ambas as drogas aceleram a produção de espécies reativas do oxigênio (Degterev et al., 1990) e do nitrogênio (Iliasova et al., 1994; Buzukov et al., 1995; Buzukov et al.,

1996) durante o metabolismo. Então, sua toxicidade possivelmente se deva ao estresse oxidativo.

O fato da fotoativação acelerar significativamente a morte das células pode ser interpretado como a formação de mais intermediários tóxicos durante a fotólise, comparando com o metabolismo no escuro, ou com a aceleração da formação das mesmas toxinas sob iluminação, ou ambos. Evidências da formação de espécies reativas durante a fotólise do Quinifuryl pela luz visível tem sido reportada (Smirnov et al., 1989; Borissevich, et al., 2003; Kuzmin et al., 1988). A formação do estado triplete excitado (Borissevich, et al., 2003), que é capaz de produzir oxigênio singlete (Henderson & Dougerthy, 1992; Ochsner, 1997; Sobolev et al., 2000), a reação do estado triplete com a droga no estado fundamental e com doadores de elétrons (Smirnov et al., 1989; Borissevich, et al., 2003; Kuzmin et al., 1988), formando o radical ânion superóxido no decurso da fotólise da droga (Smirnov et al., 1989) pode resultar na fototoxicidade do Quinifuryl.

Em contraste ao Quinifuryl, não há dados disponíveis sobre a fotólise da Nitracrina. Este fato não deixa espaço para especulações no mecanismo de fototoxicidade desta droga que, sem dúvida, merece um estudo detalhado. Nossos dados mostram que os compostos nitroheterocíclicos merecem ser estudado como possíveis candidatos para a terapia fotoquímica. Mostramos que a elevada citotoxicidade sob iluminação com luz visível não é uma propriedade específica do Quinifuryl, mas também, ocorre em compostos nitroheterocíclicos com estruturas bem diferentes. O efeito fotossensibilizante foi observado contra células de câncer diferentes como linfoleucemia de camundongo e eritroleucemia humana. Pela primeira vez foi descrito que essas drogas nitroheterocíclicas tem sua toxicidade

aumentada com a irradiação de luz. O sucesso da fototerapia com DNHC, requer o desenvolvimento paralelo de sistemas de entrega dirigida a fim de reduzir os efeitos colaterais.

Carregadores de droga.

As DNHC estudadas apresentam baixa solubilidade em água, o que nos forçou a usar soluções aquosas alcoólicas que permitiram o estudo do seu metabolismo (Degterev et al., 1990) e a atividade biomédica (Verovskiy et al., 1990). Este parece ser um problema geral associado ao uso de DNHC. A solução deste problema, no entanto, parece residir no transporte de DNHC hidrofóbico dissolvido em membranas lipossomais e micelas (Yua et al., 1998; Kidchob et al., 1998). As micelas PEG-2000-estearato e o lipossomos unilamelares DSPC foram escolhidos como veículos de transporte e a citotoxicidade dos compostos livres e imobilizados foram estudados em paralelo. Quanto ao uso de carregadores de drogas, ambas as drogas foram efetivamente imobilizadas em micelas PEG-2000-estearato e lipossomos DSPC.

Mesmo imobilizadas em carregadores, as drogas continuam a serem tóxicas contra as células tumorais. A figura 6 mostra que a morte de 50% das células foi atingida em pouco mais de 5 horas de incubação para Quinifuryl livre na concentração de 2 nmol/ml e droga imobilizada em micelas com 20 nmol/ml, enquanto que, o efeito letal do Quinifuryl micelizado na concentração 2 nmol/ml foi muito baixo. As micelas protegeram as células P388 contra a toxicidade do Quinifuryl. Um efeito protetor das micelas contra a toxicidade da Nitracrina sobre

células P388 foi observado em baixa concentração da droga (0,2 nmol/ml), mas não em concentração mais alta (2 nmol/ml) (figura 7), sugerindo uma relação dose-dependente. Em contrapartida, a incorporação da droga em micelas causou um pequeno aumento de toxicidade da droga contra as células K562 (figura 8). Nenhum efeito das micelas foi observado estudando toxicidade da nitracrina contra as células de fibroblasto NIH3T3 (figura 9).

O mecanismo do efeito dos carregadores de droga deve ser mais estudado. As possíveis hipóteses são que o efeito de proteção das células tumorais observado nas figuras 6 e 8, pode estar ligado com a absorção lenta dos veículos por essas células comparando com as drogas livres. O aumento da citotoxicidade observado em baixas concentrações da Nitracrina imobilizada em micelas, comparado com a droga pura (figura 7), pode estar ligado com a grande quantidade da droga trazida pelas micelas para dentro das células.

O Quinifuryl lipossomizado continua a ser tóxico para todas as linhagens de células estudadas. Esse dado sugere que os lipossomos facilitam a entrada da droga na célula. Ambas as drogas continuam a ser altamente tóxicas contra todas as linhagens de células quando imobilizadas em lipossomos DSPC, com Nitracrina 2,5 vezes mais tóxica (figuras 10 e 11). A figura 10 mostra que a Nitracrina imobilizada em lipossomos em concentração de 1,6 nmol/ml causou a morte de 50% das células durante 8-9 horas. A tabela 6 mostra que este valor foi atingido pela Nitracrina em concentração de 2 nmol/ml por aproximadamente 6 e 7 horas para células P388 e NIH3T3, respectivamente. Analisando a Figura 10, observamos que o LC_{50} foi atingido em 8,8 horas para K562 e NIH3T3, valores próximos aos obtidos com a droga livre (7,5 e 8,5 horas, respectivamente). No

entanto, foi observada diferença nas células P388. Neste caso, a Nitracrina lipossomizada precisou de 7,9 horas para atingir o LC_{50}, enquanto que, com a droga pura, este valor foi alcançado em 3,6 horas. Comparando os resultados da figura 11 (Quinifuryl imobilizado) com a figura 6 (Quinifuryl livre) observamos que os valores de LC_{50} foram atingidos 4 vezes mais rápido no segundo caso (20 horas e 5 horas, respectivamente). O efeito tóxico depende da concentração da droga imobilizada em lipossomos (figura 12).

Podemos sugerir que ambos os compostos designados para servir como agentes anti-cancerígenos mostraram alta citotoxicidade *in vitro* contra várias linhagens de células tumorais. No entanto, estudos complementares são necessários a fim de verificar a reprodutibilidade dos resultados principais e estudar os efeitos de imobilização nos experimentos de fototoxicidade das drogas. Consideramos nossos resultados como o primeiro passo no desenvolvimento da entrega dirigida para estas drogas.

CONCLUSÕES

- As drogas nitroheterocíclicas derivadas do 1-nitroacridina (Nitracrina) e do 5-nitrofurano (Quinifuryl) mostraram alta citotoxicidade (> 2 nmol/ml) sobre as linhagens de células de leucemia humana (K562) e de camundongos (P388), comparado com as células não-transformadas (NIH3T3).

- Pela primeira vez foi descoberta fototoxicidade de ambas as drogas sobre células tumorais, que foi muito mais alta comparada com a toxicidade das mesmas no escuro.

- A citotoxicidade da Nitracrina é maior do que à do Quinifuryl, tanto no escuro como sob iluminação.

- As drogas não causam apenas a morte, mas também atenuam a proliferação das células que sobreviveram à ação da droga.

- As drogas se incorporam em células e se transformam metabolicamente em seu interior, o que, provavelmente, é o mecanismo responsável pela morte celular.

- Ambas as drogas podem ser efetivamente imobilizadas em micelas PEG-2000-estearato e lipossomos DSPC.

- As duas drogas imobilizadas em micelas, continuam apresentado citotoxicidade contra as células tumorais.

REFERÊNCIAS BIBLIOGRÁFICAS

ADAMS, G.E. Redox, radiation, and reductive bioactivation. Failla Memorial Lecture. **Radiat. Res.** v.132, p. 129 - 139, 1992.

ADAMS, G.E. & STRATFORD I.J. Bioreductive drugs for cancer therapy: the search for tumor specificity. Intern. **J. Radiat. Oncol. Biol. Phys.** v. 29, p.231 - 238, 1994.

BARTOSZEK, A., DACKIEWICZ, P., SKLADANOWSKI, A. & KONOPA, J. In vitro DNA crosslinking by Ledakrin, an antitumor derivative of 1-nitro-9-aminoacridine. **Chemico-Biological Interactions.** v.103, p. 141 - 151, 1997.

BETHEA B., FULLMER B., SYED S., SELTZER G., TIANO J., RISCHKO G., GILLESPIE L., BROWN D. & GASPARRO F.P. Psoralen photobiology and photochemotherapy: 50 years of science and medicine. **J. Dermatol. Sci**., v.19, p. 78 - 88, 1998.

BLATUN, L.A., SVETUKHIN, A.M. & AGAFONOV, V.A. Clinic-laboratory effectiveness of modern ointments with a polyethylene glycol base in the treatment of purulent wounds. **Antibiotc Khimioterapia** v.44, p. 25 - 31, 1999.

BREMNER, J.C.M., BRADLEY J.K., ADAMS, G.E., NAYLOR, M.A., SANSOM, J.M. & STRATFORD, I.J. Comparing the anti-tumor effect of several bioreductive drugs when used in combination with photodynamic therapy (PDT). **Intern. J. Radiat. Oncol. Biol. Phys**. v. 29, p 329 - 332, 1994.

BORISSEVITCH, I.E, DAGHASTANLI, N.A. & DEGTEREV, I.A. Primary processes of photodecomposition of 2-(5'-nitro-2'-furanyl)ethenyl-4-{N-[4'-(N,N-diethylamino)-1'-methylbutyl]carbamoyl}quinoline. Effect of oxygen and compound concentration. **J. Photochem. Photobiol. A: Chemistry**, v.159, p. 213 - 217, 2003.

BUZUKOV, A. A., ILIASOVA, V. B., TABAK, M., TATARSKAYA, N. K. & DEGTEREV, I. A. Metabolic denitration of Quinifuryl and Nitracrine in mouse liver homogenate. **Pharmac. Chem. J.** (Moscow) v. 29, p. 3 - 8, 1995.

BUZUKOV, A.A., ILIASOVA, V.B., TABAK, M., TATARSKAYA, N.K., MEIRELLES, N.C. & DEGTEREV, I.A. An ESR and spectrophotometric study of the denitration of nitroheterocyclic drugs by liver homogenates and their metabolic consumption by liver microsomes from cytochrome P-450-induced mice, **Chem.-Biol. Interact**. v.100, p. 113 - 124, 1996.

CHELVI, P.T., JAIN, S.K. & RALHAN, R. Heat-mediated selective delivery of liposome-associated melphalan in murine melanoma. **Melanoma Res**. v. 5, p. 321 - 326, 1995.

CHAN, W.S; MARSHALL, J.F; LAM, G.Y.F. & HART, I.R. Tissue uptake, distribution and potency of the photoactivatable dye chloroaluminum sulfonated in mice bearing transplantable tumors. **Cancer Res**. v.48, p. 3040 - 3044, 1998.

COWAN, D.S., MATEJOVIC, J.F., WARDMAN, P., MCCLELLAND, R.A. & RAUTH, A.M. Radiosensitizing and cytotoxic properties of DNA targeted phenanthridine-linked nitroheterocycles of varying electron affinities. **Int. J. Radiat. Biol.** v. 66, p. 729 - 738, 1994.

DEGTEREV, I.A., BUZUKOV, A.A., SHARF, V.G., POPOV, K.N., SEREBRIANIY, A.M. & ZAIKOV, G.E. Comparative study of in vitro ledakrine metabolism in microsomes of EAC-cells and mouse liver, **Pharmac. Chem. J**. v.20, p. 412 - 417, 1986.

DEGTEREV, I.A., TATARSKAYA, N.K. & ZAIKOV, G.E. Kinetic investigation of nitrofuran microsomal biotransformation on the example of Quinifur. **Pharmac. Chem. J.** v. 23, p. 530 - 537, 1989

DEGTEREV, I.A., BUZUKOV, A.A., TATARSKAYA, N.K., LEONOVA, YU.E. & SUKOVA, N.M. Metabolism of hetrocyclic compounds in mouse liver microssomes. **Pharmacol. Chem. J.** v. 24, p. 9 - 16, 1990.

DEGTEREV, I.A., BUZUKOV, A.A., SHARF, V.G., POPOV, K.N., SEREBRIANIY, A.M. & ZAIKOV, G.E. Comparative study of in vitro ledakrine metabolism in microssomes of EAC-cells and mouse liver. **Pharmac. Chem. J.** v. 20, p. 412 - 417, 1991.

DEGTEREV, I.A., NOGUEIRA P.C.L., MARSAIOLI A.J. & VERCESI A.E. Microsomal metabolism of quinifuryl - a nitrofuryl-ethenyl-quinoline antiseptic possessing antitumor activity *in vitro*, **Europ. J. Drug Metab. Pharmac.** v. 24, p. 15 - 22, 1999.

DAGHASTANLI, N.A., ROSSA, M.M., SELISTRE-DE-ARAJO, H.S., TEDESCO, A.C., BORISSEVITCH, IU.E., DEGTEREV, I.A. Citotoxicity of the nitroheterocyclic compounds, Quinifuryl and nitracrine, towards leukaemic and normal cells on the dark and under illumination with visible light. **J. Photochem. Photobiol. B: Biology**, v. 75, p. 27 - 32, 2004.

DAGHASTANLI, N.A., DEGTEREV, I.A., TEDESCO A.C. & BORISSEVITCH, I.E. Photocitotoxicity of Quinifuryl, a 5-Nitrofuran-Etheyl-Quinoline antiseptic, towards P388 Mouse Leukemia Cells. **Braz. J. Med. Biol. Res**. v. 37, p. 1873 - 1879, 2004a.

DALL'AMICO R., ZULIAN F., MONTINI G., ANDRETTA B., MURER L., ROSSETTI F., LIVI U., ZACCHELLO G. & ZACCHELLO F. Applications of extracorporeal photochemotherapyin 'non-oncological' diseases. **Intern. J. Artif. Organs**, v.16 (Suppl. 5), p. 733 - 737, 1996.

DOCAMPO R. Sensitivity of parasites to free radical damage by antiparasitic drugs, **Chem.-Biol. Interact.** v. 73, p. 1- 8, 1990.

FOOTE, C.S. Chemical mechanisms of photodynamic action. **Proc. SPIE Institute "Advanced Optical Technologies on Photodynamic Therapy"** v. 6, p.115 - 126, 1990.

FRANKO, A.J. Misonidazole and other hypoxia markers: metabolism and applications. **Int. J. Radiat. Oncol. Biol. Phys**., v.12, p. 1195 - 1202, 1986.

FRESHNEY, R.I. Measurement of Viability and Citotoxicity. Culture of Animal Cells. (3d Ed.),Chp. 19. WILEY-LISS, NY. p. 287 - 307, 1994.

GARETH, J.R. Cancer Guide for Family. Dorling Kindersley Publisher. 3d Ed. v.7, p.115, 2001.

GNIAZDOWSKI, M., SZMIGIERO, L. Nitracrine and its congeners - an overview. **Gen. Pharmacol**. v. 26, p. 473 - 481, 1995.

GREGOREADIS, G. Engineiering liposomes or drug delivery: progress and problems. **Trends in Biotechnology**, v. 13, p. 527 - 537, 1995.

GORLEWSKA, K., MAZERSKA, Z., SOWIN´SKI, P. & KONOPA, J. Products of metabolic activation of the antitumor drug Ledakrin (Nitracrine) in Vitro. Chem. Res. Toxicol. v. 14, p.1 - 10, 2001.

HAY, M.P., LEE, H.H., WILSON, W.R., ROBERTS, P.B. & DENNY, W.A. Hypoxia-selective antitumor agents, bis(nitroimidazoles) and related Bis(nitroheterocycles): development of derivatives with higher rates of metabolic activation under hypoxia and improved aqueous solubility. **Med. Chem.**, v. 38, p. 1928 - 1941, 1995.

HENDERSON, B. W. & T. R. DOUGERTHY. How does photodynamic therapy work? **Photochem. Photobiol**. v.55, p.145 - 157, 1992.

ILIASOVA, V.B., BUZUKOV, A.A., TABAK, M. & DEGTEREV, I.A. On the mechanism of metabolic denitration of nitroheterociclic compounds. **Biofizica**, Moscow. v. 39, p. 219 - 225, 1994.

JORI, G. Tumor photosensitizers: approaches to enhance the selectivity and efficiency of photodynamic therapy. **J. Photochem. Photobiol. B: Biology** v. 36, p. 87- 93, 1996.

JOSEPHY, P.D., MASON, R.P. Nitroimidazoles, In: Bioactivation of Foreign Compounds, M.W. Anders (Ed.), Academic Press, New York; p. 161 - 222, 1985.

KICK, G.; MESSER, G. & PLEWIG, G. The history of photodynamic therapy. **Hautarzt**.v. 47, p. 644 - 649, 1996.

KIDCHOB, T., KIMURA, S. & IMANISHI, Y. Amphiphilic poly(Ala)-b-poly(Sar) microspheres loaded with hydrophobic drug. **J. Control. Release**., v.51, p. 241 - 248, 1998.

KWONA, G.S. & OKANOB, T. Polymeric micelles as new drug carriers. **Adv. Drug Deliv. Rev**., v. 21, p. 107 - 116, 1996.

KWONA G.S. Diblock copolymer nanoparticles for drug delivery. **Crit. Rev. Therap. Drug Carrier Syst.**, v. 15, p. 481 - 512, 1998.

KUZMIN, V.A.; LEVIN P.P.; BORISSEVITCH, YU.E; DEGTEREV, I.A. & SMIRNOV, S.M. Triplet exciplex of nitrofuran derivative with aromatic amines. Proc. Acad. Sci. USSR, **Chemistry**, N 7, p. 1510 - 1514, 1988.

MCCALLA, D.R. Nitrofurans, in: **Antibiotics**, F.E. Hahn (Ed.), Springer Verlag, New York; v. 5, p. 176 - 213, 1979.

MOAN, J., BERG, K. Photochemotherapy of cancer: experimental research. **Photochem. Photobiol**. v. 55, p. 931 - 948, 1992.

MOSMANN, T. Rapid colorimetric assay for cellular growth and survival: application to proliferation and cytotoxicity assays. **J. Immunol. Methods** v. 65, p. 55 - 63, 1983.

MONKS, A., SCUDIERO, D., SKEHAN, P., SHOEMAKER, R., PAULL, K., VISTICA, D., HOSE, C., LANGLEY, J., CRONISE, P. & VAIGRO-WOLFF, A. Feasibility of a high-flux anticancer drug screen using a diverse panel of cultured human tumor cell lines. **JNCI**; v. 83, p. 757 - 766, 1991.

OCHSNER, M. Photophysical and photobiological processes in the photodynamic therapy of tumors. **J. Photochem. Photobiol. B: Biology**, v. 39, p. 1-18, 1997.

PARK, J.W., HONG, K., KIRPOTIN, D.B., MEYER, O., PAPAHADJOPOULOS, D. & BENZ, C.C. Anti-HER2 immunoliposomes for targeted therapy of human tumors. **Cancer Let**. v.118, p. 153 - 160, 1997.

RAUTH, A.M., MELO, T. & MISRA, V. Bioreductive therapies: na overview of drugs and their mecanisms of action. **Intern. J. Rad. Oncol. Biol. Phys**. v. 47: 755 - 762, 1998.

ROSSA, M.M; ROCHA-E-SILVA, T.A.A; TERRUGGI, C.H.B; TEDESCO, A.C; SELISTRE-DE-ARAUJO, H.S; BORISSEVICH, I.E. & DEGTEREV, I.A. Comparision of the citotoxicity of two nitroheterocyclic drugs (NHCD) towards transformed and non-transformed cells. **Pharmacological Research** v.48, p. 369 - 375, 2003.

SMIRNOV, S.M., ZHURAV, M.A., TATARSKAYA, N.K., BORISSEVICH, I.E., DEGTEREV, I.A. Phototransformation of Quinifuryl. Nitroanion Radical Formation. **Khimicheskaia Fisika (Chemical Physics)**, v. 8, p. 1723 - 1725, 1989.

SOBOLEV, A.S; JANS, D.A. & ROSENKRANZ, A.A. Targeted intracellular delivery of photosensitiziers. **Progress in Biophysics & Molecular Biology** v. 73, p. 51 - 90, 2000.

TATARSKAYA, N.K., ZHURAV, M.A., SMIRNOV S.M., DEGTEREV, I.A., TARASOV, V.F., BORISSEVICH, I.E. & ZAIKOV, G.E. Effect of compound and oxygen concentration on primary processes of Quinifuryl phototransformation of Quinifuryl. Izvestia Acad. Nauk SSSR (Proceed. Acad. Sci. USSR, **Chemistry**) v. 5, p. 804 - 809, 1989.

VAN IPERENA, H.P., GERARD, M. J. & VAN HENEGOUWENA, B. Singlete oxygen producing photosensitizers in photophoresis. **J. Photochem. Photobiol. B: Biology** v. 38, p. 203 - 208, 1997.

VEROVSKIY, V.N., DEGTEREV, I.A., SUKHOVA, N.M., BUZUKOV, A.A., LEONOVA, E.YU. & TATARSKAYA, N.K. Interrelation between structure, microsomal metabolizing activation, mouse toxicity, cytotoxicity and antitumor activity of heterocyclic- and nitroheterocyclic compounds. In vitro and in vivo study, **Pharmac. Chem. J.** v. 24, p. 20 - 24, 1990.

VIODE, C., BETTACHE, N., CENAS, N., KRAUTH-SIEGEL, R.L., CHAUVIERE, G., BAKALARA, N. & PERIE, J. Enzymatic reduction studies of nitroheterocycles. **Biochem. Pharmacol**. v. 57, p. 549 - 557, 1999.

VORONINA, S.S., TATARSKAYA, N.K., DEGTEREV, I.A., SEREBRIANIY, A.M., PELEVINA, I.I. & SUKHOVA, N.M. Radiosensitizing activity and metabolismo of some nitrofuran derivatives. 1. M-106. **Radiobiologia (Radiobiology)**, v. 25, p. 748 - 751, 1985.

WAINWRIGHT, M., GRICE, N.G. & PYE, L.E.C. Phenothiazine photosensitizers: part II. 3,7-Bis(arylamino)phenothiazines1. **Dyes and Pigments.** v. 42, p. 45 - 51, 1999.

WILSON, W.R., DENNY, W.A., STEWART, G.M., FENN, A. & PROBERT, J.C. Reductive metabolism and hypoxia-selective toxicity of nitracrine. **J. Radiat. Oncol. Biol. Phys.** v. 12, p. 1235 - 1238, 1986.

WOOD, P.J., HORSMAN, M.R., KHALIL, A.A., STEIBERG, F., STREFFER, C., OVERGAARD, J., STRATFORD, I.J. & ADAMS, G.E. A comparison of the physiological effects of RSU1069 and RB6145 in the SCCVII murine tumour. **Acta Oncol**. v. 35, p. 989 - 994, 1996.

YOSHIMURA, M.; NAMURA, S., AKAMATSU, H. & HORIO, T. Antimicrobial effects of phototherapy and photochemotherapy in vivo and in vitro. **British J. Dermatol.** v. 135, p. 528 - 532, 1996.

YUA, B.G., OKANOB, T., KATAOKAC, K. & KWONA, G.S. Polymeric micelles for drug delivery: solubilization and haemolytic activity of amphotericin B. **J. Control. Release** v. 53, p. 131 - 136, 1998.

ANEXOS

Artigos Publicados durante o doutoramento:

ROSSA, M.M; ROCHA-E-SILVA, T.A.A; TERRUGGI, C.H.B; TEDESCO, A.C; SELISTRE-DE-ARAUJO, H.S; BORISSEVICH, I.E. & DEGTEREV, I.A. Comparision of the citotoxicity of two nitroheterocyclic drugs (NHCD) towards transformed and non-transformed cells. **Pharmacological Research**, v.48, p. 369-375. 2003.

DAGHASTANLI, N.A., ROSSA, M.M., SELISTRE-DE-ARAJO, H.S., TEDESCO, A.C., BORISSEVITCH, I.E. & DEGTEREV, I.A. Citotoxicity of the nitroheterocyclic compounds, Quinifuryl and Nitracrine, towards leukaemic and normal cells on the dark and under illumination with visible light. **J. Photochem. Photobiol. B: Biology,** v.75, p. 27-32. 2004.

ROCHA-E-SILVA, T.A.A; ROSSA, M.M; RANTIN, F.T., TUNDISI, T.M., TUNDISI, J.G. & DEGTEREV, I.A. Comparision of liver mixed-function oxygenase and antioxidant enzymes of vertebrates under tropical conditions. **Comparative Biochemistry and Physiology***, part C*, v.1378, p. 155-165. 2004.

COMPARISON OF THE CYTOTOXICITY OF TWO NITROHETEROCICLIC DRUGS (NHCD) TOWARDS TRANSFORMED AND NON-TRANSFORMED CELLS.

Marcelo M. Rossa[1], Thomaz A. A. Rocha-e-Silva[1], Cristina H. B. Terruggi[1], Antonio C. Tedesco[2], Heloisa S. Selistre-de-Araujo[1], Iouri E. Borissevich[3], Igor A. Degterev[4*]

1- Department of Physiological Sciences, Federal University of São Carlos, São Carlos, Brazil
2- Department of Chemistry, University of São Paulo, Riberão Preto, Brazil
3- Department of Physics and Mathematics, University of São Paulo, Riberão Preto, Brazil
4- Department of Chemical and Biochemical Kinetics, Institute of Biochemical Physics, Russian Academy of Sciences, Moscow, Russian Federation

ABSTRACT

The cytotoxicity of two nitroheterocyclic compounds, Nitracrine (Ledakrine, C-283), 1-nitro-9(3'3'-dimethylaminopropylamino) acridine and Quinifuryl (M-106), 2-(5`-nitro-2`-furanyl) ethenyl-4-{N-[4-(N,N-diethylamino)-1`-methylbutyl] carbamoyl} quinoline, towards two lines of leukaemic cells and a line of non-transformed cells, was determined under normoxia conditions. Although both drugs showed significant cytotoxicity to all cell lines (LC_{50} for 24 hr $\leq$ 2 μM) with that of Nitracrine exceeding Quinifuryl, their toxicity towards murine leukaemia P388 was substantially higher, compared to murine fibroblasts NIH3T3. In addition, the rate of cell death was also 2-3-fold higher in case of P388 cells versus NIH3T3. Interestingly, human erythroleukaemia K562 cells were shown to uptake the drugs 10 min after their addition to the tissue culture

medium, while the LC_{50} values were reached after a substantial delay of $\geq$ 3 hr. This delay might be due to the intracellular transformation of drugs required for cell killing.

* Corresponding author. Present address: DSF/ICB/UFSCar, Rodovia Washington Luis km 235, São Carlos, SP 13565-905, Brazil. Tel/fax: (55) (016) 260-8327; e-mail: vigordgt@power.ufscar.br

Abbreviations:

NHCD – nitroheterocyclic drugs, LC_{50} – lethal concentration 50%, TE – toxic effect, DMEM - Dulbecco's modified Eagle's medium, FBS - fetal bovine serum.

Key words:

cytotoxicity, nitroheterocyclic drug, lympholeukaemia P388, erythroleukaemia K562, fibroblasts NIH-3T3.

INTRODUCTION.

Nitroheterocyclic compounds (NHCD), which are typically used as antibiotics, have been, over the years, also shown to possess prominent anticancer activity. The anticancer therapeutic potential of the NHCDs is based on their cytotoxic, radiosensitising, and chemosensitising properties towards tumour cells. The most widely used among them are derivatives of 5-nitroimidazole, 5-nitrofuran, and 1-nitroacridine.

We have previously analyzed the cytotoxicity of a large group of nitroheterocyclic compounds, which were derivative from 5-nitrofuran and 1-nitroacridine, towards melanoma B16 and murine lympholeukaemia P388 cells [1]. Nitracrine, which is a 1-nitroacridine derivative, and Quinifuryl, a 5-nitrofuryl-vynyl-quinoline derivative, displayed the highest cytotoxicity among studied compounds.

In contrast to Nitracrine, which is a well established antitumor agent [2-4], this activity of Quinifuryl has not been thoroughly characterized. It was previously shown to display the highest toxicity towards two tumour cell lines *in vitro*, compared to a number of other 5-nitrofuran derivatives, and low toxicity towards tumour (P388)-bearing mice [1], whereas another report demonstrated its radiosensitising activity [5]. Additionally, Quinifuryl has been reported to be highly photolabile, producing the ROS during illumination with visible light [6,7], and we have recently discovered light-dependent elevation in its toxicity towards different tumour cell lines (manuscript in preparation). This observation makes Quinifuryl a possible candidate for cancer phototherapy. Since our initial studies [1] showed significantly higher tolerance (~ 30 times) of tumour (P388) – bearing animals to Quinifuryl than to Nitracrine, a more detailed comparison of

Quinifuryl's cytotoxicity to Nitracrine *in vitro* was performed to establish its *in vitro* potency in order to gain insight into the cause of low *in vivo* cytotoxicity.

It has been hypothesized that NHCD might posses specific toxicity toward hypoxic tumour cells, which is particularly relevant for Nitracrine, since its cytotoxic effect is attributed to DNA cross-linking [2-4]. However, based on other data, the role of oxygen metabolism in NHCD action cannot be discounted. NHCD are well known to activate oxygen in biological tissues, transferring one electron from cytochrome c (P450) reductase to oxygen molecule [8]. In particular, Quinifuryl and Nitracrine were both shown to highly accelerate the ROS production in melanoma B16, limpholeukemia P388 cells [1] and Erlich's carcinoma cells [9]. Thus, oxidative stress may be a possible mechanism for drug toxicity towards tumour cells under normoxic conditions. In the present study we examined cellular toxicity of both drugs towards murine leukaemia P388, fibroblast NIH3T3 and human erythroleukaemia K562 cells under these conditions, because they may be more relevant for the drug's mode of action *in vivo*. In addition, analyses of drugs metabolism in cells were also performed to determine their susceptibility to biotransformation and to determine the role of this process in NHCD toxicity.

Since elevated toxicity to the transformed, as opposed to the non-transformed, cells is a highly desirable feature in anticancer drugs, special emphasis has been placed on the comparisons of the drugs effects in highly tumorogenic, leukaemic (P388) and non-tumorogenic (NIH3T3) murine cells.

MATERIALS AND METHODS.

Drugs.

Quinifuryl (M-106), 2-(5`-nitro-2`-furanyl) ethenyl-4-{N-[4-(N,N-diethylamino)-1`-methylbutyl] carbamoyl} quinoline was synthesized and purified by Dr. N. M. Sukhova (Institute of Organic Synthesis, Riga, Latvian Republic). Nitracrine (Ledakrine, C-283), 1-nitro-9(3'3'-dimethylaminopropylamino) acridine was purchased from Polfa (Poland). Structural authenticity of both drugs was verified by NMR analysis. Structural formulas of both drugs are present in Fig. 1.

Cells.

$P388D_1$ cells, a mouse lymphocyte cell line, and immortalized mouse fibroblast NIH-3T3 cells were obtained from the American Type Culture Collection (ATCC). The human K562 leukaemia cell line (proerythrocytes), which was derived originally from the patient with erythroleukaemia [10], was kindly provided by Dr. S. Niewiarowski (Temple University, PA, USA). P388 cells were cultured in Fisher's media supplemented with 10 % heat inactivated horse serum in 175 cm^2 culture flasks at 37^0C with 5 % CO_2. K562 and NIH-3T3 cells were cultured as a suspension or a monolayer, respectively, in Dulbecco's modified Eagle's medium (DMEM) supplemented with heat-inactivated 10% fetal bovine serum (FBS), 1% L-glutamine, 50 units/ml penicillin, 50 mg/ml streptomycin, 250 mg/ml Anfotericin-B at 37^0C in a water-jacketed CO_2 incubator (Cellstar, USA).

The cellular density was measured with hemocytometer and viability was assessed by counting of trypan blue dye-excluded cells.

Cytotoxicity assays.

The activity of each compound on each cell line was determined by the MTT assay. The tetrazolium salt 3-(4,5-dimethylthiazol-2-yl)-2-5 diphenyl tetrazolium bromide (MTT)

is taken up into cells and reduced in a mitochondria-dependent reaction to yield a formazan product. The ability of cells to reduce MTT provides an indication of mitochondrial integrity and activity that, in turn, may be interpreted as a measure of viability [11].

For MTT assays, cells were seeded in DMEM containing 5% FBS into wells of 96-well ELISA-type plates and exposed to a range of drug concentrations for time intervals from 1 h to 24 hr. The initial seeding densities ranged from $2x10^4$–$6x10^4$ cells/well. Cell viability was assessed by trypan blue dye exclusion at the beginning of each experiment and was always higher than 96%. Drug concentrations ranged from 0.08-20 nmol/ml, for Quinifuryl, and from 0.02-2 nmol/ml, for Nitracrine.

At the end of the drug exposure period, plates were centrifuged to pellet cells and a drug-contained supernatants were displaced with either MTT dissolved in PBS (*Procedure 1*) or with fresh medium (*Procedure 2*). In the latter case, the cells were incubated for the additional 2-3 cell population-doubling times (36-72 hr) with daily media change, followed by MTT assay (*Procedure I*).

Plates with MTT were incubated in the dark for 4 hr, after which the water-insoluble MTT-formazan crystals were dissolved in DMSO, and absorbance was recorded in an ELISA plate reader Dynex MRX (Dynex Technologies Inc.) at 570 nm.

Drug concentration dependence and time-dependence of cell death were calculated as a toxic effect (TE): $TE = [DC]/[Cell]^{control}$, were $[Cell]^{control}$ is cell concentration, in control wells (cells incubated for the same time length with no compound) and [DC] – dead cell concentration. [DC] is calculated as $[Cell]^{control} - [Cell]^{final}$, were $[Cell]^{final}$, is the live cell concentration in wells exposed to drug. The above expression was developed based on the formulas for the growth inhibition power described in [12]. Cell concentration was

measured using a calibration curve made for all cell lines tested using MTT-staining method.

The cytotoxic effect (LC_{50}) of the tested compounds was estimated as 100 x (T-T_0)/T_0=-50, where T_0 and T are optical densities of the test well at time zero (when the compound is added) and after exposure to test compound [12].

Uptake of drugs into K562 cells.

Drug uptake into K562 cells was measured using the following procedure. Each drug was added to 1 ml of cell suspension ($1x10^6$ cells/ml) in 20 mM HEPES buffer to a final drug concentration of 2 nmol/ml. Mixtures were incubated at 37^0C for time intervals ranging from 0 min to 3 hr with continuous shaking on an orbital shaker (Forma Scientific, USA). Following incubation, cells were pelleted and repeatedly washed until no spectra of a drug could be detected in supernatant. Cell pellets were subsequently lysed in 0.5% Triton X-100 solution in Milli-Q water. Absorption spectra of the lysates prepared from the cells incubated with a drug were measured against that of control untreated cells, incubated under identical conditions, and compared with spectra of intact drug recorded against the lysates prepared from control cells.

Statistic analysis.

The data are presented as the mean ± SD of two to five independent series of experiments with five to six repetitions in each. Statistic analysis was performed the Student's t -test. The Tukey test with 95% confidence was applied to compare the means. Statistic analyses were done using the InStat software program for Windows (GraphPads software, San Diego, USA).

RESULTS

Dose-dependence of the toxic effects (TE) of both drugs was determined first and is shown in Fig. 2. The TE values were calculated as the ratio of numbers of the cells dying during incubation with the drug to the initial cell concentrations (for details see Materials and Methods). Cells incubated without drug served as a control in each series of experiments. Normally, no significant amounts of dead cells were observed in control wells up to 24 hr incubation.

The majority of the experimental data was obtained following Procedure 1 (Materials and Methods), according to which MTT-dye incubation was performed immediately following drug treatment. This approach limits the observed results only to the direct cytotoxic effect of the drug. Table 1 shows the LC_{50} values calculated based on the results of two to five independent series of experiments with six repetitive measurements in each series.

The results of the experiments (Table 1) clearly show that both drugs are somewhat toxic toward all cell lines ($LC_{50} \leq 2$ μM) and require less than 24 hr to reach LC_{50} values (Table 2). On the other hand, Nitracrine displays significantly higher cytotoxicity as than Quinifuryl (Tables 1 and 2). In addition, murine limpholeukaemia P388 cells were more sensitive to both drugs, as compared to non-transformed murine NIH-3T3 cells (Table 2). Respective data, presented in Table 3, show that toxic effects observed after 12 hours incubation of P388 cells with these drugs were significantly higher (0.79 and 0.64 for Quinifuryl and Nitracrine, respectively) than those in NIH-3T3 cells (0.43 and 0.38 for Quinifuryl and Nitracrine, respectively). Furthermore, the incubation times required to

reach LC_{50} values with 2 μM concentrations of both drugs were 2-3 times more for both NIH-3T3 cells (16 hr and 8.5 hr for Quinifuryl and Nitracrine, respectively) and K562 cells (21 hr and 8.4 hr for Quinifuryl and Nitracrine, respectively) as opposed to P388 cells (5.3 hr and 3.5 hr for Quinifuryl and Nitracrine, respectively) as it shown in Table 2.

In order to estimate cytostatic effects of the drugs, results, obtained in parallel experiments utilizing Procedures 1 and 2 (see Materials and Methods), were compared. Briefly, cells were incubated with drugs for 12 hr in two ELISA-type plates. In one plate the toxic effect was measured immediately after that, whereas, in the second plate, drugs were replaced with complete medium and cells were allowed to proliferate for the additional 72 hr (K562 and NIH-3T3) or 36 hr (P388) (three cell population doublings of each cell type). Subsequently, the medium was replaced with MTT-dye and toxicity was measured. The results, obtained using this method (Table 3), show that drugs not only caused death, but also attenuated proliferation of the surviving cells.

Since Quinifuryl, despite its cytotoxicity *in vitro*, showed very little effect *in vivo* [1], one possible explanation is its rapid intracellular metabolism. In order to address this possibility, first, the uptake of Quinifuryl and Nitracrine into K562 cells was measured. The cellular uptake of drugs could be visually detected, since the pellets of K562 cells turned bright yellow after 10 min of incubation with Quinifuryl (drug is yellow coloured), while pellets of control cells remained uncoloured. Incubation with Nitracrine resulted in time dependent cell pellet colour change from yellow to greyish-brown. Following incubations with the drugs, cells were pelleted, washed twice, and lysed. Difference spectra were recorded against the intracellular content of control cells that were incubated for 6 hr under the same conditions (for more details see Material and Methods). Spectra of intact drugs

were also recorded versus the control cell lysate to estimate the degree of drug biotransformation.

Kinetics of the changes in a relative Quinifuryl concentration in the supernatant versus the cell pellet are shown in Fig 3. The balance was calculated as a sum of the drug concentration in the incubation mixture and the cell lysate. Our attempts to measure the Nitracrine balance failed because of the much lower extinction coefficient of this compound as compared to Quinifuryl (3.9 mM^{-1}. cm^{-1} and 26.2 $mM^{-1}.cm^{-1}$, respectively, as determined in this study).

Figure 4 shows dynamics of spectral changes in K562 cell lysates after cell incubation with either Quinifuryl (Panel A) or Nitracrine (Panel B) for different lengths of time. Specific absorption of Quinifuryl (396 nm) was increased for the initial 30 min following drug addition and then decreased with time. This loss of Quinifuryl correlated with the appearance of a through near 248 nm and of a peak at 276 nm, which corresponds to a through at the same wavelength observed in a spectrum of an intact drug.

Following first 10 min of Nitracrine incubation, difference spectra of cellular content showed appearance of a peak at 409 nm and a corresponding through at 430 nm with fluctuated value of $\Delta A^{409-430}$, which shifted by 6 nm in comparison to the intact drug. After 1 hr incubation, however, two new peaks appeared in the spectra at 573 nm and 627 nm with variable absolute and relative absorption. Overall, spectral changes shown in Fig. 4 most likely reflect substantial biotransformation of both drugs in K562 cells.

DISCUSSION

Nitracrine, which is an antitumour drug used clinically for the last several years [13], is a potent hypoxia-selective cytotoxic agent *in vitro* (for reviews see [3,4,14]). For instance, its toxicity against the Chinese hamster ovary cell line AA8 under hypoxic conditions was found to be ~ 10^5 times higher than that of misonidazole [15]. On the other hand, Quinifuryl, is an antiseptic used in surgery for the treatment of wounds and burns [16] and its antitumour activity is not well established.

The results of our study demonstrate that under normoxic conditions both drugs are highly toxic towards three cell lines tested and the LC_{50} values obtained after 24 hr incubation are ≤ 2 μM (Table 1, Fig. 2). Both drugs induced death rapidly with the exposure time needed for Quinifuryl to achieve LC_{50} being between 5 to 21 hr and from 3.5 to 8.5 hr for Nitracrine (Table 2). In addition to the cytotoxic effects, both drugs attenuated proliferation by the surviving cells (Table 3).

Even though both drugs appeared somewhat toxic to non-tumour cells (NIH3T3), murine lympholeukaemia P388 cells were much more sensitive to both compounds. Also, P388 cells were killed significantly faster by both drugs (~ 2.5-3 times) compared to NIH3T3 cells (Table 2).

Despite our findings that Nitracrine was more toxic than Quinifuryl towards all studied cells (Tables 1 and 2), the latter still shows significant promose since its lower antitumour activity may be offset by the decreased non-specific toxicity towards host, tumour (P388)-bearing mice, which was nearly 30 times lower compared to Nitracrine [1].

Interestingly, despite the fact that both drugs entered the cells following 10 min incubation (Fig. 4), the LC_{50} were achieved by both drugs only after > 3 hr incubation (Table 2) and no significant cell death was observed after 1 hour incubation (data not shown). This "delay induction" may be needed for the build-up of either intracellular concentration of the drug itself or its toxic intermediates resulting from intracellular metabolism (Fig. 3). Since our data, presented in figure 4, suggest rapid drug metabolism, the latter assumption might be more likely.

Metabolic decomposition of the chromophore of Quinifuryl in normal tissues (λ_{max}=396 nm, ε=26 $M^{-1}.cm^{-1}$, as measured in this work), i.e. "drug bleaching", is a perfect instrument for kinetic and mechanistic studies of drug metabolism (for instance, see [17]). As shown in Fig. 3, the intracellular content of Quinifuryl increased for the first 90 min following drug incubation, reflecting compound accumulation, and then started to decrease. Concomitantly with the drug loss, a peak near 280 nm appeared in a place of a through in the spectrum of intact compound (Fig. 4A). These changes are probably due to the intracellular drug transformation.

In the early work we had been found that, in contrast to Quinifuryl, Nitracrine was not bleached during metabolism, but showed a longwave shift of its spectrum maximum in the visible region [17]. Time dependent spectral monitoring of the intracellular content of the Nitracrine-treated K562 cells indeed showed 6 nm shift in compound spectral maximum compared with the intact Nitracrine (Fig. 4B). These spectra also possessed a through at ~ 420 nm with the A^{409}/A^{420} ratio changing with time of drug incubation. Two additional new peaks also appeared in the red region following 1 hr of drug incubation. Overall, these changes clearly indicate intracellular drug transformation.

CONCLUSION.

The results, reported and discussed above, show that two representatives of different families of nitroheterocyclic drugs, Quinifuryl and Nitracrine, possess high cytotoxicity towards leukaemic cells *in vitro*, which may be a result of an intracellular metabolism of the drugs.

It should also be noted that Quinifuryl, deserves special attention as a possible candidate for cancer therapy, considering its high cytotoxicity *in vitro* and relatively low non-specific toxicity to host-animals.

Acknowledgements. This work was supported by Brazilian agencies: CNPq, FAPESP, and CAPES.

REFERENCES

1. Verovskiy VN, Degterev IA, Sukhova NM, Buzukov AA, Leonova EYu, Tatarskaya NK. Interrelation between structure, microssomal metabolising activation, mouse toxicity, cytotoxicity and antitumour activity of heterocyclic- and nitroheterocyclic compounds. *In vitro* and *in vivo* study. Pharmac. Chem. J. 1990; 24: 20 – 24.

2. Wilson WR, Denny WA, Stewart GM, Fenn A, Probert JC. Reductive metabolism and hypoxia-selective toxicity of nitracrine. Int J Radiat Oncol Biol Phys 1986; 12: 1235–1238.

3. Gniazdowski M, Szmigiero L. Nitracrine and its congeners - an overview. Gen Pharmacol 1995; 26: 473-481.

4. Gorlewska K, Mazerska Z, Sowin´ski P, Konopa J. Products of metabolic activation of the antitumor drug Ledakrin (Nitracrine) in Vitro. Chem Res Toxicol 2001; 14:1-10.

5. Voronina SS, Tatarskaia NK, Degterev IA, Serebriany AM, Pelevina II. Radiosensitising activity and metabolism of nitrofuran derivatives. Preparation M-106. Radiobiology (Moscow) 1985; 25: 748-751.

6. Smirnov S.M., Zhurav M.A., Tatarskaya N.K., Borisevich Y.E., Degterev I.A. Phototransformation of quinifur. nitroanion radical formation, Chemical Physics (Moscow) 1989; 8: 17 – 23.

7. Tatarskaya NK, Zhurav MA, Smirnov SM, Degterev IA, Tarasov VF, Borisevich YE, Zaikov GE. Effect of compound and oxygen concentration on primary processes of quinifur phototransformation. Proceed Acad Sci USSR, Chemistry 1989; N 5: 804 –809.

8. Josephy PD, Mason RP. Nitroimidazoles. In: Anders MW, ed. Bioactivation of Foreign Compounds. New York: Academic Press, 1985:161-222,

9. Degterev IA, Buzukov AA, Sharf VG, Popov KN, Serebrianiy AM, Zaikov GE. () Comparative study of in vitro ledakrine metabolism in microssomes of EAC-cells and mouse liver. Pharmac Chem J 1986; 20: 412 – 417.

10. Klein E, Ben-Bassat H, Neumann H, Ralph P, Zeuthen J, Polliac A, Vanky F. Properties of the K562 cell line, derived from a patient with chronic myeloid leukemia. Int J Cancer 1976; 18: 421–431.

11. Mosmann T. Rapid colorimetric assay for cellular growth and survival: application to proliferation and cytotoxicity assays. J Immunol Methods 1983; 65: 55-63.

12. Monks A, Scudiero D, Skehan P, Shoemaker R, Paull K, Vistica D, Hose C, Langley J, Cronise P, Vaigro-Wolff A. Feasibility of a high-flux anticancer drug screen using a diverse panel of cultured human tumor cell lines. JNCI 1991; 83: 757–66.

13. WHO Chronicle (1976) Vol. 30 (Suppl. 3), p 11, World Health Organization, Geneva.

14. Gniazdowski M, Filipski J, Chorazy M. Nitracrine. In Hahn FE ed. Antibiotics V/2. Berlin: Springer, 1979; 275-297.

15. Wilson WR, Denny WA, Twigden SJ, Baguley BC, Probert JC. Selective toxicity of nitracrine to hypoxic mammalian cells. Br. J. Cancer 1984; 49: 215-23.

16. Blatun LA, Svetukhin AM, Pal'tsyn AA, Liapunov NA, Agafonov VA. Clinic-laboratory effectiveness of modern ointments with a polyethylene glycol base in the treatment of purulent wounds. Antibiot. Khimioterapia 1999; 44: 25-31.

17. Degterev IA, Buzukov AA, Tatarskaya NK, Leonova EYu, Sukhova NM. Metabolism of heterocyclic compounds in mouse liver microsomes, Pharmac Chem J 1990; 24: 9 -16.

FIGURE 1.

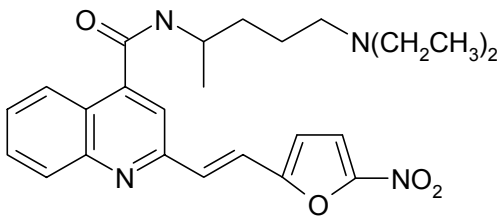

Quinifuryl:

2-(5'–nitro-2'–furanyl) ethenyl-4-{N-[4–(N,N-diethylamino)-1'–methylbutyl] carbamoyl}quinoline.

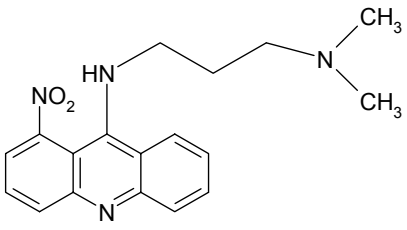

Nitracrine:

1-nitro-9(3'3'- dimethylaminopropylamino)acridine.

FIGURE 2.

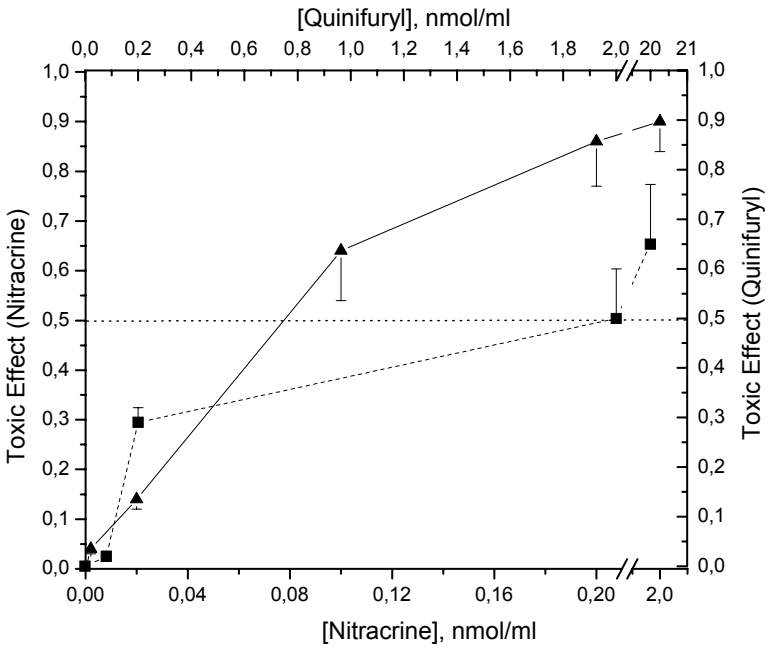
[Quinifuryl], nmol/ml
0,0 0,2 0,4 0,6 0,8 1,0 1,2 1,4 1,6 1,8 2,0 20 21
Toxic Effect (Nitracrine)
Toxic Effect (Quinifuryl)
0,0 0,1 0,2 0,3 0,4 0,5 0,6 0,7 0,8 0,9 1,0
0,00 0,04 0,08 0,12 0,16 0,20 2,0
[Nitracrine], nmol/ml

FIGURE 3.

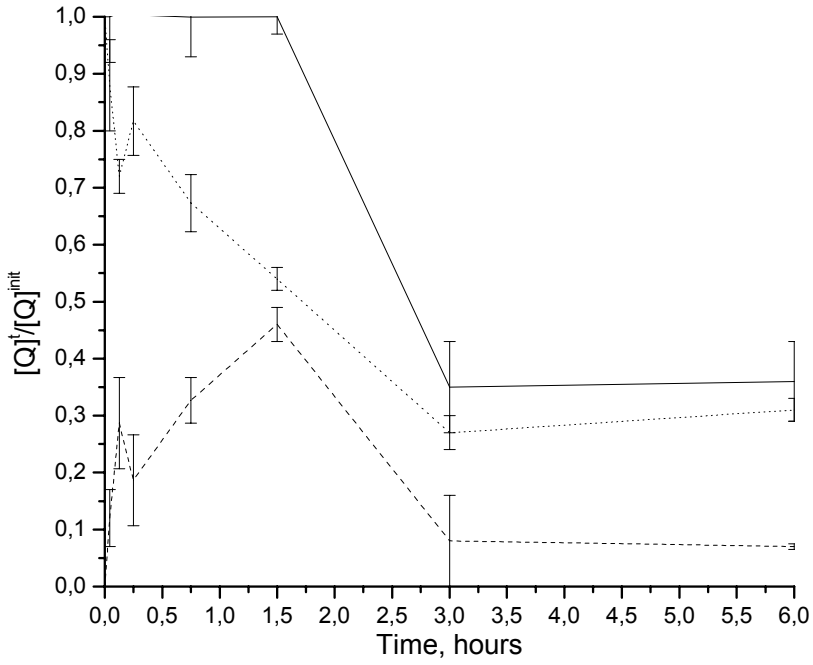
1,0
0,9
0,8
0,7
0,6
0,5
0,4
0,3
0,2
0,1
0,0
[Q]t/[Q]init
0,0
0,5
1,0
1,5
2,0
2,5
3,0
3,5
4,0
4,5
5,0
5,5
6,0
Time, hours

FIGURE 4.

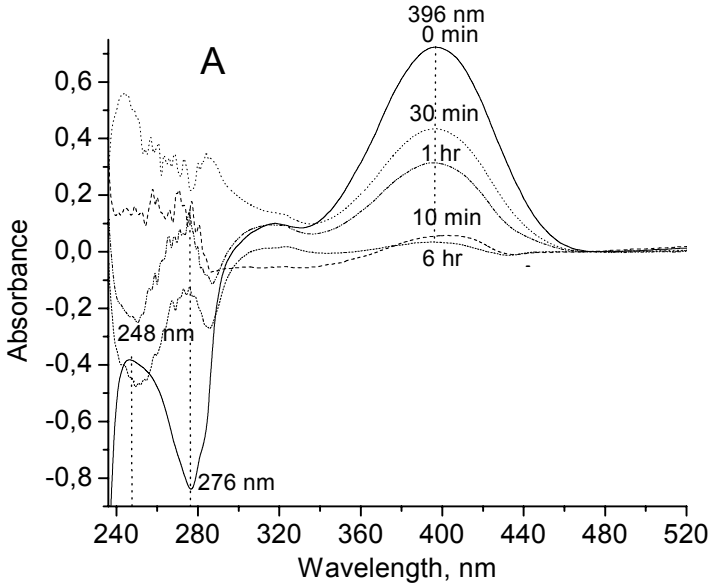
A
396 nm
0 min
30 min
1 hr
10 min
6 hr
248 nm
276 nm
Absorbance
Wavelength, nm
0,6
0,4
0,2
0,0
-0,2
-0,4
-0,6
-0,8
240
280
320
360
400
440
480
520

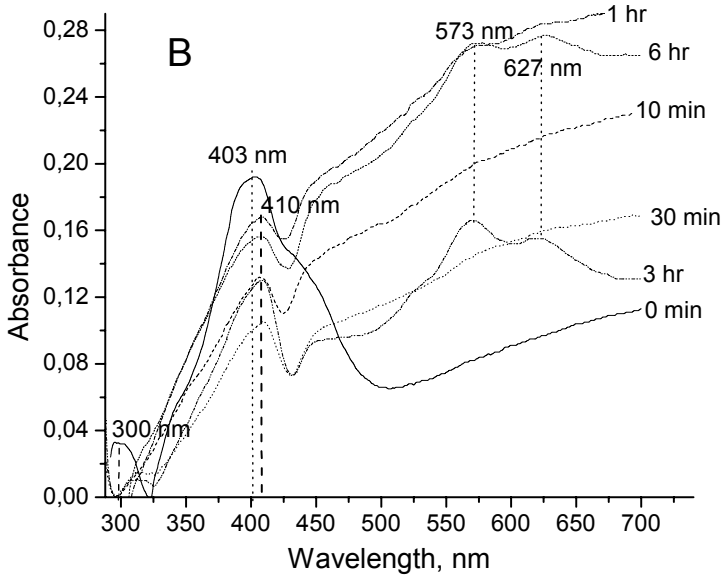
B
573 nm
1 hr
6 hr
627 nm
10 min
403 nm
410 nm
30 min
3 hr
0 min
300 nm
Absorbance
Wavelength, nm
0,28
0,24
0,20
0,16
0,12
0,08
0,04
0,00
300
350
400
450
500
550
600
650
700

TABLE 1. Values of LC_{50} for Quinifuryl and Nitracrine measured at different time lengths.

Cell line	Compound	Time, hr	LC_{50}, μM
K562	Quinifuryl	24	2±0.9
		12	12±2.2
	Nitracrine	24	0.12±0.07
		6	2.2±0.06
P388	Quinifuryl	24	1.1±0.2
	Nitracrine	24	0.16±0.06
		6	0.5±0.13
NIH3T3	Quinifuryl	24	1.2±0.17
		12	11±2.1
	Nitracrine	24	0.13±0.04
		12	1.4±0.2

Each LC_{50} value represents (M ± SD) of two to five completely independent series of experiments with five to six repetitive.

TABLE 2. Time lengths for which the LC_{50} achieved (T^{LC50}) for free compounds

Cell	Compound	Conc., μM	T^{LC50}, hour
K562	Quinifuryl	20	6.5±0.6[a]
		2	21±2.7[b]
	Nitracrine	2	8.4±0.6[c]
NIH-3T3	Quinifuryl	20	3.7±0.2[d]
		2	16±0.2[e]
	Nitracrine	2	8.5±0.4[f]
		0.2	17±2[g]
P388	Quinifuryl	2	5.3±0.7[h]
	Nitracrine	2	3.5±0.1[i]
		0.2	12±2[j]

Data concerning free drugs represent (M ± SD) of two to five completely independent series of experiments with five to six repetitive. * Significant differences were found between T^{LC50} values as follows: $p < 0.01$ (b vs h, c vs i, e vs h, f vs i), $p < 0.05$ (a vs d, g vs j, b vs e). No significant differences (NS) were observed between c and f.

TABLE 3. Toxic effects (TE) of Quinifuryl and Nitracrine observed for 12 hr drug incubation with appropriate cells (TE_{12}) and measured either immediately after drugs withdrawn (Procedure 1) or after followed three 3 cell population doubling time (Procedure 2) (for procedure details see Materials and Methods).

Compound	Cell line								
	K562			P388			NIH3T3		
	TE_{12}	TE_{72}	P	TE_{12}	TE_{36}	p	TE_{12}	TE_{72}	p
Quinifuryl, 2 μM	0.47± 0.08	0.58± 0.05	NS	0.79± 0.01	0.89± 0.04	< 0.05	0.43± 0.16	0.96± 0.01	< 0.05
Nitracrine, 0.2 μM	0.63± 0.09	0.81± 0.06	< 0.01	0.64± 0.11	0.88± 0.03	< 0.05	0.38± 0.1	0.94± 0.005	< 0.05

Each LC_{50} value represents (M ± SD) of one series of experiments with six repetitive. The experiments with each drug followed both procedures were performed in parallel.

FIGURE LEGENDS

FIGURE 1. Structures of Quinifuryl and Nitracrine.

FIGURE 2. Dependence of K562 cell death on concentration of Nitracrine (▲) and Quinifuryl (■). Time of drug incubation with cells: 24 hr.

FIGURE 3. Kinetic of changes of Quinifuryl specific absorbance at 396 nm during drug incubation with K562 cells in supernatant (dotted line), in cell content (dashed line), and balance (solid line). $A_r = A^i/A^0$, where A^0 and A^i – intensities of these peak before and during drug incubation. Balance - $A^i_s + A^i_c/A^0$, where A^i_s and A^i_c are absorbance discovered in supernatant and cell content, respectively. Data represent (M ± SD) of three measurements.

FIGURE 4. Difference absorption spectra of K562 cell content after incubation with Quinifuryl (A) and Nitracrine (B) for various time lengths followed by cell wash and lyses. Solid lines represent spectra of respective drugs before incubation with cells. All spectra were recorded against content of intact cells that was incubated in parallel with no additives. Each measurement made in three repetitive.

CYTOTOXICITY OF NITROHETEROCYCLIC COMPOUNDS, QUINIFURYL AND NITRACRINE, TOWARDS LEUKAEMIC AND NORMAL CELLS ON THE DARK AND UNDER ILLUMINATION WITH VISIBLE LIGHT.

Marcelo M. Rossa[1], Nasser A. Daghastanli[2], Heloisa S. Selistre-de-Araujo[1]

Antonio C. Tedesco[3], Iouri E. Borissevitch[2] , Igor A. Degterev[2,4]*

[1]Department de Ciências Fisiológicas, Universidade Federal de São Carlos, São Carlos, Brasil.

[2]Departamento de Física e Matemática, Faculdade de Filosofia Ciências e Letras de Ribeirão Preto, Universidade de São Paulo, Av. Bandeirantes 3900, CEP 14040-901, Ribeirão Preto, SP, Brazil.

[3]Departamento de Química, Faculdade de Filosofia Ciência e Letras de Ribeirão Preto, Universidade de São Paulo, Av. Bandeirantes 3900, CEP 14040-901, Ribeirão Preto, SP, Brazil.

[4]Department of Chemical & Biological Kinetics, Institute of Biochemical Physics, Russian Academy of Sciences, Kosygin Str. 4, 117333 Moscow, Russian Federation.

Keywords: Photochemotherapy, photocytotoxicity, nitroheterocyclic compounds, Quinifuryl, Nitracrine, lympholeukaemia P388, human erythroleukaemia K562, fibroblast NIH3T3.

*Corresponding author. Present address: Departamento de Física e Matemática, Faculdade de Filosofia Ciências e Letras de Ribeirão Preto, Universidade de São Paulo, Av.

Bandeirantes 3900, Vila Monte Alegre, CEP 14040-901, Ribeirão Preto, SP, Brasil. Phone: 55 (016) 602-3862, FAX: 55 (016) 633-9949 E-mail: igor@dfm.ffclrp.usp.br

ABSTRACT

The cytotoxicity of two nitroheterocyclic compounds (NHCD), Nitracrine, 1-nitro-9(3_3_-dimethylaminopropylamino) acridine and Quinifuryl, 2-(5`-nitro-2`-furanyl) ethenyl-4-{*N*-[4-(*N*,*N*-diethylamino)-1`-methylbutyl] carbamoyl}quinoline, towards two lines of leukaemic cells and a line of non-transformed cells, was measured in comparison, on the dark and under illumination with visible light (350-450 nm). Both drugs showed highly elevated cytotoxicity when illuminated with LC_{50} values 7÷35 times lower after 1 h illumination compared to 1 h incubation of cells incubation with drug on the dark. Cytotoxicity of Nitracrine toward all cell lines studied exceeded that of Quinifuryl, both on the dark and under illumination, so that ≈ 10 times lower concentration of former drug was needed to reach the same toxicity as the latter. General toxic effect was calculated as a direct cell kill and a cell proliferation arrest. The effect > 80% for both drugs was achieved after 1 h cell illumination with as low drug concentrations as 0.2 μM for Quinifuryl and 0.02 μM for Nitracrine.

INTRODUCTION

Photochemotherapy (PCT) is a mode of cancer treatment based on a supply a target (cancer) tissue with a photoactive agent (photosensitizer) followed by illumination of tumor with light to produce species that are highly toxic to a target [1-3]. The extensive search of new agents for PCT is continued [3-7] and studies on the mechanism of their phototoxicity are developing [8,9].

Quinifuryl is an antiseptic in surgery for the treatment of wounds and burns [10]. Our previous analysis of cytotoxicity has demonstrated that Quinifuryl displayed the high cytotoxicity ($LC_{50} \leq 2\mu M$) towards melanoma B16 [11], murine lympholeukaemia P388 cells [11,12], and human erythroleukaemia K562 cells [12]. At the same time, this compound was shown to be photolabile absorbing intensively visible light ($\lambda^{max} = 396$ nm, $\varepsilon_{396} = 2.47 \times 10^4$ $M^{-1}cm^{-1}$ [12] and producing reactive species during photoexcitation [13-15]. This fact led us to an assumption that the illumination of tumor cells with the visible light may result in the drug cytotoxicity potentiation.

The aim of the present work was to extend number of cellular targets for Quinifuryl in order to confirm intensified photocytotoxicity of this compound and to compare the photocytotoxic potency of Quinifuryl with that of Nitracrine, a 1-nitroacridine derivative, known as a potent hypoxia-selective agent *in vitro* [16,17] and used clinically as antitumor drug [18]. Our previous analysis of cytotoxicity has demonstrated that Nitracrine and Quinifuryl displayed the high cytotoxicity ($LC_{50} \leq$

2μM) towards melanoma B16 [11], murine lympholeukaemia P388 cells [11,12], and human erythroleukaemia K562 cells.

Quinifuryl possesses the optical absorption more intense that this of Nitracrine (Nitracrine – ε_{400}= 4 x 10^3 $M^{-1}cm^{-1}$, Quinifuryl – ε_{396} = 2.47 x 10^4 $M^{-1}cm^{-1}$, respectively, [12]). No study of Nitracrine photocitotoxicity was ever made.

In this work cellular toxicity of drugs towards murine leukemia P388, fibroblast NIH3T3, and human erythroleukaemia K562 cells was measured on the dark and under illumination with visible light.

MATERIALS AND METHODS.

Drugs. Quinifuryl (M-106), 2-(5`-nitro-2`-furanyl) ethenyl-4- {*N*- [4-(*N*, *N*-diethylamino)-1`-methylbutyl] carbamoyl} quinoline, a representative of a family of 5-nitrofuran-ethenyl-quinoline drugs, was synthesized and purified by Dr. N. M. Sukhova. Nitracrine (Ledakrine, C-283), 1-nitro-9 (3`, 3`-dimethylaminopropylamino) acridine was purchased from Polfa. Structural authenticity of both drugs was verified by NMR analysis. Structural formulas of both drugs are present in Fig. 1.

Cells. The human K562 leukemia cell line (proerythrocytes), which was originally derived from the patient with erythroleukaemia [19], was kindly provided by Dr. S. Niewiarowski (Temple University, PA, USA). $P388D_1$ cells, a mouse macrophage monocyte line that grows in semi-suspension, and immortalized mouse fibroblast NIH3T3 cells were obtained from the American Type Culture Collection. P388 cells were cultured in Fisher's media supplemented with 10 % heat inactivated horse serum in 175cm^2 culture flasks at 37^{o}C with 5% CO_2. K562 and NIH3T3 cells were cultured as a suspension or a monolayer, respectively, in Dulbecco's modified Eagle's medium (DMEM) supplemented

Excluído: cm 2

Excluído:

with heat-inactivated 10% fetal bovine serum (FBS), 1% l-glutamine, 50 units/ml penicillin, 50 mg/ml streptomycin, 250 mg/ml Anfotericin-B at 37 .C in a water-jacketed CO_2 incubator (Cellstar, USA). The day before an experiment, cells were seeded at 5 x 10^5 cells/mL. The number of cells in suspension was calculated using a Neubauer chamber (0.0025mm^2). A slow magnetic stirring was used to maintain the suspension in homogeneous state. All preparations were made under subdued red light (λ > 550 nm) at room temperature (22^{o}C).

Excluído: l

Excluído: of low illumination intensity

The toxicity test was based on the MTT assay and performed in two ways measuring either direct killer effect of a drug (Test 1) or general toxic effect that included a cell proliferation arrest (Test 2) [12]. The tetrazolium salt 3-(4,5-dimethylthiazol-2-yl)-2-5 diphenyl tetrazolium bromide (MTT) is reduced into leaving cells to yield a colored product that may be interpreted as a measure of viability [20]. For MTT assays, cells were seeded in DMEM containing 5% FBS into wells of 96-well ELISA-type plates and exposed to a range of either drug concentrations from 0,02 to 2 μM for time intervals either from 1 to 24 h (experiments on the dark) or from 10 to 90 min (experiments under illumination). At the end of the drug exposure period, plates were centrifuged to pellet cells and drug-contained supernatants were displaced with either MTT dissolved in PBS (*Test 1*) or with fresh medium (Test 2). In the latter case, the cells were incubated for the 2–3 cell population-doubling times (36–72 h) with daily media change, followed by MTT assay. In both tests, plates with MTT were incubated in the dark for 4 h, after which the water-insoluble MTT-formazan crystals were dissolved in DMSO, and absorbance was recorded in an ELISA plate reader Dynex MRX (Dynex Technologies Inc.) at 570 nm. The initial

seeding densities ranged from 2×10^4 to 6×10^4 cells/well. Cell viability was assessed by TB dye exclusion at the beginning of each experiment and was always higher than 96%.

Irradiation. Samples, containing cells and drug, and controls, containing cells in the absence of drug, were irradiated directly in ELISA-type plates, in the spectral range from 350 to 450 nm using standard light source with tungsten lamp (150 W) and the glass filter (5-57 KOPP color glass filter). The intensity of irradiation was 22mW/cm^2, as measured by a Spectra-Physics 407A radiometer.

Calculation of the results. Drug concentration dependence and time dependence of cell death were calculated as a toxic effect (TE): TE = [DC]/[Cell]^{control}, where [Cell]^{control} is cell concentration, in control wells (cells incubated for the same time length with no compound) and [DC] is the dead cell concentration. [DC] was calculated as [Cell]^{control} - [Cell]^{final}, were [Cell]^{final} is the live cell concentration in wells exposed to drug [12]. Cell concentration was measured using a calibration curve made for all cell lines tested using MTT-staining method. The LC_{50} of the tested compounds was estimated as $100 \times (T\text{-}T_0)/T_0 = 50$, where T_0 and T are optical densities of the test well at time zero (when the compound is added) and after exposure to test compound [21]. The LC_{50} was measured after 1 h cell incubation with either drug on the dark or under illumination.

Statistic analysis. The data are presented as the mean ± S.D. of two to five independent series of experiments with five to six repetitions in each. Statistic analysis was performed on the Student's *t*-test. The Turkey's test with 95% confidence was applied to compare the means. Statistic analyses were done using the InStat software program for Windows (GraphPads software, San Diego, USA).

RESULTS

Excluído: ¶
Inserido: ¶
Excluído: ¶
Excluído: 200

One example of a drug cytotoxicity measurements are present in Fig. 2 that shows a development of toxic effect (TE) toward human K562 erythroleukaemia cells as a function of cell incubation time with drug either under illumination with visible light (Panel A) or on the dark (Panel B). The TE values were calculated as was described in the Materials and Methods. Cells incubated without drug served as a control in each series of experiments. Normally, no significant amounts of dead cells were observed in control wells up to 24 h incubation on the dark and up to 1.5 h illumination.

Both drugs were much more cytotoxic under illumination than on the dark. Death of 50% of cells were achieved under illumination for 45 min and 48 min for 2 μM of Quinifuryl and for 0.2 μM of Nitracrine, respectively (Fig. 2A), while on the dark it took 8.5 hr for Nitracrine and 18.4 hr for Quinifuryl (Fig. 2B). Nitracrine possesses higher cytotoxicity than Quinifuryl on the dark and under illumination. So that 10-times lower concentration of Nitracrine produced the same (illumination, Fig. 2A) or higher (on the dark, 2B) toxic effects towards K562 cells than Quinifuryl.

The majority of the experimental data was obtained following Test 1 (Materials and Methods), according to which MTT-dye incubation was performed immediately following drug treatment. This approach limits the observed results only to the direct killer effect of the drug. Table 1 shows that the LC_{50} values observed after 1 hour illumination were lower, compared to the dark experiments, by at least order of magnitude. All cells were more sensitive to Nitracrine, compared to Quinifuryl, both on the dark and under illumination.

The cell kill (Test 1) and general toxicity (Test 2) experiments were performed in parallel. Briefly, cells were incubated with drugs in a pare of ELISA-type plates for either 12 h on the dark or 1 h under illumination with filtered visible light (350-450 nm). In each pare, one plate was subjected to the measurement of toxic effect immediately after a drug withdrawal (Test 1). In the second plate, drugs were replaced with complete medium and cells were allowed to proliferate for the 2-3 population-doubling time that were either 72 h (K562 and NIH3T3) or 36 h (P388). Subsequently, the medium was replaced with MTT-

dye and the TE was measured as a ratio of dead cells to initial cell amount (see Materials and Methods. The direct killer effect (Test 1) and general toxic effect (Test 2) of both drugs towards three cell lines measured in parallel are present in Table 2.

Being applied at the same concentration, both drugs kill cells much rapidly when illuminated with visible light. Table 3 shows the incubation times required to reach death of 50% of cells at different drug concentrations either on the dark or under illumination with visible light.

DISCUSSION

The results of our previous works have shown that Quinifuryl and Nitracrine, representatives of two different groups of nitroheterocyclics, are highly toxic (($LC_{50} \leq 2$ μM) toward various lines of tumor cells on the dark: melanoma B16 [11], mouse limpholeukaemia P388 [11,12], human K562 erythroleukaemia cell [12], with Nitracrine always displayed higher cytotoxicity than Quinifuryl.

The results presented in this work show that the illumination with visible light sharply decreased lethal concentrations of both agents (Table 1) and shortened time of the lethal effect run up (Table 3).

Table 2 shows that the killer effects (Test 1) of both drugs, when illuminated with visible light for 1 h, were similar to those observed after 12 h drug incubation with either cells on the dark. The effect of Nitracrine was higher, compared to Quinifuryl, both on the dark and under illumination. Significant toxicity toward P388 and NIH3T3 cells was observed for low concentration (0.2 μM) of Quinifuryl under illumination, while negligible (P388) or no (NIH3T3) toxicity was observed for 12 h of drug incubation with these cells on the dark. These results also show that drugs not only caused death, but also attenuated proliferation of the surviving cells. In contrast to direct killer effect, general toxicity (Test 2) of both drugs toward P388 and NIH3T3 cells after 1 h illumination and 12 h of the dark incubation was similar.

Mechanisms of dark-cytotoxicity of Quinifuryl and Nitracrine are, probably, due to their metabolism. Both drugs were metabolized in normal tissues [22-24] and cancer cells [11,22]. Nitracrine is believed to produce reactive intermediate(s) during metabolism that causes DNA modification [17]. Both drugs accelerate the production of reactive oxygen [23] and nitrogen [25-27] species during metabolism. Thus, their toxicity may also be due to oxidative stress.

The fact that the photoactivation significantly accelerates cell killing should be interpreted as either formation more toxic intermediates during photolysis, compared to the dark metabolism, or acceleration of the same toxins formation under illumination, or both. Evidence of reactive species formation during photolysis of Quinifuryl by visible light was reported in our previous works [13-15]. The formation of the triplet excited state [14], which is capable to produce singlet oxygen [1-3], the reaction of the triplet state with the drug in the ground state and with electron donors [13-15], forming of superoxide anion radical in the course of drug photolysis [13] could result in the Quinifuryl phototoxicity.

In contrast to Quinifuryl, there is no data available on the Nitracrine photolysis. This fact creates no room for speculations on the mechanism of photocytotoxicity of this drug that, undoubtedly, deserves special study.

The above data show that nitroheterocyclic compounds deserve study as possible candidates for photochemistry therapy. Differently from cited work, we had shown here that elevated cytotoxicity under illumination with visible light is not specific property of Quinifuryl, but also resides to nitroheterocyclic compound of quite different structure. Photosensitizing effect was observed with cancer cells as different as mouse limpholeukaemia and human erythroleukemia.

REFERENCES

1. **Henderson, B. W. and T. R. Dougerthy (1992) How does photodynamic therapy work? *Photochem. Photobiol.* 55, 145-157.**
2. **Ochsner, M. (1997) Photophysical and photobiological processes in the photodynamic therapy of tumors. *J. Photochem. Photobiol. B:Biology* 39,1-18.**
3. Sobolev, A. S., D. A. Jans and A. A. Rosenkranz (2000) Targeted intracellular delivery of photosensitizers. *Prog. Biophys. Mol. Bio.* **73**, 51-90.
4. Franck, B. and A. Nonn (1995) Novel porphyrinoids for chemistry and medicine by biomimetic syntheses. *Angew. Chem. Int. Ed. Engl*. **34**, 1795-1811.
5. Oertel, M., S. I. Schastak, A. Tannapfel, R. Hermann, U. Sack, J. Mossner and F. Berr (2003) Novel bacteriochlorine for high tissue-penetration: photodynamic properties in human biliary tract cancer cells in vitro and in mouse tumour model. *J. Photochem. Photobiol. B: Biology* **71**, 1-10
6. Bourre, L., G. Simonneaux, Y. Ferrand, S. Thibaut, Y.Lajat, and T. Patrice (2003) Synthesis, and in vitro and in vivo evaluation of a diphenylchlorin sensitizer for photodynamic therapy. *J. Photochem. Photobiol. B: Biology* **69**, 179-192.
7. Kassab, K. (2002) Photophysical and photosensitizing properties of selected cyanines. *J. Photochem. Photobiol. B: Biology* **68**,15-22.
8. Dobrucki, J. W. (2001) Interaction of oxygen-sensitive luminescent probes Ru(phen)32+ and Ru(bipy)32+ with animal and plant cells in vitro: Mechanism of photoxicity and conditions for non-invasive oxygen measurements. *J. Photochem. Photobiol. B: Biology* **65**,136-144.

9. Bohm, F., R. Edge, S. Foley, L. Lange, and T. G. Truscott (2002) Antioxidant inhibition of porphyrin-induced cellular phototoxicity. *J. Photochem. Photobiol. B: Biology* **65**, 177-183.

10. Blatun, L. A., A. M. Svetukhin, A. A. Pal'tsyn, N. A. Liapunov, and V. A. Agafonov (1999) Clinic-laboratory effectiveness of modern ointments with a polyethylene glycol base in the treatment of purulent wounds. *Antibiot. Khimioterapia* **44**, 25–31.

11. Verovskiy, V. N., I. A. Degterev, N. M. Sukhova, A. A. Buzukov, E. Yu. Leonova., N. K. Tatarskaya (1990) Interrelation between structure, microsomal metabolizing activation, mouse toxicity, cytotoxicity and antitumor activity of heterocyclic- and nitroheterocyclic compounds. In vitro and in vivo study. *Pharmac. Chem. J.* **24**, 20–24.

12. Rossa, M. M., T. A. A. Rocha-e-Silava, C. H. B. Terruggi, A. C. Tedesco, H. S. Selistre-de-Araujo, I. E. Borissevich, I. A. Degterev (2003) Comparison of the cytotoxicity of two nitroheterocyclic drugs (NHCD) towards transformed and non-transformed cells. *Pharm. Res.* **48**, 369-375.

13. Smirnov, S. M., M. A. Jurav, N. K. Tatarskaja, Yu. E. Borisevich, I. A. Degterev (1989) Quinifur photoreduction Nitroanionradical formation. *Chemical Physics* (Moscow) **8**, 1723-1725.

14. Borissevich, I. E., N. A. Daghastanli, I. A. Degterev (2003) Primary processes of photodecomposition of 2-(5'-nitro-2'-furanyl)ethenyl-4-{N-[4'-(N,N-diethylamino)-1'-methylbutyl]carbamoyl}quinoline. Effect of oxygen and compound concentration. *J Photochem. Photo.iol A:Chemistry* **159**, 213-217.

15. Kuzmin, V. A., P. P. Levin, Yu. E. Borisevich, I. A. Degterev, S. M. Smirnov (1988) Triplet Excipleks of Nitrofuran Derivative with Aromatic Amines. *Proceed. Acad. Sci. USSR, Chemistry,* N 7, pp. 1510 – 1514.

16. Gniazdowski, M. and L. Szmigiero (1995) Nitracrine and its congeners—an overview. *Gen. Pharmacol.* **26**, 473–81.

17. Gorlewska, K., Z. Mazerska, P. Sowin'ski, J. Konopa (2001) Products of metabolic activation of the antitumor drug Ledakrin (Nitracrine) in Vitro. *Chem Res Toxicol.* **14**, 1–10.

18. WHO Chronicle, vol. 30 (Suppl. 3). Geneva: World Health Organization; 1976. p. 11

19. Klein E., H. Ben-Bassat, H. Neumann, P. Ralph, J. Zeuthen, A. Polliac, F. Vanky (1976) Properties of the K562 cell line, derived from a patient with chronic myeloid leukemia. *Int. J. Cancer* **18**, 421–31.

20. Mosmann, T. (1983) Rapid colorimetric assay for cellular growth and survival: application to proliferation and cytotoxicity assays. *J. Immunol. Methods* **65**, 55-63.

21. Monks A, D. Scudiero, P. Skehan, R. Shoemaker, K. Paull, D. Vistica, C. Hose, J. Langley, P. Cronise, A. Vaigro-Wolff (1991) Feasibility of a high-flux anticancer drug screen using a diverse panel of cultured human tumor cell lines. *JNCI* **83,** 757–66.

22. Degterev, I. A., A. A. Buzukov, V. G. Sharf, K. N. Popov, A. M. Serebrianiy, G. E. Zaikov (1986) Comparative study of in vitro ledakrine metabolism in microsomes of EAC-cells and mouse liver, *Pharmac. Chem. J.* **20**, 412 – 417.

23. Degterev, I. A., A. A. Buzukov, N. K. Tatarskaya, E. Yu. Leonova, N. M. Sukhova (1990) Metabolism of heterocyclic compounds in mouse liver microsomes, *Pharmac. Chem. J.* **24**, 9 -16.

24. Degterev, I. A., P. C. L. Nogueira, A. J. Marsaioli, A. E. Vercesi (1999) Microsomal metabolism of quinifuryl - a nitrofuryl-ethenyl-quinoline antiseptic possessing antitumor activity *in vitro, Europ. J. Drug Metab. Pharmac.* **24**, 15-22.

25. Iliasova, V. B., A. A. Buzukov, M. Tabak, I. A. Degterev (1994) On the mechanism of metabolic denitration of nitroheterocyclic compounds. *Biofizika* (Moscow) **39**, 219 – 225.

26. Buzukov, A. A., V. B. Iliasova, M. Tabak, N. K. Tatarskaya, I. A. Degterev (1995) Metabolic denitration of Quinifuryl and Nitracrine in mouse liver homogenate. *Pharmac. Chem. J. (Moscow)* **29**, 3 – 8.

27. Buzukov, A. A., V.B. Il'asova, M. Tabak, N. C. Meirelles, I. A. Degterev (1996) An ESR and spectrophotometric study of the denitration of nitroheterocyclic drugs by liver homogenates and their metabolic consumption by liver microsomes from cytochrome P-450-induced mice. *Chem.-Biol. Interact.* **100**, 113 – 124.

LEGENDS TO FIGURES

FIGURE 1. Structures of Quinifuryl and Nitracrine.

FIGURE 2. Photocytotoxicity (A) and cytotoxicity on the dark (B) of Quinifuryl (●) and Nitracrine (■) towards human erythroleukemia K562 cells as measured by method dye inclusion (MTT). Vertical dashed lines show time needed to rich kill of 50% of cells. Drug concentrations were as follows: Quinifuryl – 2.0 μM; Nitracrine - 0.2 μM. Conditions: cell concentration was ~ $1x10^6$ in Na-phosphate buffer, pH7.4; mixtures were illuminated at room temperature with filtered (350-450 nm) light of tungsten lamp (200W) at 22^0C with the irradiation intensity of 22 mW/cm^2. Toxic effect was measured as $[DC]/[Cell]^{control}$, where $[Cell]^{control}$ is cell concentration, in control wells (cells incubated for the same time length with no compound) and [DC] is the dead cell concentration. Each point represents M±SD of six measurements.

Table 1. The LC_{50} for Quinifuryl and Nitracrine measured after 1 h of cells incubation with drug either on the dark or under illumination with visible light.

Drug	LC_{50}, μM	
	Dark	Illumination
P388 cells		
Quinifuryl	79.7±18.1	11.8±3.8
Nitracrine	7.7±1.3	0.23±0.15
NIH3T3 cells		
Quinifuryl	18.6±6.0	1.6±0.7
Nitracrine	16.2±2.8	0.6±0.6
K562 cells		
Quinifuryl	*15.4±2.4	1.48±0.33
Nitracrine	*8.9±0.8	0.16±0.04

* - no significant cytotoxicity was observed after 1 h of K562 cells incubation with either drug, thus cytotoxicity on the dark was measured after 12 h of cell incubation with drugs.

Table 2. Direct kill effect (Test 1) and general toxicity (Test 2) of Quinifuryl and Nitracrine toward P388 cells either on the dark or under illumination with visible light.

Drug	[Drug], μM	TOXIC EFFECT			
		Dark, 12 h		Illumination, 1h	
		Test 1	Test 2	Test 1	Test 2
P388 cells					
Quinifuryl	2.0	*0.48±0.1	0.97±0.16	*0.76±0.27	0.93±0.20
	0.2	*0.014±0.002	n. m.	*0.13±0.04	0.84±0.24
Nitracrine	0.2	0.59±0.2	0.97±0.15	*0.64±0.17	0.99±0.26
	0.02	*0.14±0.05	n. m.	*0.49±0.13	0.97±0.26
NIH3T3 cells					
Quinifuryl	2.0	*0.59±0.13	0.96±0.01	*0.43±0.16	0.93±0.04
	0.2	*0.0±0.06	0.0±0.12	*0.35±0.12	0.87±0.12
Nitracrine	2.0	0.56±0.1	0.96±0.15	n. m.	0.89±0.20
	0.2	*0.38±0.1	0.94±0.01	*0.65±0.14	0.89±0.12
	0.02	*0.25±0.03	0.89±0.2	*0.41±0.11	n. m.
K562 cells					
Quinifuryl	2.0	*0.33±0.1	n. m.	*0.68±0.15	n. m.
Nitracrine	0.2	0.63±0.03	n. m.	0.68±0.17	n. m.

In each row, symbol (*) marks statistically significant difference ($P < 0.01$) between the results of Test 1. No significant differences were observed between Tests 2 on the dark and under illumination in each series of experiments.

Table 3. Time for which death of 50% of cells achieved (τ_{50})

Drug	[Drug], μM	τ_{50}, min	
		Dark	Illumination
P388 cells			
Quinifuryl	20.0	231±51	25±7
	2.0	350±118	76±9
	0.2	1540±90	96±11
Nitracrine	0.2	390±179	76±9
	0.02	431±43	97±13
NIH3T3 cells			
Quinifuryl	2.0	408±67	34±18
	0.2	> 500	56±17
Nitracrine	0.2	191±13	31±15
	0.02	622±115	58±28
K562 cells			
Quinifuryl	2.0	n. m.	45±5
Nitracrine	0.2	n. m.	48±7

QUINIFURYL

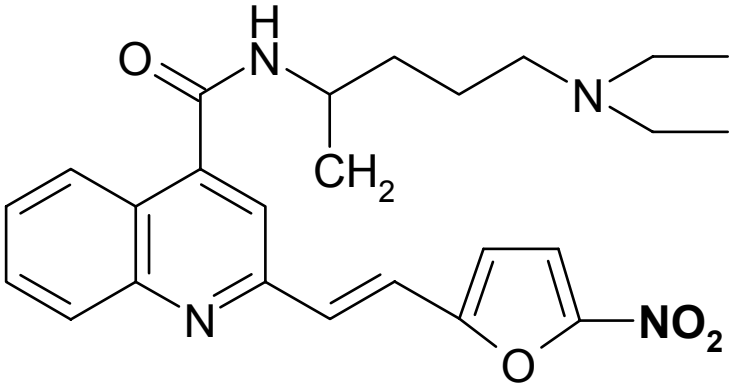

NITRACRINE

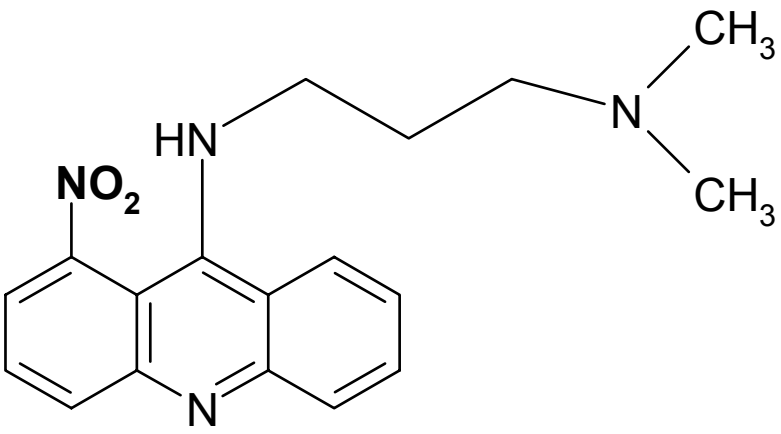

Figure 1.

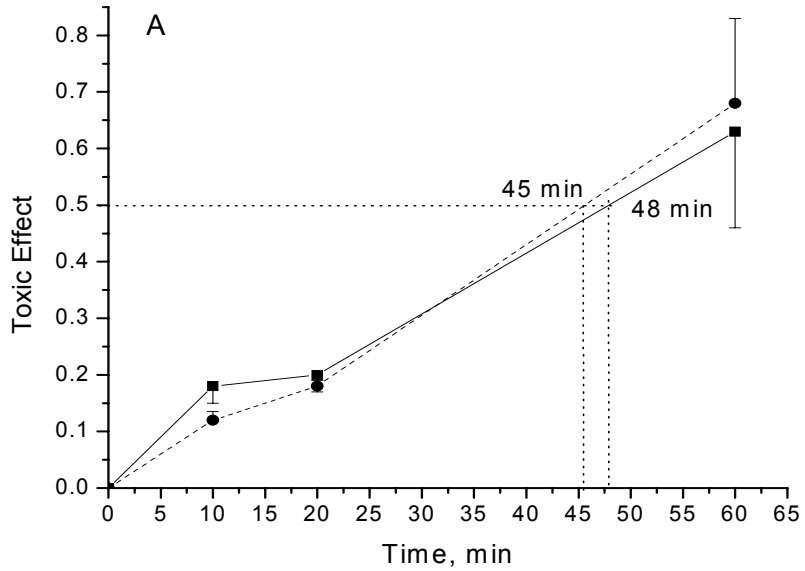
A
Toxic Effect
Time, min
45 min
48 min
0.0
0.1
0.2
0.3
0.4
0.5
0.6
0.7
0.8
0
5
10
15
20
25
30
35
40
45
50
55
60
65

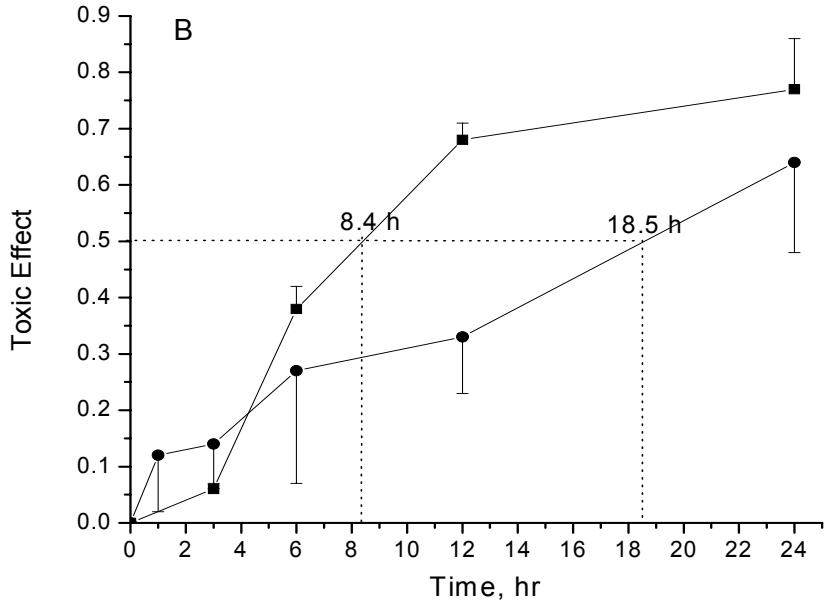
B
Toxic Effect
Time, hr
8.4 h
18.5 h
0.0
0.1
0.2
0.3
0.4
0.5
0.6
0.7
0.8
0.9
0
2
4
6
8
10
12
14
16
18
20
22
24

Figure 2.

ACADEMIC PRESS

Pharmacological Research xxx (2003) xxx–xxx

Pharmacological research

www.elsevier.com/locate/yphrs

Comparison of the cytotoxicity of two nitroheterociclic drugs (NHCD) towards transformed and non-transformed cells

Marcelo M. Rossa [a], Thomaz A.A. Rocha-e-Silva [a], Cristina H.B. Terruggi [a], Antonio C. Tedesco [b], Heloisa S. Selistre-de-Araujo [a], Iouri E. Borissevich [c], Igor A. Degterev [d,*]

[a] *Department of Physiological Sciences, Federal University of São Carlos, São Carlos, Brazil*
[b] *Department of Chemistry, University of São Paulo, Riberão Preto, Brazil*
[c] *Department of Physics and Mathematics, University of São Paulo, Riberão Preto, Brazil*
[d] *Department of Chemical and Biochemical Kinetics, Institute of Biochemical Physics, Russian Academy of Sciences, Moscow, Russia*

Accepted 9 May 2003

Abstract

The cytotoxicity of two nitroheterocyclic compounds (NHCD), Nitracrine, 1-nitro-9(3′3′-dimethylaminopropylamino) acridine (Polfa, Poland) and Quinifuryl, 2-(5′-nitro-2′-furanyl) ethenyl-4-{*N*-[4-(*N*,*N*-diethylamino)-1′-methylbutyl] carbamoyl}quinoline (Dr. N. M. Sukhova, Institute of Organic Synthesis, Riga, Latvian Republic), towards two lines of leukaemic cells and a line of non-transformed cells, was determined under normoxia conditions. Although both drugs showed significant cytotoxicity to all cell lines (LC_{50} for 24 h, $\leq$2 μM) with that of Nitracrine exceeding Quinifuryl, their toxicity towards murine leukaemia P388 was substantially higher, compared to murine fibroblasts NIH3T3. In addition, the rate of cell death was also two- to three-fold higher in case of P388 cells versus NIH3T3. Interestingly, human erythroleukaemia K562 cells were shown to uptake the drugs 10 min after their addition to the tissue culture medium, while the LC_{50} values were reached after a substantial delay of 3 h. This delay might be due to the intracellular transformation of drugs required for cell killing.

Keywords: Cytotoxicity; Nitroheterocyclic drug; Lympholeukaemia P388; Erythroleukaemia K562; Fibroblasts NIH3T3

1. Introduction

Nitroheterocyclic compounds (NHCD), which are typically used as antibiotics, have been, over the years, also shown to possess prominent anticancer activity. The anticancer therapeutic potential of the NHCDs is based on their cytotoxic, radiosensitising, and chemosensitising properties towards tumour cells. The most widely used among them are derivatives of 5-nitroimidazole, 5-nitrofuran, and 1-nitroacridine.

We have previously analyzed the cytotoxicity of a large group of NHCD, which were derivative from 5-nitrofuran and 1-nitroacridine, towards melanoma B16 and murine lympholeukaemia P388 cells [1]. Nitracrine, which is a 1-nitroacridine derivative, and Quinifuryl, a 5-nitrofuryl-vynyl-quinoline derivative, displayed the highest cytotoxicity among studied compounds.

In contrast to Nitracrine, which is a well established antitumor agent [2–4], this activity of Quinifuryl has not been thoroughly characterized. It was previously shown to display the highest toxicity towards two tumour cell lines in vitro, compared to a number of other 5-nitrofuran derivatives, and low toxicity towards tumour (P388)-bearing mice [1], whereas another report demonstrated its radiosensitising activity [5]. Additionally, Quinifuryl has been reported to be highly photolabile, producing the ROS during illumination with visible light [6,7], and we have recently discovered light-dependent elevation in its toxicity towards different tumour cell lines (manuscript in preparation). This observation makes Quinifuryl a possible candidate for cancer phototherapy. Since our initial studies [1] showed significantly higher tolerance (∼30 times) of tumour (P388)-bearing animals to

Abbreviations: NHCD, nitroheterocyclic drugs; LC_{50}, lethal concentration 50%; TE, toxic effect; DMEM, Dulbecco's modified Eagle's medium; FBS, fetal bovine serum

* Corresponding author. Present address: DSF/ICB/UFSCar, Rodovia Washington Luis km 235, São Carlos, SP 13565-905, Brazil. Tel.: +55-16-260-8327; fax: +55-16-260-8327.
E-mail address: vigordgt@power.ufscar.br (I.A. Degterev).

1043-6618/03/$ – see front matter © 2003 Published by Elsevier Science Ltd.
doi:10.1016/S1043-6618(03)00183-X

Quinifuryl than to Nitracrine, a more detailed comparison of Quinifuryl's cytotoxicity to Nitracrine in vitro was performed to establish its in vitro potency in order to gain insight into the cause of low in vivo cytotoxicity.

It has been hypothesized that NHCD might posses specific toxicity toward hypoxic tumour cells, which is particularly relevant for Nitracrine, since its cytotoxic effect is attributed to DNA cross-linking [2–4]. However, based on other data, the role of oxygen metabolism in NHCD action cannot be discounted. NHCD are well known to activate oxygen in biological tissues, transferring one electron from cytochrome c (P450) reductase to oxygen molecule [8]. In particular, Quinifuryl and Nitracrine were both shown to highly accelerate the ROS production in melanoma B16, limpholeukemia P388 cells [1] and Erlich's carcinoma cells [9]. Thus, oxidative stress may be a possible mechanism for drug toxicity towards tumour cells under normoxic conditions. In the present study we examined cellular toxicity of both drugs towards murine leukaemia P388, fibroblast NIH3T3, and human erythroleukaemia K562 cells under these conditions, because they may be more relevant for the drug's mode of action in vivo. In addition, analyses of drugs metabolism in cells were also performed to determine their susceptibility to biotransformation and to determine the role of this process in NHCD toxicity.

Since elevated toxicity to the transformed, as opposed to the non-transformed, cells is a highly desirable feature in anticancer drugs, special emphasis has been placed on the comparisons of the drugs effects in highly tumorogenic, leukaemic (P388), and non-tumorogenic (NIH3T3) murine cells.

2. Materials and methods

2.1. Drugs

Quinifuryl (M-106), 2-(5′-nitro-2′-furanyl) ethenyl-4-{*N*-[4-(*N*,*N*-diethylamino)-1′-methylbutyl] carbamoyl} quinoline was synthesized and purified by Dr. N. M. Sukhova. Nitracrine (Ledakrine, C-283), 1-nitro-9(3′3′-dimethylaminopropylamino) acridine was purchased from Polfa. Structural authenticity of both drugs was verified by NMR analysis. Structural formulas of both drugs are present in Fig. 1.

2.2. Cells

$P388D_1$ cells, a mouse lymphocyte cell line, and immortalized mouse fibroblast NIH3T3 cells were obtained from the American Type Culture Collection (ATCC). The human K562 leukaemia cell line (proerythrocytes), which was derived originally from the patient with erythroleukaemia [10], was kindly provided by Dr. S. Niewiarowski (Temple University, PA, USA). P388 cells were cultured in Fisher's media supplemented with 10% heat inactivated horse serum in 175 cm^2 culture flasks at 37 °C with 5% CO_2. K562 and NIH3T3 cells were cultured as a suspension or a monolayer, respectively, in Dulbecco's modified Eagle's medium (DMEM) supplemented with heat-inactivated 10% fetal bovine serum (FBS), 1% L-glutamine, 50 units/ml penicillin, 50 mg/ml streptomycin, 250 mg/ml Anfotericin-B at 37 °C in a water-jacketed CO_2 incubator (Cellstar, USA).

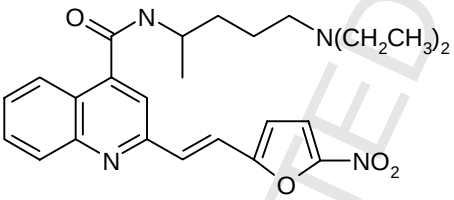

Quinifuryl:

2-(5'–nitro-2'–furanyl) ethenyl-4-{N-[4–(N,N-diethylamino)-1'–methylbutyl] carbamoyl}quinoline.

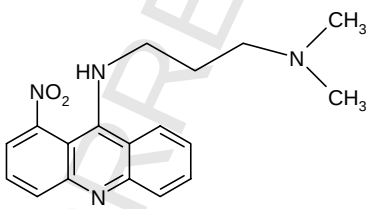

Nitracrine:

1-nitro-9 3'3'- dimethylaminopropylamino)acridine.

Fig. 1. Structures of Quinifuryl and Nitracrine.

The cellular density was measured with hemocytometer and viability was assessed by counting of trypan blue dye-excluded cells.

2.3. Cytotoxicity assays

The activity of each compound on each cell line was determined by the MTT assay. The tetrazolium salt 3-(4,5-dimethylthiazol-2-yl)-2-5 diphenyl tetrazolium bromide (MTT) is taken up into cells and reduced in a mitochondria-dependent reaction to yield a formazan product. The ability of cells to reduce MTT provides an indication of mitochondrial integrity and activity that, in turn, may be interpreted as a measure of viability [11].

For MTT assays, cells were seeded in DMEM containing 5% FBS into wells of 96-well ELISA-type plates and exposed to a range of drug concentrations for time intervals from 1 to 24 h. The initial seeding densities ranged from 2×10^4 to 6×10^4 cells/well. Cell viability was assessed by trypan blue dye exclusion at the beginning of each experiment and was always higher than 96%. Drug concentrations ranged from 0.08 to 20 nmol/ml, for Quinifuryl, and from 0.02 to 2 nmol/ml, for Nitracrine.

At the end of the drug exposure period, plates were centrifuged to pellet cells and a drug-contained supernatants were displaced with either MTT dissolved in PBS (*Procedure 1*) or with fresh medium (*Procedure 2*). In the latter case, the cells were incubated for the additional 2–3 cell population-doubling times (36–72 h) with daily media change, followed by MTT assay (*Procedure I*).

Plates with MTT were incubated in the dark for 4 h, after which the water-insoluble MTT-formazan crystals were dissolved in DMSO, and absorbance was recorded in an ELISA plate reader Dynex MRX (Dynex Technologies Inc.) at 570 nm.

Drug concentration dependence and time-dependence of cell death were calculated as a toxic effect (TE): $TE = [DC]/[Cell]^{control}$, where $[Cell]^{control}$ is cell concentration, in control wells (cells incubated for the same time length with no compound) and [DC] is the dead cell concentration. [DC] is calculated as$[Cell]^{control} - [Cell]^{final}$, were $[Cell]^{final}$, is the live cell concentration in wells exposed to drug. The above expression was developed based on the formulas for the growth inhibition power described in [12]. Cell concentration was measured using a calibration curve made for all cell lines tested using MTT-staining method.

The cytotoxic effect (LC_{50}) of the tested compounds was estimated as $100 \times (T - T_0)/T_0 = -50$, where T_0 and T are optical densities of the test well at time zero (when the compound is added) and after exposure to test compound [12].

2.4. Uptake of drugs into K562 cells

Drug uptake into K562 cells was measured using the following procedure. Each drug was added to 1 ml of cell suspension (1×10^6 cells/ml) in 20 mM HEPES buffer to a final drug concentration of 2 nmol/ml. Mixtures were incubated at 37 °C for time intervals ranging from 0 min to 3 h with continuous shaking on an orbital shaker (Forma Scientific, USA). Following incubation, cells were pelleted and repeatedly washed until no spectra of a drug could be detected in supernatant. Cell pellets were subsequently lysed in 0.5% Triton X-100 solution in Milli-Q water. Absorption spectra of the lysates prepared from the cells incubated with a drug were measured against that of control untreated cells, incubated under identical conditions, and compared with spectra of intact drug recorded against the lysates prepared from control cells.

2.5. Statistic analysis

The data are presented as the mean ± S.D. of two to five independent series of experiments with five to six repetitions in each. Statistic analysis was performed on the Student's *t*-test. The Tukey test with 95% confidence was applied to compare the means. Statistic analyses were done using the InStat software program for Windows (GraphPads software, San Diego, USA).

3. Results

Dose-dependence of the TEs of both drugs was determined first and is shown in Fig. 2. The TE values were calculated as the ratio of numbers of the cells dying during incubation with the drug to the initial cell concentrations (for details see Section 2). Cells incubated without drug served as a control in each series of experiments. Normally, no significant amounts of dead cells were observed in control wells up to 24 h incubation.

The majority of the experimental data was obtained following Procedure 1 (Section 2), according to which MTT-dye incubation was performed immediately following drug treatment. This approach limits the observed results only to the direct cytotoxic effect of the drug. Table 1 shows the LC_{50} values calculated based on the results of two to five independent series of experiments with six repetitive measurements in each series.

The results of the experiments (Table 1) clearly show that both drugs are somewhat toxic toward all cell lines ($LC_{50} \leq 2$ μM) and require less than 24 h to reach LC_{50} values (Table 2). On the other hand, Nitracrine displays significantly higher cytotoxicity than Quinifuryl (Tables 1 and 2). In addition, murine limpholeukaemia P388 cells were more sensitive to both drugs, as compared to non-transformed murine NIH3T3 cells (Table 2). Respective data, presented in Table 3, show that toxic effects observed after 12 h incubation of P388 cells with these drugs were significantly higher (0.79 and 0.64 for Quinifuryl and Nitracrine, respectively) than those in NIH3T3 cells (0.43 and 0.38 for Quinifuryl and Nitracrine, respectively). Furthermore, the incubation times

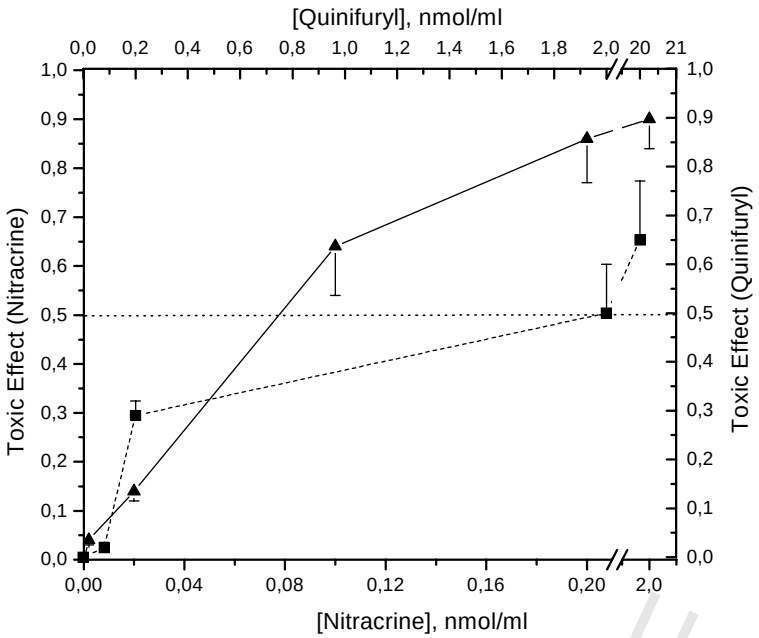

Fig. 2. Dependence of K562 cell death on concentration of Nitracrine (▲) and Quinifuryl (■). Time of drug incubation with cells is 24 h.

required to reach LC_{50} values with 2 μM concentrations of both drugs were 2–3 times more for both NIH3T3 cells (16 and 8.5 h for Quinifuryl and Nitracrine, respectively), and K562 cells (21 and 8.4 h for Quinifuryl and Nitracrine, respectively) as opposed to P388 cells (5.3 and 3.5 h for Quinifuryl and Nitracrine, respectively) as shown in Table 2.

In order to estimate cytostatic effects of the drugs, results, obtained in parallel experiments utilizing Procedures 1 and 2 (see Section 2), were compared. Briefly, cells were incubated with drugs for 12 h in two ELISA-type plates. In one plate the TE was measured immediately after that, whereas, in the second plate, drugs were replaced with complete medium and cells were allowed to proliferate for the additional 72 h (K562 and NIH3T3) or 36 h (P388; three cell population doublings of each cell type). Subsequently, the medium was replaced with MTT-dye and toxicity was measured. The results, obtained using this method (Table 3), show that drugs not only caused death, but also attenuated proliferation of the surviving cells.

Since Quinifuryl, despite its cytotoxicity in vitro, showed very little effect in vivo [1], one possible explanation is its rapid intracellular metabolism. In order to address this possibility, first, the uptake of Quinifuryl and Nitracrine into K562 cells was measured. The cellular uptake of drugs could be visually detected, since the pellets of K562 cells turned bright yellow after 10 min of incubation with Quinifuryl (drug is yellow colored), while pellets of control cells remained uncolored. Incubation with Nitracrine resulted in time-dependent cell pellet colour change from yellow to

Table 1
Values of LC_{50} for Quinifuryl and Nitracrine measured at different time lengths

Cell line	Compound	Time (h)	LC_{50} (μM)
K562	Quinifuryl	24	2 ± 0.9
		12	12 ± 2.2
	Nitracrine	24	0.12 ± 0.07
		6	2.2 ± 0.06
P388	Quinifuryl	24	1.1 ± 0.2
	Nitracrine	24	0.16 ± 0.06
		6	0.5 ± 0.13
NIH3T3	Quinifuryl	24	1.2 ± 0.17
		12	11 ± 2.1
	Nitracrine	24	0.13 ± 0.04
		12	1.4 ± 0.2

Each LC_{50} value represents ($M \pm$ S.D.) of two to five completely independent series of experiments with five to six repetitive.

Table 2
Time lengths for which the LC_{50} achieved ($\hat{O}^{LC50}$) for free compounds

Cell	Compound	Concentration (μM)	$\hat{O}^{LC_{50}}$ (h)
K562	Quinifuryl	20	6.5 ± 0.6 a
		2	21 ± 2.7 b
	Nitracrine	2	8.4 ± 0.6 c
NIH3T3	Quinifuryl	20	3.7 ± 0.2 d
		2	16 ± 0.2 e
	Nitracrine	2	8.5 ± 0.4 f
		0.2	17 ± 2 g
P388	Quinifuryl	2	5.3 ± 0.7 h
	Nitracrine	2	3.5 ± 0.1 i
		0.2	12 ± 2 j

Data concerning free drugs represent ($M \pm$S.D.) of two to five completely independent series of experiments with five to six repetitive. * Significant differences were found between $\hat{O}^{LC_{50}}$ values as follows: $P < 0.01$ (b vs. h, c vs. i, e vs. h, f vs. i), $P < 0.05$ (a vs. d, g vs. j, b vs. e). No significant differences (NS) were observed between c and f.

Table 3
Toxic effects (TE) of Quinifuryl and Nitracrine observed for 12 h drug incubation with appropriate cells (TE_{12}) and measured either immediately after drugs withdrawn (Procedure 1) or after followed three 3 cell population-doubling time (Procedure 2; for procedure details see Section 2)

Compound	Cell line								
	K562			P388			NIH3T3		
	TE_{12}	TE_{72}	P	TE_{12}	TE_{36}	P	TE_{12}	TE_{72}	P
Quinifuryl, 2 μM	0.47 ± 0.08	0.58 ± 0.05	NS	0.79 ± 0.01	0.89 ± 0.04	<0.05	0.43 ± 0.16	0.96 ± 0.01	<0.05
Nitracrine, 0.2 μM	0.63 ± 0.09	0.81 ± 0.06	<0.01	0.64 ± 0.11	0.88 ± 0.03	<0.05	0.38 ± 0.1	0.94 ± 0.005	<0.05

Each LC_{50} value represents ($M \pm$ S.D.) of one series of experiments with six repetitive. The experiments with each drug followed both procedures were performed in parallel.

greyish-brown. Following incubations with the drugs, cells were pelleted, washed twice, and lysed. Difference spectra were recorded against the intracellular content of control cells that were incubated for 6 h under the same conditions (for more details see Section 2). Spectra of intact drugs were also recorded versus the control cell lysate to estimate the degree of drug biotransformation.

Kinetics of the changes in a relative Quinifuryl concentration in the supernatant versus the cell pellet are shown in Fig. 3. The balance was calculated as a sum of the drug concentration in the incubation mixture and the cell lysate. Our attempts to measure the Nitracrine balance failed because of the much lower extinction coefficient of this compound as compared to Quinifuryl (3.9 and 26.2 mM/cm, respectively, as determined in this study).

Fig. 4 shows dynamics of spectral changes in K562 cell lysates after cell incubation with either Quinifuryl (panel A) or Nitracrine (panel B) for different lengths of time. Specific absorption of Quinifuryl (396 nm) was increased for the initial 30 min following drug addition and then decreased with time. This loss of Quinifuryl correlated with the appearance of a through near 248 nm and of a peak at 276 nm, which corresponds to a through at the same wavelength observed in a spectrum of an intact drug.

Following first 10 min of Nitracrine incubation, difference spectra of cellular content showed appearance of a peak at 409 nm and a corresponding through at 430 nm with fluctuated value of $\Delta A^{409-430}$, which shifted by 6 nm in comparison to the intact drug. After 1 h incubation, however, two new peaks appeared in the spectra at 573 and 627 nm with absolute variable and relative absorption. Overall, spectral changes shown in Fig. 4 most likely reflect substantial biotransformation of both drugs in K562 cells.

4. Discussion

Nitracrine, which is an antitumour drug used clinically for the last several years [13], is a potent hypoxia-selective cytotoxic agent in vitro (for reviews see [3,4,14]). For in-

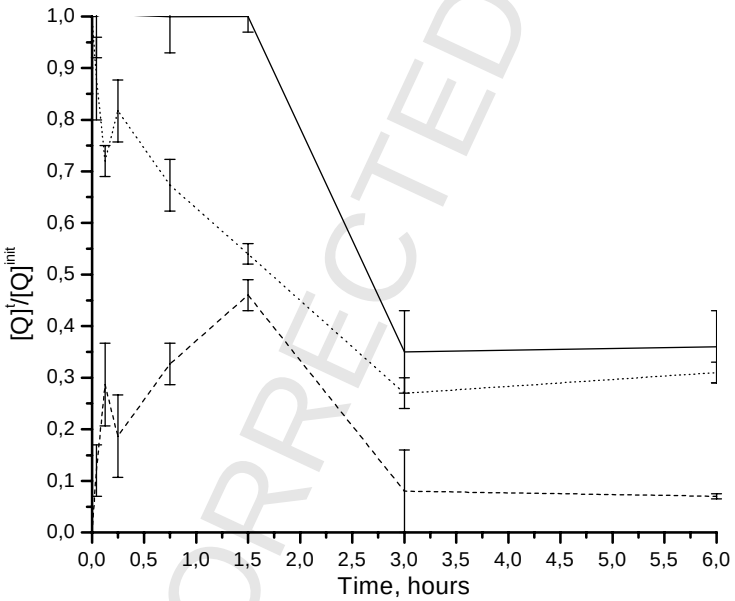

Fig. 3. Kinetic of changes of Quinifuryl specific absorbance at 396 nm during drug incubation with K562 cells in supernatant (dotted line), in cell content (dashed line), and balance (solid line). $A_r = A^i/A^0$, where A^0 and A^i are intensities of these peak before and during drug incubation. Balance $= A^i_s + A^i_c/A^0$, where A^i_s and A^i_c are absorbance discovered in supernatant and cell content, respectively. Data represent ($M \pm$ S.D.) of three measurements.

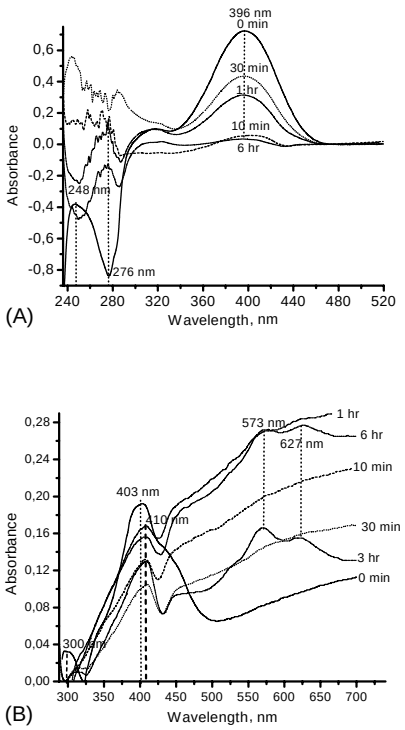

Fig. 4. Difference absorption spectra of K562 cell content after incubation with Quinifuryl (A) and Nitracrine (B) for various time lengths followed by cell wash and lyses. Solid lines represent spectra of respective drugs before incubation with cells. All spectra were recorded against content of intact cells that was incubated in parallel with no additives. Each measurement made in three repetitive.

stance, its toxicity against the Chinese hamster ovary cell line AA8 under hypoxic conditions was found to be $\sim 10^5$ times higher than that of misonidazole [15]. On the other hand, Quinifuryl, is an antiseptic used in surgery for the treatment of wounds and burns [16] and its antitumour activity is not well established.

The results of our study demonstrate that under normoxic conditions both drugs are highly toxic towards three cell lines tested and the LC_{50} values obtained after 24 h incubation are $\leq 2\,\mu M$ (Table 1, Fig. 2). Both drugs induced death rapidly with the exposure time needed for Quinifuryl to achieve LC_{50}, being between 5 and 21 h and from 3.5 to 8.5 h for Nitracrine (Table 2). In addition to the cytotoxic effects, both drugs attenuated proliferation by the surviving cells (Table 3).

Even though both drugs appeared somewhat toxic to non-tumour cells (NIH3T3), murine lympholeukaemia P388 cells were much more sensitive to both compounds. Also, P388 cells were killed significantly faster by both drugs (~2.5–3 times) compared to NIH3T3 cells (Table 2).

Despite our findings that Nitracrine was more toxic than Quinifuryl towards all studied cells (Tables 1 and 2), the latter still shows significant promose since its lower antitumour activity may be offset by the decreased non-specific toxicity towards host, tumour (P388)-bearing mice, which was nearly 30 times lower compared to Nitracrine [1].

Interestingly, despite the fact that both drugs entered the cells following 10 min incubation (Fig. 4), the LC_{50} were achieved by both drugs only after >3 h incubation (Table 2) and no significant cell death was observed after 1 h incubation (data not shown). This "delay induction" may be needed for the build-up of either intracellular concentration of the drug itself or its toxic intermediates resulting from intracellular metabolism (Fig. 3). Since our data, presented in Fig. 4, suggest rapid drug metabolism, the latter assumption might be more likely.

Metabolic decomposition of the chromophore of Quinifuryl in normal tissues ($\lambda_{max} = 396$ nm, $\varepsilon = 26$ M/cm, as measured in this work), i.e. "drug bleaching," is a perfect instrument for kinetic and mechanistic studies of drug metabolism (for instance, see [17]). As shown in Fig. 3, the intracellular content of Quinifuryl increased for the first 90 min following drug incubation, reflecting compound accumulation, and then started to decrease. Concomitantly with the drug loss, a peak near 280 nm appeared in a place of a through in the spectrum of intact compound (Fig. 4A). These changes are probably due to the intracellular drug transformation.

In the early work we had found that, in contrast to Quinifuryl, Nitracrine was not bleached during metabolism, but showed a longwave shift of its spectrum maximum in the visible region [17]. Time dependent spectral monitoring of the intracellular content of the Nitracrine-treated K562 cells indeed showed 6 nm shift in compound spectral maximum compared with the intact Nitracrine (Fig. 4B). These spectra also possessed a through at ~420 nm with the A^{409}/A^{420} ratio changing with time of drug incubation. Two additional new peaks also appeared in the red region following 1 h of drug incubation. Overall, these changes clearly indicate intracellular drug transformation.

5. Conclusion

The results, reported and discussed above, show that two representatives of different families of nitroheterocyclic drugs, Quinifuryl and Nitracrine, possess high cytotoxicity towards leukaemic cells in vitro, which may be a result of an intracellular metabolism of the drugs.

It should also be noted that Quinifuryl, deserves special attention as a possible candidate for cancer therapy, considering its high cytotoxicity in vitro and relatively low non-specific toxicity to host animals.

Acknowledgements

This work was supported by Brazilian agencies: CNPq, FAPESP, and CAPES.

References

[1] Verovskiy VN, Degterev IA, Sukhova NM, Buzukov AA, Leonova EYu, Tatarskaya NK. Interrelation between structure, microssomal metabolising activation, mouse toxicity, cytotoxicity and antitumour activity of heterocyclic- and nitroheterocyclic compounds. In vitro and in vivo study. Pharma Chem J 1990;24:20–4.

[2] Wilson WR, Denny WA, Stewart GM, Fenn A, Probert JC. Reductive metabolism and hypoxia-selective toxicity of nitracrine. Int J Radiat Oncol Biol Phys 1986;12:1235–8.

[3] Gniazdowski M, Szmigiero L. Nitracrine and its congeners—an overview. Gen Pharmacol 1995;26:473–81.

[4] Gorlewska K, Mazerska Z, Sowin'ski P, Konopa J. Products of metabolic activation of the antitumor drug Ledakrin (Nitracrine) in Vitro. Chem Res Toxicol 2001;14:1–10.

[5] Voronina SS, Tatarskaia NK, Degterev IA, Serebriany AM, Pelevina II. Radiosensitising activity and metabolism of nitrofuran derivatives. Preparation M-106. Radiobiology (Moscow) 1985;25:748–51.

[6] Smirnov SM, Zhurav MA, Tatarskaya NK, Borisevich YE, Degterev IA. Phototransformation of quinifur nitroanion radical formation. Chemical Physics (Moscow) 1989;8:17–23.

[7] Tatarskaya NK, Zhurav MA, Smirnov SM, Degterev IA, Tarasov VF, Borisevich YE, et al. Effect of compound and oxygen concentration on primary processes of quinifur phototransformation. Proc Acad Sci USSR, Chem 1989;N 5:804–9.

[8] Josephy PD, Mason RP. Nitroimidazoles. In: Anders MW, editor. Bioactivation of foreign compounds. New York: Academic Press; 1985. p. 161–222.

[9] Degterev IA, Buzukov AA, Sharf VG, Popov KN, Serebrianiy AM, Zaikov GE. Comparative study of in vitro ledakrine metabolism in microssomes of EAC-cells and mouse liver. Pharma Chem J 1986;20:412–7.

[10] Klein E, Ben-Bassat H, Neumann H, Ralph P, Zeuthen J, Polliac A, et al. Properties of the K562 cell line, derived from a patient with chronic myeloid leukemia. Int J Cancer 1976;18:421–31.

[11] Mosmann T. Rapid colorimetric assay for cellular growth and survival: application to proliferation and cytotoxicity assays. J Immunol Methods 1983;65:55–63.

[12] Monks A, Scudiero D, Skehan P, Shoemaker R, Paull K, Vistica D, et al. Feasibility of a high-flux anticancer drug screen using a diverse panel of cultured human tumor cell lines. JNCI 1991;83:757–66.

[13] WHO Chronicle, vol. 30 (Suppl. 3). Geneva: World Health Organization; 1976. p. 11.

[14] Gniazdowski M, Filipski J, Chorazy M. Nitracrine. In: Hahn FE, editor. Antibiotics V/2. Berlin: Springer; 1979. p. 275–97.

[15] Wilson WR, Denny WA, Twigden SJ, Baguley BC, Probert JC. Selective toxicity of nitracrine to hypoxic mammalian cells. Br J Cancer 1984;49:215–23.

[16] Blatun LA, Svetukhin AM, Pal'tsyn AA, Liapunov NA, Agafonov VA. Clinic-laboratory effectiveness of modern ointments with a polyethylene glycol base in the treatment of purulent wounds. Antibiot Khimioterapia 1999;44:25–31.

[17] Degterev IA, Buzukov AA, Tatarskaya NK, Leonova EYu, Sukhova NM. Metabolism of heterocyclic compounds in mouse liver microsomes. Pharma Chem J 1990;24:9–16.

Available online at www.sciencedirect.com
SCIENCE DIRECT®
Journal of Photochemistry and Photobiology B: Biology 75 (2004) 27–32
Journal of Photochemistry and Photobiology B:Biology
www.elsevier.com/locate/jphotobiol

Cytotoxicity of nitroheterocyclic compounds, Quinifuryl and Nitracrine, towards leukaemic and normal cells on the dark and under illumination with visible light

Nasser A. Daghastanli [a], Marcelo M. Rossa [b], Heloisa S. Selistre-de-Araujo [b], Antonio C. Tedesco [c], Iouri E. Borissevitch [a], Igor A. Degterev [a,d,*]

[a] *Departamento de Física e Matemática, Faculdade de Filosofia Ciências e Letras de Ribeirão Preto, Universidade de São Paulo, Av. Bandeirantes 3900, CEP 14040-901, Ribeirão Preto, SP, Brazil*
[b] *Department de Ciências Fisiológicas, Universidade Federal de São Carlos, São Carlos, Brazil*
[c] *Departamento de Química, Faculdade de Filosofia Ciência e Letras de Ribeirão Preto, Universidade de São Paulo, Av. Bandeirantes 3900, CEP 14040-901, Ribeirão Preto, SP, Brazil*
[d] *Department of Chemical and Biological Kinetics, Institute of Biochemical Physics, Russian Academy of Sciences, Kosygin Str. 4, 117333 Moscow, Russian Federation*

Received 8 April 2004; accepted 27 April 2004
Available online 7 June 2004

Abstract

The cytotoxicity of two nitroheterocyclic compounds (NHCD), Nitracrine, 1-nitro-9(3-3-dimethylaminopropylamino) acridine and Quinifuryl, 2-(5′-nitro-2′-furanyl) ethenyl-4-{*N*-[4-(*N,N*-diethylamino)-1′-methylbutyl] carbamoyl} quinoline, towards two lines of leukaemic cells and a line of non-transformed cells, was measured in comparison, on the dark and under illumination with visible light (350–450 nm). Both drugs showed highly elevated cytotoxicity when illuminated with LC_{50} values 7–35 times lower after 1 h illumination compared to 1 h incubation of cells incubation with drug on the dark. Cytotoxicity of Nitracrine toward all cell lines studied exceeded that of Quinifuryl, both on the dark and under illumination, so that ≈10 times lower concentration of former drug was needed to reach the same toxicity as the latter. General toxic effect was calculated as a direct cell kill and a cell proliferation arrest. The effect >80% for both drugs was achieved after 1 h cell illumination with as low drug concentrations as 0.2 μM for Quinifuryl and 0.02 μM for Nitracrine.

Keywords: Photochemotherapy; Photocytotoxicity; Nitroheterocyclic compounds; Quinifuryl; Nitracrine; Lympholeukaemia P388; Human erythroleukaemia K562; Fibroblast NIH3T3

1. Introduction

Photochemotherapy (PCT) is a mode of cancer treatment based on a supply a target (cancer) tissue with a photoactive agent (photosensitizer) followed by illumination of tumor with light to produce species that are highly toxic to a target [1–3]. The extensive search of new agents for PCT is continued [3–7] and studies on the mechanism of their phototoxicity are developing [8,9].

Quinifuryl is an antiseptic in surgery for the treatment of wounds and burns [10]. Our previous analysis of cytotoxicity has demonstrated that Quinifuryl displayed the high cytotoxicity ($LC_{50} \leqslant 2$ μM) towards melanoma B16 [11], murine lympholeukaemia P388 cells [11,12], and human erythroleukaemia K562 cells [12]. At the same time, this compound was shown to be photolabile absorbing intensively visible light ($\lambda^{max} = 396$ nm, $\varepsilon_{396} = 2.47 \times 10^4$ $M^{-1}\,cm^{-1}$ [12] and producing reactive species during photoexcitation [13–15]. This fact led us to an assumption that the illumination of tumor cells with the visible light may result in the drug cytotoxicity potentiation.

* Corresponding author. Tel.: +55-016-602-3862; fax: +55-016-633-9949.
E-mail address: igor@dfm.ffclrp.usp.br (I.A. Degterev).

1011-1344/$ - see front matter © 2004 Elsevier B.V. All rights reserved.
doi:10.1016/j.jphotobiol.2004.04.005

The aim of the present work was to extend number of cellular targets for Quinifuryl in order to confirm intensified photocytotoxicity of this compound and to compare the photocytotoxic potency of Quinifuryl with that of Nitracrine, a 1-nitroacridine derivative, known as a potent hypoxia-selective agent in vitro [16,17] and used clinically as antitumor drug [18]. Our previous analysis of cytotoxicity has demonstrated that, as well as Quinifuryl, Nitracrine also displayed the high cytotoxicity ($LC_{50} \leqslant 2$ μM) towards melanoma B16 [11], murine lympholeukaemia P388 cells [11,12], and human erythroleukaemia K562 cells and always displayed higher cytotoxicity than Quinifuryl.

Quinifuryl possesses the optical absorption more intense than this of Nitracrine (Nitracrine $-\ \varepsilon_{400} = 4 \times 10^3$ $M^{-1}\,cm^{-1}$, Quinifuryl $-\ \varepsilon_{396} = 2.47 \times 10^4$ $M^{-1}\,cm^{-1}$, respectively, [12]). No study of Nitracrine photocytotoxicity was ever made.

In this work cellular toxicity of drugs towards murine leukemia P388, fibroblast NIH3T3, and human erythroleukaemia K562 cells was measured on the dark and under illumination with visible light.

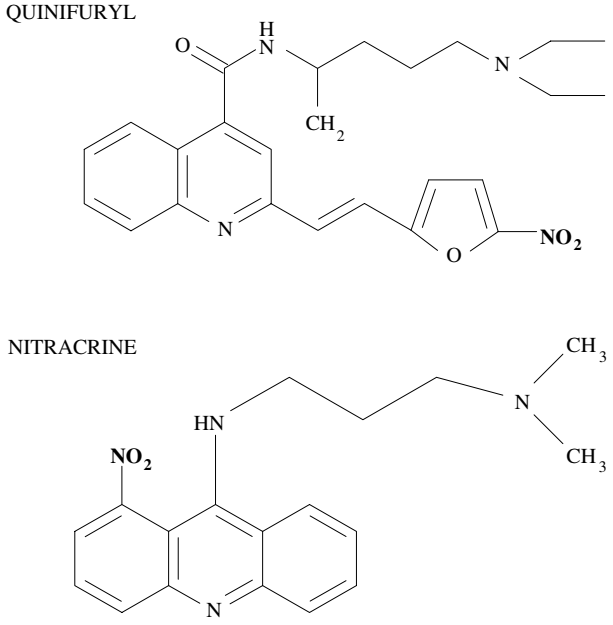

Fig. 1. Structures of Quinifuryl and Nitracrine.

2. Materials and methods

2.1. Drugs

Quinifuryl (M-106), 2-(5′-nitro-2′-furanyl) ethenyl-4-{*N*-[4-(*N,N*-diethylamino)-1′-methylbutyl] carbamoyl} quinoline, a representative of a family of 5-nitrofuran-ethenyl-quinoline drugs, was synthesized and purified by Dr. N.M. Sukhova. Nitracrine (Ledakrine, C-283), 1-nitro-9 (3′,3′-dimethylaminopropylamino) acridine was purchased from Polfa. Structural authenticity of both drugs was verified by NMR analysis. Structural formulas of both drugs are present in Fig. 1.

2.2. Cells

The human K562 leukemia cell line (proerythrocytes), which was originally derived from the patient with erythroleukaemia [19], was kindly provided by Dr. S. Niewiarowski (Temple University, PA, USA). $P388D_1$ cells, a mouse macrophage monocyte line that grows in semi-suspension, and immortalized mouse fibroblast NIH3T3 cells were obtained from the American Type Culture Collection. P388 cells were cultured in Fisher's media supplemented with 10% heat inactivated horse serum in 175 cm^2 culture flasks at 37 °C with 5% CO_2. K562 and NIH3T3 cells were cultured as a suspension or a monolayer, respectively, in Dulbecco's modified Eagle's medium (DMEM) supplemented with heat-inactivated 10% fetal bovine serum (FBS), 1% L-glutamine, 50 units/ml penicillin, 50 mg/ml streptomycin, 250 mg/ml Anfotericin-B at 37 °C in a water-jacketed CO_2 incubator (Cellstar, USA). The day before an experiment, cells were seeded at 5×10^5 cells/ml. The number of cells in suspension was calculated using a Neubauer chamber (0.0025 mm^2). A slow magnetic stirring was used to maintain the suspension in homogeneous state. All preparations were made under subdued red light ($\lambda > 550$ nm) at room temperature (22 °C).

The toxicity test was based on the MTT assay and performed in two ways measuring either direct killer effect of a drug (Test 1) or general toxic effect that included a cell proliferation arrest (Test 2) [12]. The tetrazolium salt 3-(4,5-dimethylthiazol-2-yl)-2-5 diphenyl tetrazolium bromide (MTT) is reduced into leaving cells to yield a colored product that may be interpreted as a measure of viability [20]. For MTT assays, cells were seeded in DMEM containing 5% FBS into wells of 96-well ELISA-type plates and exposed to a range of either drug concentrations from 0.02 to 2 μM for time intervals either from 1 to 24 h (experiments on the dark) or from 10 to 90 min (experiments under illumination). At the end of the drug exposure period, plates were centrifuged to pellet cells and drug-contained supernatants were displaced with either MTT dissolved in PBS (Test 1) or with fresh medium (Test 2). In the latter case, the cells were incubated for the 2–3 cell population-doubling times (36–72 h) with daily media change, followed by MTT assay. In both tests, plates with MTT were incubated in the dark for 4 h, after which the water-insoluble MTT-formazan crystals were dissolved in DMSO, and absorbance was recorded in an ELISA plate reader Dynex MRX (Dynex Technologies Inc.) at 570 nm. The initial seeding densities ranged from 2×10^4 to 6×10^4

cells/well. Cell viability was assessed by TB dye exclusion at the beginning of each experiment and was always higher than 96%.

2.3. Irradiation

Samples, containing cells and drug, and controls, containing cells in the absence of drug, were irradiated directly in ELISA-type plates, in the spectral range from 350 to 450 nm using standard light source with tungsten lamp (150 W) and the glass filter (5–57 KOPP color glass filter). The intensity of irradiation was 22 mW/cm^2, as measured by a Spectra-Physics 407A radiometer.

2.4. Calculation of the results

Drug concentration dependence and time dependence of cell death were calculated as a toxic effect (TE): TE = [DC]/[Cell]^{control}, where [Cell]^{control} is cell concentration, in control wells (cells incubated for the same time length with no compound) and [DC] is the dead cell concentration. [DC] was calculated as [Cell]^{control}–[Cell]^{final}, were [Cell]^{final} is the live cell concentration in wells exposed to drug [12]. Cell concentration was measured using a calibration curve made for all cell lines tested using MTT-staining method. The LC_{50} of the tested compounds was estimated as $100 \times (T - T_0)$ $T_0 = 50$, where T_0 and T are optical densities of the test well at time zero (when the compound is added) and after exposure to test compound, respectively [21]. The LC_{50} was measured after 1 h cell incubation with either drug on the dark or under illumination.

2.5. Statistic analysis

The data are presented as the mean ± SD of two to five independent series of experiments with five to six repetitions in each. Statistic analysis was performed on the Student's *t*-test. The Turkey's test with 95% confidence was applied to compare the means. Statistic analyses were done using the InStat software program for Windows (GraphPads software, San Diego, USA).

3. Results

One example of a drug cytotoxicity measurements are present in Fig. 2 that shows a development of toxic effect (TE) toward human K562 erythroleukaemia cells as a function of cell incubation time with drug either under illumination with visible light (Panel A) or on the dark (Panel B). The TE values were calculated as was described in Section 2. Cells incubated without drug served as a control in each series of experiments. Normally, no significant amounts of dead cells were observed in control wells up to 24 h incubation on the dark and up to 1.5 h illumination.

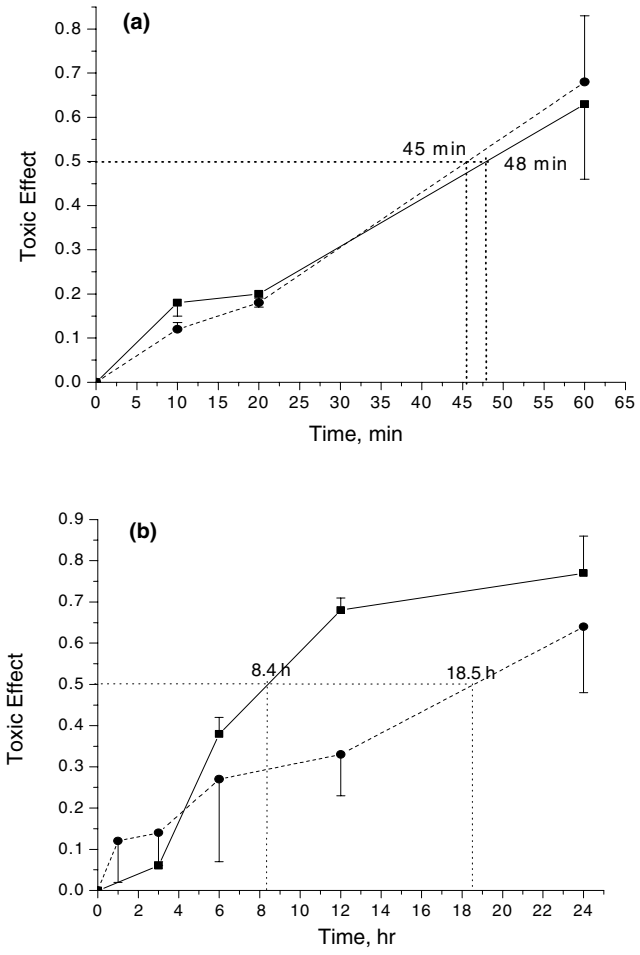

Fig. 2. Photocytotoxicity (a) and cytotoxicity on the dark (b) of Quinifuryl (●) and Nitracrine (■) towards human erythroleukemia K562 cells as measured by method dye inclusion (MTT). Vertical dashed lines show time needed to reach kill of 50% of cells. Drug concentrations were as follows: Quinifuryl – 2.0 μM; Nitracrine – 0.2 μM. Conditions: cell concentration was $\sim 1 \times 10^6$ in Na-phosphate buffer, pH 7.4; mixtures were illuminated at room temperature with filtered (350–450 nm) light of tungsten lamp (200 W) at 22 °C with the irradiation intensity of 22 mW/cm^2. Toxic effect was measured as [DC]/[Cell]^{control}, where [Cell]^{control} is cell concentration, in control wells (cells incubated for the same time length with no compound) and [DC] is the dead cell concentration. Each point represents M ± SD of six measurements.

Both drugs were much more cytotoxic under illumination than on the dark. Death of 50% of cells were achieved under illumination for 45 and 48 min for 2 μM of Quinifuryl and for 0.2 μM of Nitracrine, respectively (Fig. 2(a)), while on the dark it took 8.5 h for Nitracrine and 18.4 h for Quinifuryl (Fig. 2(b)). Nitracrine possesses higher cytotoxicity than Quinifuryl on the dark and under illumination. So that 10-times lower concentration of Nitracrine produced the same (illumination, Fig. 2(a)) or higher (on the dark, Fig. 2(b)) toxic effects towards K562 cells than Quinifuryl.

Table 1
The LC_{50} for Quinifuryl and Nitracrine measured after 1 h of cells incubation with drug either on the dark or under illumination with visible light

Drug	LC_{50} (μM)	
	Dark	Illumination
P388 cells		
Quinifuryl	79.7 ± 18.1	11.8 ± 3.8
Nitracrine	7.7 ± 1.3	0.23 ± 0.15
NIH3T3 cells		
Quinifuryl	18.6 ± 6.0	1.6 ± 0.7
Nitracrine	16.2 ± 2.8	0.6 ± 0.6
K562 cells		
Quinifuryl	[a]15.4 ± 2.4	1.48 ± 0.33
Nitracrine	[a]8.9 ± 0.8	0.16 ± 0.04

[a] No significant cytotoxicity was observed after 1 h of K562 cells incubation with either drug, thus cytotoxicity on the dark was measured after 12 h of cell incubation with drugs.

Table 3
Time for which death of 50% of cells achieved (τ_{50})

Drug	[Drug] (μM)	τ_{50} (min)	
		Dark	Illumination
P388 cells			
Quinifuryl	20.0	231 ± 51	25 ± 7
	2.0	350 ± 118	76 ± 9
	0.2	1540 ± 90	96 ± 11
Nitracrine	0.2	390 ± 179	76 ± 9
	0.02	431 ± 43	97 ± 13
NIH3T3 cells			
Quinifuryl	2.0	408 ± 67	34 ± 18
	0.2	>500	56 ± 17
Nitracrine	0.2	191 ± 13	31 ± 15
	0.02	622 ± 115	58 ± 28
K562 cells			
Quinifuryl	2.0	n.m.	45 ± 5
Nitracrine	0.2	n.m.	48 ± 7

The majority of the experimental data was obtained following Test 1 (Section 2), according to which MTT-dye incubation was performed immediately following drug treatment. This approach limits the observed results only to the direct killer effect of the drug. Table 1 shows that the LC_{50} values observed after 1 h illumination were lower, compared to the dark experiments, by at least order of magnitude. All cells were more sensitive to Nitracrine, compared to Quinifuryl, both on the dark and under illumination.

The cell kill (Test 1) and general toxicity (Test 2) experiments were performed in parallel. Briefly, cells were incubated with drugs in a pare of ELISA-type plates for either 12 h on the dark or 1 h under illumination with filtered visible light (350–450 nm). In each pair, one plate was subjected to the measurement of toxic effect immediately after a drug withdrawal (Test 1). In the second plate, drugs were replaced with complete medium and cells were allowed to proliferate for the 2–3 population-doubling time that were either 72 h (K562 and NIH3T3) or 36 h (P388). Subsequently, the medium was replaced with MTT-dye and the TE was measured as a ratio of dead cells to initial cell amount (see Section 2). The direct killer effect (Test 1) and general toxic effect (Test 2) of both drugs towards three cell lines measured in parallel are present in Table 2.

Table 2
Direct killer effect (Test 1) and general toxicity (Test 2) of Quinifuryl and Nitracrine toward P388 cells either on the dark or under illumination with visible light

Drug	[Drug] (μM)	Toxic effect			
		Dark (12 h)		Illumination (1 h)	
		Test 1	Test 2	Test 1	Test 2
P388 cells					
Quinifuryl	2.0	*0.480.1	0.97 ± 0.16	*0.76 ± 0.27	0.93 ± 0.20
	0.2	*0.014 ± 0.002	n.m.	*0.13 ± 0.04	0.84 ± 0.24
Nitracrine	0.2	0.59 ± 0.2	0.97 ± 0.15	*0.64 ± 0.17	0.99 ± 0.26
	0.02	*0.14 ± 0.05	n.m.	*0.49 ± 0.13	0.97 ± 0.26
NIH3T3 cells					
Quinifuryl	2.0	*0.59 ± 0.13	0.96 ± 0.01	*0.43 ± 0.16	0.93 ± 0.04
	0.2	*0.0 ± 0.06	0.0 ± 0.12	*0.35 ± 0.12	0.87 ± 0.12
Nitracrine	2.0	0.56 ± 0.1	0.96 ± 0.15	n.m.	0.89 ± 0.20
	0.2	*0.38 ± 0.1	0.94 ± 0.01	*0.65 ± 0.14	0.89 ± 0.12
	0.02	*0.25 ± 0.03	0.89 ± 0.2	*0.41 ± 0.11	n.m.
K562 cells					
Quinifuryl	2.0	*0.33 ± 0.1	n.m.	*0.68 ± 0.15	n.m.
Nitracrine	0.2	0.63 ± 0.03	n.m.	0.68 ± 0.17	n.m.

In each row, symbol (*) marks statistically significant difference ($P < 0.01$) between the results of Test 1. No significant differences were observed between Tests 2 on the dark and under illumination in each series of experiments.

Being applied at the same concentration, both drugs kill cells much rapidly when illuminated with visible light. Table 3 shows the incubation times required to reach death of 50% of cells at different drug concentrations either on the dark or under illumination with visible light.

4. Discussion

The results presented in this work show that the illumination with visible light sharply decreased lethal concentrations of both Quinifuryl and Nitracrine (Table 1) and shortened time of the lethal effect run up (Table 3).

Table 2 shows that the killer effects (Test 1) of both drugs, when illuminated with visible light for 1 h, were similar to those observed after 12 h drug incubation with either cells on the dark. These results show that drugs not only caused death, but also attenuated proliferation of the surviving cells. In contrast to direct killer effect, general toxicity (Test 2) of both drugs toward P388 and NIH3T3 cells after 1 h illumination and 12 h of the dark incubation was similar. The effect of Nitracrine was higher, compared to Quinifuryl, both on the dark and under illumination. Significant toxicity toward P388 and NIH3T3 cells was observed for low concentration (0.2 μM) of Quinifuryl under illumination, while negligible (P388) or no (NIH3T3) toxicity was observed for Quinifuryl in the same concentration for 12 h of drug incubation with these cells on the dark.

Mechanisms of dark-cytotoxicity of Quinifuryl and Nitracrine are, probably, due to their metabolism. Both drugs were metabolized in normal tissues [22–24] and cancer cells [11,12]. Nitracrine is believed to produce reactive intermediate(s) during metabolism that causes DNA modification [17]. Both drugs accelerate the production of reactive oxygen [23] and nitrogen [25–27] species during metabolism. Thus, their toxicity may also be due to oxidative stress.

The fact that the photoactivation significantly accelerates cell killing should be interpreted as either formation more toxic intermediates during photolysis, compared to the dark metabolism, or acceleration of the same toxins formation under illumination, or both. Evidence of reactive species formation during photolysis of Quinifuryl by visible light was reported in our previous works [13–15]. The formation of the triplet excited state [14], which is capable to produce singlet oxygen [1–3], the reaction of the triplet state with the drug in the ground state and with electron donors [13–15], forming of superoxide anion radical in the course of drug photolysis [13] could result in the Quinifuryl phototoxicity.

In contrast to Quinifuryl, there is no data available on the Nitracrine photolysis. This fact creates no room for speculations on the mechanism of photocytotoxicity of this drug that, undoubtedly, deserves special study.

The above data show that nitroheterocyclic compounds deserve study as possible candidates for photochemistry therapy. Differently from cited work, we had shown here that elevated cytotoxicity under illumination with visible light is not specific property of Quinifuryl, but also resides to nitroheterocyclic compound of quite different structure. Photosensitizing effect was observed with cancer cells as different as mouse limpholeukaemia and human erythroleukemia.

References

[1] B.W. Henderson, T.R. Dougerthy, How does photodynamic therapy work? Photochem. Photobiol. 55 (1992) 145–157.
[2] M. Ochsner, Photophysical and photobiological processes in the photodynamic therapy of tumors, J. Photochem. Photobiol. B: Biology 39 (1997) 1–18.
[3] A.S. Sobolev, D.A. Jans, A.A. Rosenkranz, Targeted intracellular delivery of photosensitizers, Prog. Biophys. Mol. Biol. 73 (2000) 51–90.
[4] B. Franck, A. Nonn, Novel porphyrinoids for chemistry and medicine by biomimetic syntheses, Angew. Chem. Int. Ed. Engl. 34 (1995) 1795–1811.
[5] M. Oertel, S.I. Schastak, A. Tannapfel, R. Hermann, U. Sack, J. Mossner, F. Berr, Novel bacteriochlorine for high tissue-penetration: photodynamic properties in human biliary tract cancer cells in vitro and in mouse tumour model, J. Photochem. Photobiol. B: Biology 71 (2003) 1–10.
[6] L. Bourre, G. Simonneaux, Y. Ferrand, S. Thibaut, Y. Lajat, T. Patrice, Synthesis, and in vitro and in vivo evaluation of a diphenylchlorin sensitizer for photodynamic therapy, J. Photochem. Photobiol. B: Biology 69 (2003) 179–192.
[7] K. Kassab, Photophysical and photosensitizing properties of selected cyanines, J. Photochem. Photobiol. B: Biology 68 (2002) 15–22.
[8] J.W. Dobrucki, Interaction of oxygen-sensitive luminescent probes Ru (phen)32+ and Ru (bipy)32+ with animal and plant cells in vitro: Mechanism of photoxicity and conditions for non-invasive oxygen measurements, J. Photochem. Photobiol. B: Biology 65 (2001) 136–144.
[9] F. Bohm, R. Edge, S. Foley, L. Lange, T.G. Truscott, Antioxidant inhibition of porphyrin-induced cellular phototoxicity, J. Photochem. Photobiol. B: Biology 65 (2002) 177–183.
[10] L.A. Blatun, A.M. Svetukhin, A.A. Pal'tsyn, N.A. Liapunov, V.A. Agafonov, Clinic-laboratory effectiveness of modern ointments with a polyethylene glycol base in the treatment of purulent wounds, Antibiot. Khimioterapia 44 (1999) 25–31.
[11] V.N. Verovskiy, I.A. Degterev, N.M. Sukhova, A.A. Buzukov, E. Yu. Leonova, N.K. Tatarskaya, Interrelation between structure, microsomal metabolizing activation, mouse toxicity, cytotoxicity and antitumor activity of heterocyclic- and nitroheterocyclic compounds. In vitro and in vivo study, Pharmacol. Chem. J. 24 (1990) 20–24.
[12] M.M. Rossa, T.A.A. Rocha-e-Silava, C.H.B. Terruggi, A.C. Tedesco, H.S. Selistre-de-Araujo, I.E. Borissevich, I.A. Degterev, Comparison of the cytotoxicity of two nitroheterocyclic drugs (NHCD) towards transformed and non-transformed cells, Pharmacol. Res. 48 (2003) 369–375.
[13] S.M. Smirnov, M.A. Jurav, N.K. Tatarskaja, E. Yu. Borisevich, I.A. Degterev, Quinifur photoreduction Nitroanionradical formation, Chem. Phys. (Moscow) 8 (1989) 1723–1725.

[14] I.E. Borissevich, N.A. Daghastanli, I.A. Degterev, Primary processes of photodecomposition of 2-(5′-nitro-2′-furanyl) ethenyl-4-{N-[4′-(*N*,*N*-diethylamino)-1′-methylbutyl]carbamoyl} quinoline. Effect of oxygen and compound concentration, J. Photochem. Photobiol. A: Chemistry 159 (2003) 213–217.
[15] V.A. Kuzmin, P.P. Levin, E. Yu. Borisevich, I.A. Degterev, S.M. Smirnov, Triplet exciplex of nitrofuran derivative with aromatic amines, Proc. Acad. Sci. USSR, Chemistry, N 7 (1988) 1510–1514.
[16] M. Gniazdowski, L. Szmigiero, Nitracrine and its congeners – an overview, Gen. Pharmacol. 26 (1995) 473–481.
[17] K. Gorlewska, Z. Mazerska, P. Sowin'ski, J. Konopa, Products of metabolic activation of the antitumor drug Ledakrin (Nitracrine) in Vitro, Chem. Res. Toxicol. 14 (2001) 1–10.
[18] WHO Chronicle, vol. 30, Suppl. 3, World Health Organization, Geneva 1976, p. 11.
[19] E. Klein, H. Ben-Bassat, H. Neumann, P. Ralph, J. Zeuthen, A. Polliac, F. Vanky, Properties of the K562 cell line, derived from a patient with chronic myeloid leukemia, Int. J. Cancer 18 (1976) 421–431.
[20] T. Mosmann, Rapid colorimetric assay for cellular growth and survival: application to proliferation and cytotoxicity assays, J. Immunol. Meth. 65 (1983) 55–63.
[21] A. Monks, D. Scudiero, P. Skehan, R. Shoemaker, K. Paull, D. Vistica, C. Hose, J. Langley, P. Cronise, A. Vaigro-Wolff, Feasibility of a high-flux anticancer drug screen using a diverse panel of cultured human tumor cell lines, JNCI 83 (1991) 757–766.
[22] I.A. Degterev, A.A. Buzukov, V.G. Sharf, K.N. Popov, A.M. Serebrianiy, G.E. Zaikov, Comparative study of in vitro ledakrine metabolism in microsomes of EAC-cells and mouse liver, Pharmacol. Chem. J. 20 (1986) 412–417.
[23] I.A. Degterev, A.A. Buzukov, N.K. Tatarskaya, E. Yu. Leonova, N.M. Sukhova, Metabolism of heterocyclic compounds in mouse liver microsomes, Pharmacol. Chem. J. 24 (1990) 9–16.
[24] I.A. Degterev, P.C.L. Nogueira, A.J. Marsaioli, A.E. Vercesi, Microsomal metabolism of Quinifuryl – a nitrofuryl-ethenyl-quinoline antiseptic possessing antitumor activity in vitro, Eur. J. Drug Metab. Pharmacol. 24 (1999) 15–22.
[25] V.B. Iliasova, A.A. Buzukov, M. Tabak, I.A. Degterev, On the mechanism of metabolic denitration of nitroheterocyclic compounds, Biofizika (Moscow) 39 (1994) 219–225.
[26] A.A. Buzukov, V.B. Iliasova, M. Tabak, N.K. Tatarskaya, I.A. Degterev, Metabolic denitration of Quinifuryl and Nitracrine in mouse liver homogenate, Pharmacol. Chem. J. (Moscow) 29 (1995) 3–8.
[27] A.A. Buzukov, V.B. Il'asova, M. Tabak, N.C. Meirelles, I.A. Degterev, An ESR and spectrophotometric study of the denitration of nitroheterocyclic drugs by liver homogenates and their metabolic consumption by liver microsomes from cytochrome P-450-induced mice, Chem. -Biol. Interact. 100 (1996) 113–124.

ELSEVIER

Comparative Biochemistry and Physiology Part C 137 (2004) 155–165

CBP

www.elsevier.com/locate/cbpc

Comparison of liver mixed-function oxygenase and antioxidant enzymes in vertebrates

Thomaz A.A. Rocha-e-Silva[a], Marcelo M. Rossa[a], Francisco T. Rantin[a], Takako Matsumura-Tundisi[b], Jose G. Tundisi[b], Igor A. Degterev[b,c,*]

[a]*Department of Physiological Sciences/Federal University of São Carlos, Rod. Washington Luís, km 235, 13650-905 São Carlos, São Paulo, Brazil*

[b]*International Institute of Ecology, Rua Bento Carlos 750, 13560-660 São Carlos, São Paulo, Brazil*

[c]*Department of Chemical and Biochemical Kinetics/Institute of Biochemical Physics/Russian Academy of Sciences, Kosygin Str. 4, Moscow, Russian Federation*

Received 31 May 2003; received in revised form 19 December 2003; accepted 6 January 2004

Abstract

We performed a comparative analysis of cytochrome P450, cytochrome b_5, MFO associated enzymes and cytosolic antioxidant enzymes in hepatic microsomes and cytosolic fractions prepared from five animal species representing three vertebrate classes living in tropical conditions (Brazil). The data obtained show that rats have higher hepato-somatic index, specific cytochrome b_5 concentration, and NADPH-dependent cytochrome *c* (P450) activity compared to ectothermic species, SOD activity similar to those in amphibians, and specific concentration of cytochrome P450 and catalase activity lower than in a toad, but higher than in fishes and a frog. Our data indicate that tropical fishes may have reduced xenobiotic-metabolizing ability compared to the rat and amphibians. In contrast to fish and rat, amphibians have a low ratio (<0.5) of cytochrome b_5 concentration to that of P450. Most species showed cytochrome b_5 sensitivity to oxygen. Thus, the use of sodium dithionate as a reducer, rather than NADPH, may be preferential in b_5 determinations.

Keywords: Amphibians; Fish; Rat; Antioxidant enzymes; Cytochromes; Mixed-function oxidase; Hepato-somatic index; Microsomal protein index

1. Introduction

The importance of the cytochrome P450 mixed-function oxygenase (MFO) system in detoxification of xenobiotics and maintenance of homeostasis in animals of different phyla is well established. In particular, the MFO system plays a crucial role in an animal's pharmacology, metabolizing foreign compounds, such as therapeutic agents, and in its toxicology, metabolizing natural and pollutant xenobiotics. Understanding the diversity of the MFO system of different animals is important for further development of the ecosystem diagnostic for the presence of dangerous pollutants, and for the better understanding of numerous biological processes, such as xenobiotic

Abbreviations: MFO, mixed-function oxidase; HSI, hepato-somatic index; MPI. microsomal protein index; EROD, 7-ethoxyresorufin deethylase; NCCR, NADPH-dependent cytochrome *c* (P450) reductase; SOD, superoxide dismutase; CAT, catalase; BM, body mass.

*Corresponding author. *Present address*: Departamento de Física e Matemática/FFCLRP/Universidade de São Paulo, Av. Bandeirantes 3900, 14040-901, Riberão Preto, SP, Brazil. Tel./fax: +55-16-602-3862.

E-mail address: igor@dfm.ffclrp.usp.br (I.A. Degterev).

1532-0456/04/$ - see front matter © 2004 Elsevier Inc. All rights reserved.
doi:10.1016/j.cca.2004.01.007

disposition and toxicity, mechanisms of cellular adaptation and evolutionary divergence.

This is also true concerning cytosolic antioxidant enzymes. Some authors showed that antioxidant defense components, like SOD and catalase, might also effectively serve as biomarkers for the evaluation of contaminated ecosystems (Fouchecourt and Riviere, 1995; Livingstone et al., 1995; Choi et al., 1999; Niyogi et al., 2001a,b). The overall use of biomarkers needs knowledge of whether and how the above parameters depend on biological and/or biochemical peculiarities of different animal classes.

Works devoted to comparative studies of the MFO and antioxidant liver enzymes of animals of different classes are very limited. In earlier work by Miura et al. (1980) it was shown that cytochrome P450 content in liver microsomes of Japanese bullfrog (*Rana catesbeiana*) was lower than in various mammals, but higher than in trout (*Onchorynchus mykiss*) and the same as in human. Later, Schwen and Mannering (1982) have comparatively measured HSI, MPI, cytochromes P450 and b_5, and NCCR in hepatic microsomes from Wistar rat, trout (*Salmo trutta*), frog (*Rana pipiens*) and garter snake (*Thamnophis* sp.). They found cytochrome content and NCCR activity in rat much higher compared to other animals. Ertl and Winston (1998) had reviewed basal hepatic microsomal proteins and associated activities of a number of reptiles and amphibians and found them significantly lower than in rat. However, data used for this comparison were taken from different sources of the literature, thus uncertainty may exist due to different animal habitat and maintenance, test conditions, etc. To the best of our knowledge, there has only been a single extensive comparative study of a large number of animals from different vertebrate classes, reported by Nandi et al. in 1997. However, only SOD activity and cytochrome P450 content in liver were measured. These authors showed, in contrast to the above cited data, that P450 concentration in amphibians was twice as high as rats and similar to some other mammals.

In view of these considerations we performed a comparative study of liver mixed-function oxygenase and antioxidant enzymes of vertebrates of different classes in order to obtain additional baseline data. In this work, a comparative analysis of cytochrome P450, cytochrome b_5, MFO associated enzymes [NADPH-dependent cytochrome *c* (P450) reductase (NCCR) and 7-ethoxyresorufin deethylase (EROD)], cytosolic antioxidant enzymes [superoxide dismutase (SOD) and catalase (CAT)] was performed in hepatic microsomes and cytosolic fractions prepared from five animal species representing three vertebrate classes living in tropical conditions (Brazil): tropical Nile tilapia (*Oreochromis niloticus*, Cichlidae) and neotropical matrinxã (*Brycon cephalus*, Characidae), bullfrog (*R. catesbeiana*), native to Eastern North America, cane toad (*Bufo marinus*) and rat (*Rattus norvegicus*). The results obtained in this work were analyzed in comparison to data found in the literature.

2. Materials and methods

2.1. Animals

Fishes. The characid *B. cephalus* (matrinxa), and the cichlid *O. niloticus* (tilapia) were obtained from the National Center for the Study of Tropical Fish (CEPTA, Pirassununga, SP, Brazil), where they were grown in artificial, open-air reservoirs in pollutant-free water and received feed containing 25% protein ad libitum 7 days/week. Adult male and female fish (body mass 350–500 g) were killed after being kept at 25 °C for 2–3 days in our laboratory tanks equipped with recirculating and aerated water. Fish collections were made over one (matrinxã) or two (tilapia) years. Animals were collected at least once a season throughout the four seasons.

Rodents. Male Wistar rats (*R. norvegicus*) with a body mass (BM) of 220–260 g were bred at the Federal University of São Carlos. Animals had free access to food and tap water. Some groups of rats were raised at the animal facility, while other groups were transferred to our laboratory at the age of 1–2 months and housed under conditions controlled for temperature (22 ± 1 °C) and photoperiod (lights on between 08:00 and 18:00 h daily) for 1 month prior to being killed. Analyses were performed over 2 years at least once a season throughout four seasons.

Amphibians. Cane toads (*B. marinus*; 250 g BM) were collected in the field nearby Pirassununga city, São Paulo State. Frogs (*R. catesbeiana*, 300 g BM) were purchased from a commercial frog farm, where animals were kept under controlled temperature (27 °C). Animals were killed immediately after delivery to our laboratory. Both species of amphibians were collected once a year

for 2 years, in November through December (Spring–Summer).

Chemicals. NADPH, NADH and sodium dithionite (DTN) were purchased from Sigma (St. Louis, MO, USA). Heparin solution (5000 IU/ml) was purchased from Roche (Brazil).

Animal treatment and preparation of liver microsomes have been described in detail previously (Leitão et al., 2001; Rocha-e-Silva et al., 2001). Briefly, the aorta was injected with 1% heparin solution prior to killing, followed by exhaustive liver perfusion. Individual livers were dissected, rinsed repeatedly with large volumes of physiological saline, and homogenized by hand in 5 vol. of ice-cold 0.1 M potassium phosphate buffer, pH 7.4, containing 0.15 M KCl and 1 mM EDTA, and the crude homogenate was centrifuged at 43 000 $\times g$ for 40 min. Ultracentrifugation to pellet the microsomal fraction was performed at 105 000 $\times g$ for 1 h. Following isolation, the microsomal pellet was washed in 40 vol. of buffer until a colorless supernatant was obtained (usually two washes). All procedures were carried out at 0–4 °C. The resulting pellet was resuspended in 1.5–3 ml of the same buffer with or without 20% glycerol, and then homogenized by hand. The microsomal suspensions were frozen in liquid nitrogen and stored at −80 °C. Analyses were usually performed within 1 week of microsome preparation. Microsomal suspensions were prepared in 0.1 M potassium phosphate buffer, pH 7.4.

Total microsomal protein concentrations were determined by the Bradford method using bovine serum albumin (BSA) as a reference protein.

Hepatosomatic index (HSI) was measured as a ratio: liver mass/body mass $\times$ 100.

Microsomal protein index (MPI)—the content of the microsomal fraction in liver was measured as the ratio of mass of the total microsomal protein (mg) prepared from the liver to the mass of the liver (g).

Specific concentrations of cytochrome P450 and b_5 were determined using a method of Omura and Sato (1964). Usually, b_5 concentration was assessed by measuring differences in spectra of microsomes reduced with NADH (1 mM) vs. oxidized microsomes. Additionally, cytochrome b_5 concentration was measured using dithionite (DTN) as reducer (1.5 mM). P450 concentration was assessed with DTN (2 mM). Concentrations of P450 and b_5 were related to protein content of microsomes.

Specific activity of microsomal NADPH-cytochrome *c* (P450) reductase was measured according to Brattsten et al. (1980) by the increase in absorbance of reduced cytochrome *c* in the presence of NADPH at 550 nm ($\varepsilon = 21$ mM^{-1} cm^{-1}) and related to protein content of microsomes.

Specific activity of microsomal ethoxyresorufin *O*-deethylase (EROD) was measured using a fluorescence assay according to Pohl and Fouts (1980) (excitation at 550 nm, emission at 585 nm) and related to protein content of microsomes.

Specific activity of cytosolic superoxide dismutase (SOD) was measured according to Misra and Fridovich (1972). The method is based on the inhibition of spontaneous adrenalin oxidation with superoxide anion radical to adrenochrome by SOD recorded by a decrease of absorbance at 480 nm ($\varepsilon = 4.0$ nmol^{-1} cm^{-1}). Results were related to cytosolic protein.

Specific activity of cytosolic catalase (CAT) was measured according to Aebi (1984) following a decrease in the concentration of hydrogen peroxide at 240 nm ($\varepsilon = 40$ M^{-1} cm^{-1}). Results were related to the cytosolic protein.

Cytochrome concentrations and enzymatic activities, except for EROD, were measured using the Varian Cary 500 dual-beam spectrophotometer. EROD activity was determined with a Jasco FP-6500 spectrofluorimeter. All spectral measurements were performed at 25 °C.

Statistical analysis. The data are presented as the mean $\pm$ S.D. of at least three animals analyzed. One-way ANOVA with 95% confidence interval was used to compare raw data. Either the Tukey's test or Student–Newman–Keuls test were applied to compare the means. Statistical analyses were done using the InStat software program for Windows (GraphPads software, San Diego, USA).

3. Results

The HSI was highest in rats and lowest in fishes with amphibians possessing higher HSI than both fish species (Table 1). No significant difference among animals in MPI was observed (Table 1).

The highest specific content of cytochrome P450 was observed in liver microsomes from toad and rat, while rat microsomes showed significantly higher content of cytochrome b_5 than other animals (Table 1). Specific content of b_5 was measured in

Table 1
Hepatic (HSI) and microsomal protein (MPI) indexes, specific content of microsomal cytochromes P450 and b_5, activities of MFO-associated enzymes (NCCR, EROD), and liver cytosolic antioxidant activities (CAT, SOD)

Animal	HSI$\times 10^2$, g liver g BM^{-1}	MPI, mg protein g liver^{-1}	[P450], pmol mg prot^{-1}	$[b_5]^{NADH}$, pmol mg prot^{-1}	$[b_5]^{NADH}/[b_5]^{DTN}$	NCCR, nmol min^{-1} mg prot^{-1}	EROD, nmol min^{-1} mg prot^{-1}	Catalase, K mg prot^{-1}	SOD, U mg prot^{-1}
Wistar rat	4.6±2.6	2.7±1.7	620±340	505±450	0.75±0.2	270±115	50±40	3.7±1.4	5.4±1.7
A	(25)	(25)	(26)	(26)	(30)	(26)	(21)	(26)	(26)
	BC		BCDE	BCDE	BC	BCDE	BD	BCD	BC
O. niloticus	1.6±0.6	2.8±1.6	170±140	60±33	0.36±0.32	120±50	18±17	0.8±0.8	2.8±1.7
B	(49)	(41)	(34)	(37)	(22)	(40)	(31)	(40)	(39)
	AE		AD	A	ACE	A	ADC	AD	A
B. cephalus	1.1±0.2	2±2	170±70	120±70	1.3±0.6	120±80	65±40	0.7±0.3	2.1±0.3
C	(12)	(12)	(6)	(6)	(6)	(7)	(5)	(12)	(12)
	AE		AD	A	ABD	A	BD	AD	AE
B. marinus	2.8±0.9	3.5±1.0	920±250	190±60	0.7±0.3	95±30	238±94	7±4	3.8±2.0
D	(7)	(9)	(5)	(5)	(5)	(9)	(4)	(5)	(9)
			ABCE	A	C	A	ABCE	ABCE	
R. catesbeiana	3.7±1.0	2.0±0.9	85±12	31±13	0.8±0.2	110±30	34±30	2±3	4.8±0.9
E	(6)	(6)	(5)	(5)	(5)	(6)	(5)	(6)	(6)
	BC		AD	A	B	A	D	D	C

$[b_5]^{NADH}/[b_5]^{DTN}$-the ratio of cytochrome b_5 concentrations measured with either NADH or DTN as reducers and calculated based on parallel measurements of respective parameters; NCCR-NADPH-dependent cytochrome *c* (P450) reductase; EROD-7-ethoxyresorufin deethylase; CAT-catalase; K–the first order rate constant of the H_2O_2 decomposition; SOD-superoxide dismutase. Data presented as mean±S.D. and are statistically compared within each column by analysis of variance (ANOVA test, 95%) and Student–Neuman–Keuls test. Number of animals studied given in parentheses. Letters indicate statistically significant differences ($P<0.01$) of each parameter between animals.

duplicate, with either NADH or DTN as reducers, and related to the P450 concentration in an appropriate microsome preparation (Table 1).

Rats showed the highest specific activity of NCCR compared to other animals. No significant differences of this parameter were observed between fishes and amphibians (Table 1).

EROD activity was highest in toad microsomes and lowest in those from tilapia. No significant differences in this parameter were noted among frog, matrinxã and rat (Table 1).

As for antioxidant enzymes of the cytosol, there was no great interspecies difference in SOD activity, while that of rat was slightly enhanced compared to other animals, except in frog. The highest catalase activity was found in the cane toad followed by rat with no significant difference observed between frog and fishes (Table 1).

No significant seasonal differences of any parameter measured were observed in tissues of *O. niloticus* and rat when the data obtained during the four seasons were analyzed (Table 2). There also were no significant differences in HSI, MPI, content of microsomal cytochromes, and NCCR activity between male and female *O. niloticus* collected in parallel (Table 3). Thus, Table 1 represents means of pooled data.

No differences were observed between rat tissues obtained from animals maintained under conditions controlled for temperature and photoperiod and those maintained under natural conditions. Thus, these data were also pooled.

4. Discussion

The data obtained here were compared with appropriate parameters measured by other authors for specimens of the same species, if available, or the same class in order to clarify to what extent they can serve as reference material.

The HSI values for fishes, amphibians and rat studied here are similar to those reported for brown trout, leopard frog and Sprague–Dawley rat, respectively (Table 4). The averaged HSI value for tropical freshwater fish, measured in this work, was similar to those reported for brown trout and 11 species of marine tropical fishes and below the averaged data for amphibians and rats (Table 4).

Table 2
Hepatic (HSI) and microsomal protein (MPI) indexes, specific content of microsomal cytochromes P450 and b_5, activities of MFO-associated enzymes (NCCR, EROD), and cytosolic antioxidant activities (CAT, SOD). Seasonal analyses of tilapia (*O. niloticus*) and rat (*R. norvegicus*) liver tissues

Season	Month	HSI×10², g liver g BM⁻¹	MPI, mg protein g liver⁻¹	[P450] pmol mg prot⁻¹	[b_5] pmol mg prot⁻¹	NCCR, nmol min⁻¹ mg prot⁻¹	EROD, nmol min⁻¹ mg prot⁻¹	Catalase, K mg prot⁻¹	SOD, U mg prot⁻¹
O. niloticus									
Summer	December (A)	1.4±0.2 (4) B	2.3±0.8 (4) E	125±92 (4)	44±28 (4)	105±50 (4)	10±8 (4) E	1.9±0.7 (3) B, C, D, E	3.5±0.9 (3) F
	January (B)	2.0±0.5 (10) A, C, D	2.6±1 (7) E	170±200 (7)	81±58 (7)	145±75 (7)	n.m.	0.46±0.31 (7) A, F	2.95±0.8 (7) F
Autumn	April/May (C)	1.3±0.7 (14) B	3.3±1.8 (11) D	125±120 (10)	85±39 (11)	140±54 (11) E	18±13 (8)	0.40±0.35 (11) A, F	3.6±1.2 (11) F
Winter	June/July (D)	1.8±0.5 (11)	1.8±1.2 (9) C, E	215±105 (4)	49±25 (6)	120±26 (9) E	30±22 (7)	0.54±0.3 (9) A, F	2.61±0.95 (9) F
	August (E)	1.6±0.4 (6)	4.9±1.2 (6) A, B, D, F	265±120 (6)	76±32 (6)	78±23 (6) C, D	28±1 (6) A	0.50±0.24 (6) A, F	0±0 (6)
Spring	October (F)	1.3±0.5 (4) B	1.6±0.6 (4) E	78±46 (3)	48±34 (3)	84±15 (3)	n.m.	2.16±1.6 (4) B, C, D, E	5.47±0.8 (3) B, C, D, E
Average		1.6±0.6 (41)	2.8±1.6 (34)	170±140 (37)	60±33 (40)	120±50 (31)	18±17 (40)	0.8±0.8 (39)	2.8±1.7
	(49)								
Wistar rats									
Summer	December (A)	1.7±0.8 (5)	2.6±0.9 (5)	670±90 (5)	350±65 (5) C	340±150 (5) B	105±40 (5) B–F	4.0±1.3 (5)	4.6±0.4 (5)
	February/March (B)	6.4±4.2 (5)	2.5±1.2 (5)	470±230 (5)	668±326 (5) F	130±45 (5) A, F	16±1 (2)	2.8±0.9 (5) C	4.5±1.1 (5)
Autumn	April (C)	6.4±2.6 (3)	2.4±0.7 (3)	1100±600 (4)	1075±204 (4) A, F	250±86 (4)	28±10 (3)	5.3±1.4 (4) B	7.9±0.6 (4) A, B, D–F
	May (D)	5±1 (4)	5±3 (4) F	630±60 (4)	806±90 (4) F	255±75 (4)	16±6 (4)	3±2 (4)	5.3±2.7 (4)
Winter	July (E)	4.8±1.3 (4)	2.7±1.4 (4)	460±340 (4)	619±472 (4) F	260±45 (4)	28±10 (3)	4.2±0.7 (4)	4.4±0.6 (4)
Spring	November (F)	4.2±0.6 (4)	1.4±0.4 (4) D	470±250 (4)	130±122 (4) A–E	400±15 (4) B	60±30 (4)	3±0.6 (4)	6.2±0.4 (4)

Data are means±S.D. and are statistically compared within each column by ANOVA (95%) and Student–Newman–Keuls test. Number of animals studied in parentheses. Letters indicate statistically significant differences ($P<0.01$).

Table 3
Analyses of sex-dependence of hepatic (HSI) and microsomal protein (MPI) indexes, specific content of microsomal cytochromes P450 and b_5, and NCCR activity in liver of *O. niloticus*

Sex	HSI$\times 10^2$, g liver g BM^{-1}	MPI, mg protein g liver^{-1}	[P450] pmol mg prot^{-1}	[b_5] pmol mg prot^{-1}	NCCR, nmol min^{-1} mg prot^{-1}
Male	1.3±0.5 (18)	6.7±3.1 (18)	67±41 (13)	14±11 (10)	2.7±1.0 (18)
Female	1.17±0.11 (6)	6.8±2.0 (6)	67±46 (5)	18±8 (6)	3.1±1.6 (6)

Data presented as mean±S.D. (n).

Thus, it seems that liver occupies significantly less space in body of fishes, at least tropical species, compared to rats and amphibians.

In contrast to HSI, specific MPI values did not differ significantly for animals studied here (Table 1). There are vary few works reporting the HSI and MPI for vertebrates investigated here and these parameters measured for same or allied species were higher compared to those obtained here (Table 2). Nevertheless, the above consideration would also hold for the literature data that show that MPIs for rat, leopard frog (*R. pipiens*), and brown trout (*Salmo trutta*) were inside of the range for MPIs of tropical marine fish (Table 4).

Averaged data from different sources (Table 5) show similar P450 specific concentration in liver of tropical freshwater and marine fishes, rainbow trout, and frogs (approx. 0.3 nmol mg prot^{-1}), and twice as much in liver of rat and toad (0.6 nmol mg prot^{-1}). Reviewing data on basal hepatic microsomal P450 specific content in amphibians and reptiles, Ertl and Winston (1998) found it to

Table 4
Comparative data on the HSI and MPI indexes in liver from fish, amphibians and rat

Animal		HSI, F liver wt./body wt. %	MPI, mg protein/ g liver	Source
Fish	*O. niloticus*	1.6±0.6 (49)	2.8±1.6 (41)	This work
		n.m.	4.8±1.2 (16)	Leitão et al., 2001
	B. cephalus	1.1±0.3 (12)	2±2 (12)	This work
		n.m.	2.0±0.3 (8)	Leitão et al., 2001
	Colossoma macropomum (tambaqui)	n.m.	4.5±2.0 (26)	Leitão et al., 2001
	Average for tropical freshwater fish	1.35±0.5	–	
	S. trutta (brown trout)	1.0±0.1 (≥5)	23.1±0.8 (≥5)	Schwen and Mannering, 1982
	*Average for 11 species of tropical marine fish	1.13±0.47	17.6±7.7	Stegeman et al., 1997
		0.63÷1.8	6.9÷27.6	Vrolijk et al., 1994
Amphibians	*R. catesbeiana*	3.7±1.0 (6)	2.0±0.9 (6)	This work
	R. pipiens (leopard frog)	4.2±0.2 (≥5)	9.0±0.6 (≥5)	Schwen and Mannering, 1982
	B. marinus	2.8±0.9 (7)	3.5±1.0 (9)	This work
	Average for amphibians	3.6±0.9	–	
Rat		4.6±2.6 (25)	2.7±1.7 (25)	This work
		5.7±0.1 (≥5)	11.0±1.2 (≥5)	Schwen and Mannering, 1982
	Average for rat	5.2±1.9	–	

Data presented as mean±S.D.; (n) – number of specimens or (*) species studied. n.m.=not measured.

Table 5
Comparative data on content of microsomal cytochromes in liver from fish, amphibians and rat

Animal		[P450] nmol mg prot^{-1}	[b_5] nmol mg prot^{-1}	[b_5]^{NADH}/ [P450]	[b_5]^{DTN}/ [P450]	Source
Fish	[a]*O. niloticus*	0.17±0.14 (34)	0.06±0.03 (37)	0.35±0.35 (25)	1±1 (25)	This work
		0.26±0.003 (8)	0.15±0.02 (9)	0.58	n.m.	*Bainy et al., 1996
		0.46±0.13 (7)	0.06±0.01 (7)	0.13	n.m.	*Bainy et al., 1999
		0.52±0.14 (5)	n.m.	n.m.	n.m.	**Pathiratne and George, 1996
	[a]*B. cephalus*	0.17±0.07 (6)	0.12±0.07 (6)	0.9±0.7 (6)	0.7±0.5 (6)	This work
		0.23±0.13 (5)	0.11± 0.1 (5)	0.48	n.m.	Leitão et al., 2001
	[a]*C. macropomum*	0.31±0.19 (9)	0.25± 0.075 (9)	0.81	n.m.	Leitão et al., 2001
	Averaged tropical freshwater fish	0.3±0.17	0.13±0.08	0.54±0.29	n.m.	–
	[a]*O. mykiss* (rainbow trout)	0.3±0.06 (5)	n.m.	n.m.	n.m.	Pathiratne and George, 1996
	[b]Tropical marine fish species	0.3±0.2 (9)	0.11±0.085 (9)	0.27±0.08 (10)	n.m.	Stegeman et al., 1997
		0.083÷1.73	0.024÷0.611			
Amphibians	[a]*R. catesbeiana*	0.085±0.012 (5)	0.03±0.01 (5)	0.3±0.1 (5)	0.4±0.18 (5)	This work
		0.4±0.02 (18)	n.m.	n.m.	n.m.	Miura et al., 1980
	[b]Frogs	0.35±0.21 (5)	0.19±0.12 (3)	0.33±0.11		Ertl and Winston, 1998
		0.07÷0.77	0.08÷0.32	(3)	n.m.	Nandi et al., 1997
	Averaged frogs	0.30±0.20	0.11±0.11	0.32±0.1		
	[a]*B. marinus*	0.92±0.25 (5)	0.19±0.06 (5)	0.3±0.1 (5)	0.44±0.17 (5)	This work
	[b]Toads	0.32±0.22 (5)	0.12±0.06 (2)	0.47±0.1 (2)	n.m.	Ertl and Winston, 1998 Nandi et al., 1997
	Averaged toads	0.62±0.39	0.16±0.07	0.39±0.13		
[a]Rat		0.62±0.34 (26)	0.51±0.45 (26)	0.9±0.2 (26)	1.2±0.3 (26)	This work
		0.92	n.m.	n.m.	n.m.	Jewell and Winston, 1989
		~0.94	~0.44	0.47	n.m.	Schwen and Mannering, 1982
		0.15±0.03 (2)	n.m.	n.m.	n.m.	Nandi et al., 1997
	Averaged rat	0.6±0.4	0.49±0.37	0.79±0.27	n.m.	

Tilapia were artificially reared in either fish farms in São Paulo State (this work and *) or in Sri Lanka (**). [b_5]^{NADH}/[P450] and [b_5]^{DTN}/[P450] – ratios of cytochrome b_5 concentrations, measured with either NADH or DTN as reducer, to that of P450 calculated based on parallel measurements of respective parameters. Data presented as mean±S.D. Number in parentheses are either specimens ([a]) or species ([b]) studied.

fall into the lower end of the range for mammals. In particular, P450 content in frog and toad livers were from 8 to 84% of that in rat liver. However, these authors had used a value of 0.92 nmol mg prot^{-1} as reference point for rat, while this concentration is greatly variable (Table 5). In contrast, Nandi et al. (1997) who measured liver microsomal P450 in amphibians, reptiles, and mammals have shown that toad and frog had similar specific content of this enzyme (approx. 0.3 nmol mg prot^{-1}) similar to that of various mammals (mice, cow, goat), but twice as rat (0.15 nmol mg

Table 6
Comparative data on microsomal enzymatic activities in liver from fish, amphibians and rat

Animal		NCCR	EROD	EROD/[P450], min^{-1}	Source
		nmol min^{-1} mg $prot^{-1}$			
Fish	*O. niloticus*	120±50 (40)	0.018±0.017(31)[a]	0.11±0.09(19)	This work
		290±130 (3)	0.02±0.01 (3)[a]	0.13	Leitão et al., 2001
		59±8 (5)	0.52±0.1 (5)[c]	1.0	*Pathiratne and George, 1996
	B. cephalus	120±80 (7)	0.065±0.04 (5)[a]	0.6±0.45 (5)	This work
		380±150 (3)	0.025±0.006 (3)[a]	0.11	Leitão et al., 2001
	C. macropomum	420±190 (3)	0.06±0.01 (3)[a]	0.19	Leitão et al., 2001
	Averaged tropical freshwater fish	226±163	**0.04±0.03	–	
	O. mykiss	23±2 (5)	0.02±0.03 (5)[c]	0.07	Pathiratne and George, 1996
	S. trutta	~110 (≥5)	n.m.	n.m.	Schwen and Mannering, 1982
	[x]Eleven tropical marine fish species	112±90 (11)	0.06±0.04 (7)	0.2±0.14 (7)	Stegeman et al., 1997
		18÷330	0.84±0.56 (4)	1.3±1.1 (4)	Vrolijk et al., 1994
			0.023÷2.1[b]	0.029÷3.02	
	P. platessa	70±4 (5)	1.6±0.01 (5)	3.0	Pathiratne and George, 1996
Amphibians	*R. catesbeiana*	110±30 (6)	0.03±0.03 (5)[a]	0.45±0.3 (5)	This work
	[x]Three species of frog	103±25 (3)	n.m.	n.m.	Ertl and Winston, 1998
	Averaged frogs	108±23 (5)	0.03±0.03	0.45±0.3	
	B. marinus	95±30 (9)	0.24±0.09 (4)[a]	0.22±0.06 (4)	This work
	[x]Two species of toad	69±18 (2)	n.m.	n.m.	Ertl and Winston, 1998
	Averaged toads	82±26	0.24±0.09	0.22±0.06	
Rat		270±115 (26)	0.05±0.04 (26)[a]	0.06±0.04(26)	This work
		~470 (≥5)	n.m.	n.m.	Schwen and Mannering, 1982
		320±137	0.05±0.04	0.06±0.04	

All tilapia specimens were artificially reared in fish farms in São Paulo State (this work) or in Sri Lanka (*). The EROD was measured using: the fluorimetric method (a); spectrophotometric assay (b); no method described (c). The EROD/[P450]-ratio of 7-ethoxyresorufin deethylase activity (pmol/min) to concentration of P450 (pmol) calculated based on parallel measurements of respective parameters. Data presented as mean±SD; (*n*) – number of animals, ([x])–number of species studied, ** only data obtained at the same laboratory (this work and Leitão et al.) was averaged. n.m. - not measured.

$prot^{-1}$). Thus, the true correlation remains unclear between P450 concentration in frogs and toads, toads and rats, while our and literature data sets agree that concentration of this enzyme in fish liver is lower compared to rat.

This fact, along with observations that fish possesses lower, relative to body mass, size of liver compared to rat and amphibians and similar specific (per g of liver mass) MPIs (Table 4), may signify that overall xenobiotic-metabolizing ability of these animals is lower compared to above-mentioned.

In contrast to P450, cytochrome b_5 content was not significantly different in microsomes from fishes and amphibians, with rats showing the highest level of this enzyme (Table 1). As for comparison with the literature data: specific concentrations of b_5 in fish were inside of the data range for freshwater and marine tropical fish, with those in *R. catesbeiana* – lower, and *B. marinus* – higher, compared to frogs and toads, respectively (Table 5).

It is well known that DTN, in contrast to NADH, reduces molecular oxygen, thus creating an anaerobic microenvironment. The fact that all species, except *B. cephalus*, had a ratio $[b_5]^{NADH}/[b_5]^{DTN}$ below 1 (Table 1) shows that the reduced form of this enzyme is sensitive to the presence of oxygen. Thus, it seems more reasonable to compare concentrations of cytochrome P450 and b_5 assessed both in the presence of DTN. This comparison (Table 5) shows that, unlike rat and fishes, concentration of P450 in liver of amphibians was nearly twice as much than cytochrome b_5.

Rat showed the highest specific activity of the NCCR, while other animals did not significantly differ by this parameter (Table 1). When compared with the literature data, one can see that the NCCR measured in this work for amphibians were close to those reported by other authors (Table 6).

Table 7
Comparative data on CAT and SOD activities in liver from fish, amphibians and rat

Animal		Total CAT, K mg prot^{-1}	Total SOD, U mg prot^{-1}	Source
Fish	*O. niloticus*	0.8±0.8 (40)	2.8±1.7 (19)[1]	[a]This work
		n.m.	57.4±6.7 (9)[1]	[a]Bainy et al., 1996
	B. cephalus	0.7±0.3 (12)	2.1±0.3 (12)[1]	[a]This work
	C. macropomum	0.55±0.08 (10)	–*, [2]	[b]Marcon and Filho, 1999
	Average for six tropical fish species (Calcutta, India)	n.m.	8±0.8 (50)[3]	[c]Nandi et al., 1997
Amphibians	*R. catesbeiana*	2±3 (6)	4.8±0.9 (6)[1]	[a]This work
	R. tigrina	n.m.	9±0.6 (12)[3]	[c]Nandi et al., 1997
	B. marinus	7±4 (5)	3.8±2 (9)[1]	[a]This work
	B. melanosticus	n.m.	9.8±0.8 (18)[3]	[c]Nandi et al., 1997
Rat		3.7±1.4 (20)	3.7±1.4 (26)[1]	[a]This work
		n.m.	15.5±1.2 (12)[3]	[c]Nandi et al., 1997
		2.2±0.6 (8)	–**,[3]	[a]Fouchecourt and Riviere, 1995

Activities were measured in: [a] – liver cytosol; [b] – supernatant of 10 000×*g* centrifugation of liver homogenate; [b] – supernatant of 34 880×*g* centrifugation of liver homogenate. Methods of SOD activity measurement: [1] – epinephrine oxidation to adrenochrome; [2] – cytochrome *c* reduction; 3 – pyrogallol autoxidation. * – results expressed in U g liver^{-1}; ** – results expressed in SOD μg mg prot^{-1}. Data presented as mean±S.D. (*n*).

Comparisons of averaged data show that the NCCR activity is possibly decreased as follows: rat > tropical freshwater fish > tropical marine fish, frogs, and brown trout > toads, plaice (*Pleuronectes platessa*) > rainbow trout.

The same is true for EROD activity. The EROD values reported by different authors for animals of the same class or, even, the same species may vary by more than order of magnitude (Table 6). We failed to reveal an apparent reason for such great data dispersion. Neither different methods, as photometric or fluorometric (see legend to this Table), nor assay temperatures of 25 °C (Pathiratne and George, 1996 ; this work) or 30 °C (Stegeman et al., 1997; Vrolijk et al., 1994) can explain such a great difference between data reported for the same or allied species by different authors (e.g. tilapia in Table 4). It seems that interspecies comparison may be valuable for data obtained in the same laboratory. According to our data, toads showed the highest EROD result with tilapia possessing the lowest value and no significant difference was observed between frog, rat, and neotropical fish (*B. cephalus*) (Table 1). Tropical marine fish can be divided in two groups, according to the EROD activities. Seven species, out of 11, have an averaged activity (0.06±0.04) close to that measured for tropical freshwater fish in our laboratory (0.04±0.03), and those measured in this work for rat (0.05±0.04) and frog (0.03±0.03) (Table 6). Another four species had higher average EROD activity (0.84±0.56) than any other animal reported in this table except plaice (1.6±0.01). Activity of tilapia reared in Sri Lanka (Pathiratne and George, 1996) was ~30 times greater compared to both this fish grown in Brazil and rainbow trout from Sri Lanka (Table 6).

Thus, a reliable interspecies comparison of NCCR and EROD activities are not available because a dispersion of results inside one species was sometimes greater than differences between species and classes.

The highest ratios of EROD activity to P450 concentration were observed in some (four out of 11) tropical marine fish species and in *B. cephalus* with the lowest value of this ratio showed by rats (Table 6).

Our data did not show significant differences in SOD activity between toad and fishes, although this activity in frog liver microsomes was similar to that in rat and considerably higher compared to fishes. The highest catalase activity was observed in toad liver cytosol, while fishes showed the lowest values of this enzyme activity and no significant difference was detected between frog and rat (Table 1).

Data obtained in this work and those reported in the literature (Table 7) show that catalase activities in fish and rat liver measured by different

authors are in a reasonable agreement. One can see that this activity is lower in fish compared to amphibians and rats. In contrast, there is a great dispersion between SOD activities measured by different authors. In part, the dispersion may be due to either different methods employed for measurements of this activity or to the fact that SOD was measured in different fractions of liver tissues (see legend to Table 7). Great dispersion of data obtained by different authors does not permit differentiation of these three classes of vertebrates by SOD activity.

It was noted (Niyogi et al., 2001a) that one may experience significant difficulties in the practical use of antioxidant enzymes as biomarkers, because of considerable seasonal fluctuations of these activities. In contrast to this statement, we did not observe seasonal differences in either activity when analyzing data obtained with liver cytosol from rats and fishes collected during the four seasons over the course of 2 years (Table 2). Thus, the great dispersion of data concerning CAT activity for *O. niloticus* and *R. catesbeiana* was due to some unknown factor and not to seasonal fluctuation.

Sex-dependent differences in content of microsomal cytochromes, MFO-associated enzymatic activities, HSI, and MPI were reported for various fish species (Stegeman and Chevion, 1980; Pajor et al., 1990; Vrolijk et al., 1994). Vrolijk et al. (1994) did not observe significant differences in HSI and MPI of *Chaetodon capistratus* collected in Florida and Belize, while cytochrome P450 specific content was 20–36% greater in male than female and NCCR activity was ~20% greater in male among fish collected in Florida, but not in Belize. In this work, we observed no significant difference in any of these parameters when male and female, artificially reared *O. niloticus* were collected in parallel (Table 3).

Data reported here show that rats have higher HSI, specific cytochrome b_5 content, and NADPH-dependent cytochrome *c* (P450) activity compared to ectothermic species, SOD activity similar to those in amphibians, and specific concentration of cytochrome P450 and catalase activity lower than in a toad, but higher than in fishes and a frog. *O. niloticus* and *B. cephalus* possessed the lowest HSI and specific cytochrome P450 content compared to the other vertebrates, while MPIs were similar. This means that tropical fishes may have reduced xenobiotic-metabolizing ability compared to rat and amphibians. Most vertebrate species studied in this work showed sensitivity of cytochrome b_5 to oxygen. Thus, the use of sodium dithionate as a reducer, rather than NADPH, may be preferential in b_5 determinations.

Acknowledgments

The authors thank Prof. Alzir A. Batista and post-doctoral student Marcio P. de Araujo (Federal University of São Carlos) for valuable assistance in spectrophotometric measurements. This work was supported by Brazilian agencies: Conselho Nacional de Desenvolvimento Científico e Tecnológico (CNPq), Coordenação de Aperfeiçoamento de Pessoal de Nível Superior (CAPES), Fundação de Amparo à Pesquisa do Estado de São Paulo (FAPESP).

References

Aebi, H., 1984. Catalase in vitro. Method Enzymol. 105, 121–126.

Bainy, A.C.D., Saito, E., Carvalho, P.S.M., Junqueira, V.B.C., 1996. Oxidative stress in gill, erythrocytes, liver and kidney of Nile tilapia (*Oreochromis niloticus*) from a polluted site. Aquat. Toxicol. 34, 151–162.

Bainy, A.C.D, Woodin, B.R., Stegeman, J.J., 1999. Elevated levels of multiple cytochrome P450 forms in tilapia from Billings Reservoir-Sao Paulo, Brazil. Aquat. Toxicol. 44, 289–305.

Brattsten, L.B., Price, S.L., Gunderson, C.A., 1980. Microsomal oxidases in midgut and fatbody tissues of a broadly herbivorous insect larva, Spodoptera eridania Cramer (Noctuidae). Comp. Biochem. Physiol. C 66, 231–237.

Choi, J., Roche, H., Caquet, T., 1999. Characterization of superoxide dismutase activity in Chironomus riparius Mg. (Diptera, Chironomidae) larvae—a potential biomarker. Comp. Biochem. Physiol. C 124, 73–81.

Ertl, R.P., Winston, G.W., 1998. The microsomal mixed function oxidase system of amphibians and reptiles: components, activities and induction. Comp. Biochem. Physiol. C 121, 85–105.

Fouchecourt, M.-O., Riviere, J.-L., 1995. Activities of cytochrome P450-dependent monooxigenase and antioxidant enzymes in different organs of Norway rata (*Rattus norvegicus*) inhabiting reference and contaminated sites. Chemosphere 31, 4375–4386.

Jewell, C.S., Winston, G.W., 1989. Characterization of the microsomal mixed-function oxygenase system of the hepatopancreas and green gland of the red swamp crayfish, *Procambarus clarkii*. Comp. Biochem. Physiol. B 92, 329–339.

Leitão, M.A.S., Affonso, E.G., da Silva, M.E., Meirelles, N.C., Rantin, F.T., Vercesi, A.E., et al., 2001. The liver monooxigenase system of Brazilian freshwater fish. Comp. Biochem. Physiol. C 126, 29–38.

Livingstone, D.R., Lemaire, P., Matthews, A., Peters, L.D., Porte, C., Fitzpatrick, P.J., et al., 1995. Assessment of the impact of organic pollutants on goby (*Zosterisessor ophi-*

ocephalus) and mussel (*Mytilus galloprovincialis*) from the Venice Lagoon, Italy: Biochemical studies. Mar. Environ. Res. 39, 235–240.

Marcon, J.L., Filho, D.W., 1999. Antioxidant processes of the wild tambaqui, *Colossoma macropomum* (Osteichthyes, Serrasalmidae) from the Amazon. Comp. Biochem. Physiol. C 123, 257–263.

Misra, H.P., Fridovich, I., 1972. The role of superoxide anion in the autoxidation of epinephrine and a single assay for superoxide dismutase. J. Biol. Chem. 247, 3170–3174.

Miura, Y., Hisaki, H., Ueta, N., 1980. Effect of detergents on the microsomal cytochrome *P*-450-dependent monooxygenases from frog and rat liver. Comp. Biochem. Physiol. B 67, 541–547.

Nandi, A., Mukhopadhyay, C.K., Ghosh, M.K., Chattopadhyay, D.J., Chatterjee, I.B., 1997. Evolutionary significance of vitamin C biosynthesis in terrestrial vertebrates. Free Radical Biol. Med. 22, 1047–1054.

Niyogi, S., Biswas, S., Sarker, S., Datta, A.G., 2001a. Seasonal variation of antioxidant and biotransformation enzyme. Mar. Environ. Res. 52, 13–26.

Niyogi, S., Biswas, S., Sarker, S., Datta, A.G., 2001b. Antioxidant enzymes in brackish water oyster, *Saccostrea cucullata* as potential biomarkers of polyaromatic hydrocarbon pollution in Hooghly Estuary (India): seasonality and its consequences. Sci. Total Environ. 281, 237–246.

Omura, T., Sato, R., 1964. The carbon monoxide-binding pigment of liver microsomes. II. Solubilization, purification, and properties. J. Biol. Chem. 239, 2379–2385.

Pajor, A.M., Stegeman, J.J., Thomas, P., Woodin, B.R., 1990. Feminization of the hepatic microsomal cytochrome P-450 system in brook trout by estradiol, testosterone, and pituitary factors. J. Exp. Zool. 253, 52–60.

Pathiratne, A., George, S., 1996. Comparison of xenobiotic metabolizing enzymes of tilapia with those of other fish species and interspecies relationships between gene families. Mar. Environ. Res. 42, 293–296.

Pohl, R.J., Fouts, J.R., 1980. A rapid method for assaying the metabolism of 7-ethoxyresorufin by microsomal subcellular fractions. Anal. Biochem. 107, 150–155.

Rocha-e-Silva, T.A.A., Farley, B., Nonaka, K.O., Selistre-de-Araujo, H.H.S., Rantin, F.T., Degterev, I.A., 2001. The spectral characteristics of an unknown compound that altered cytochrome P450 spectra from spectra from vertebrate microsomes suggest that it is a functional protein. Comp. Biochem. Physiol. C 130, 53–66.

Schwen, R.J., Mannering, G.J., 1982. Hepatic cytochrome P-450-dependent monooxygenase systems of the trout, frog and snake.-1. Components. Comp. Biochem. Physiol. B 71, 431–436.

Stegeman, J.J., Chevion, M., 1980. Sex differences in cytochrome *P*-450 and mixed function oxygenase activity in gonadally mature trout. Biochem. Pharmacol. 29, 553–558.

Stegeman, J.J., Woodin, B.R., Singh, H., Oleksiak, M.F., Celander, M., 1997. Cytochromes P450 (CYP) in tropical fishes: catalytic activities, expression of multiple CYP proteins and high levels of microsomal P450 in liver of fishes from Bermuda. Comp. Biochem. Physiol. C 116, 61–75.

Vrolijk, N.H., Targett, N.M., Woodin, B.R., Stegeman, J.J., 1994. Toxicological and ecological applications of biotransformation enzymes in the tropical teleost *Chaetodon capistratus*. Mar. Biol. 119, 151–158.